Cellular interactions during zebrafish adult stripe formation and implications for pigment pattern evolution

Larissa Blythe Patterson

A dissertation

submitted in partial fulfillment of the

requirements for degree of

Doctor of Philosophy

University of Washington

2014

Reading Committee:

David Parichy, Chair

Billie Swalla

David Raible

Program Authorized to Offer Degree:

Biology

University of Washington

Abstract

Cellular interactions during zebrafish adult stripe formation and implications for pigment pattern evolution

Larissa Blythe Patterson

Chair of the Supervisory Committee:
Professor David Parichy
Biology

Pigment patterns are among the most striking of traits, yet we know very little about the interactions required for organizing pigment cells during adult pattern formation or how evolutionary changes in pigment cell development generate different patterns. As an adult the zebrafish, *Danio rerio* displays a pattern of dark horizontal stripes composed of black melanophores alternating with light interstripes composed of yellow xanthophores. Previous work showed that melanophore–xanthophore interactions are critical for stripe organization, but did not explain why stripes develop where they do. Here I investigate the role of a third pigment cell, the iridescent iridophore, in zebrafish stripe development and pigment pattern evolution. I show that in *D. rerio,* iridophores are the first pigment cell type to develop during adult stripe formation and that they do so precisely at the location of the first interstripe. By ablating iridophores in wild-type and mutants I found that iridophores play a role in organizing both xanthophores and melanophores into stripes. Additionally, I found that iridophores express *colony stimulating factor 1* (*csf1*) and that localized Csf1 expression is sufficient to direct localized xanthophore development. Next, I asked whether differences in these interactions could

play a role in the evolutionary loss of stripes in the closely related species, *D. albolineatus.* I found that iridophores are also required for stripe termination in *D. rerio*, but that *D. albolineatus* fails to develop iridophores at times and locations critical for stripe development. Instead, I found that *D. albolineatus* developed precocious xanthophores. Early, widespread xanthophore development in *D. albolineatus* was associated with similarly widespread and early expression of *csf1*, a change associated with *cis*-regulatory evolution at the Colony stimulating factor-1a (Csf1a) locus. Finally, to test if these changes in xanthophore and iridophore development are sufficient to explain the loss of stripes in *D. albolineatus,* I expressed *csf1* similarly to *D. albolineatus* in *D. rerio*. Under these conditions, xanthophores and melanophores were intermingled, iridophore development was repressed and stripes were absent, as in *D. albolineatus*. These results suggest that changes in the timing of pigment cell differentiation can have downstream effects on pattern formation and likely contribute to evolutionary diversification in this group.

Acknowledgements

My deepest thanks to the many undergrads, graduate students, post doctoral fellows and research technicians who have helped with fish care over the years. This work wouldn't have been possible without you. Many thanks to Tiffany Gordon, Erine Budi, Sarah McMenamin, Emily Bain, Jessica Spiewak and Anna McCann, you all made the long days in the lab feel a little less like work. Thanks to all the faculty and grad students who have provided feedback on this work. Finally, thanks to Amazon Fresh for bringing groceries to my door on the weeks I couldn't find the time to get to the store.

I have a special appreciation for the following:

My supervisor for guidance and support, and especially for his patience with my many, many questions:
David Parichy

My committee for their personal and professional guidance:
David Raible, Billie Swalla, Leo Pallanck

My family for helping me to cultivate my sense of curiosity and for their steadfast support throughout this long journey:
Mom, Dad, Josh, Kristin
Aunt Kristen, Uncle David Ned
Grandma and Grandpa Patterson, Grandpa John

and

Mike, for helping me through the tough parts.

TABLE OF CONTENTS

LIST OF FIGURES

Introduction

Pigment patterns are one of the most striking and memorable traits of any animal. Pigment patterns are critical for survival and reproduction, serving important roles in crypsis and warning coloration, as well as promoting social interactions such as mate choice and shoaling preference [1-3]. Pigment patterns have long garnered the attention of both geneticists and mathematicians seeking to understand the mechanisms underlying pattern formation. Theoretical work by Alan Turing suggested stable patterns could be generated by the interactions of two diffusible molecules [4]. Later work showed Turing mechanisms do not require diffusion but instead can be produced through interactions involving local activation and long-range inhibition producing stable patterns [5, 6]. This opens the door to pattern generation through the activity of direct cell-cell interactions [7]. However, validating the biological relevance of these models has been somewhat hampered by the identification of molecules involved in generating them. In fact, the genetic basis for differences in pattern development has only been identified in a hand full of cases [8-15]. Additionally, it remains unclear how much pattern development relies upon positional cues provided by the environment or forms autonomously as is predicted by reaction-diffusion mechanisms.

Recent work in *Drosophila* and *Heliconius* butterflies, suggest patterns in these groups do not arise autonomously but instead require a developmental pre-pattern [10, 16]. Analysis of male-specific wing spot development in *Drosophila* present some of the most detailed and elegant studies of the developmental and evolutionary basis of pattern formation [8-10, 17]. Insects have no specialized pigment cells. Instead, pigment is secreted by epithelial cells and polymerized in the overlying cuticle [18, 19]. Melanin (black pigment) synthesis requires activity of the Yellow protein and at early pupal stages, patterns of yellow expression in the wing prefigure sites of

adult melanin distribution. *D. guttifera* males have 16 black spots located on wing veins and at their junctions with crossviens or the wing margin [10]. The evolution of *cis*-regulatory elements in the *yellow* locus makes its expression responsive to *wingless* [10]. An ancient ancestral pattern of *wingless* expression in the wing margins and crossveins, drives yellow expression in *D. guttifera* at sites of pigment spots [10]. This interaction was later co-opted again in the *D. guttifera* lineage by changes in *wingless* expression that increase its locations and therefore the sites of pigment spots [10]. In this case, a pre-pattern established by the ancestral expression pattern of a morphogen (*wingless*) provides positional information for later pigmentation. The development of wingspots in *Bicyclus* butterflies is also dependent upon morphogen sources [20, 21] and recent work identified evolutionary changes at the *Wnt5* locus as the source black pattern variation in mimetic Heliconius butterflies [16].

In vertebrates, pigment cells are derived from the neural crest. Birds and mammals have a single pigment cell type the melanocyte that can produce two pigments eumelanin or pheomelanin [22]. These pigments are transferred from the melanocyte to developing skin, feathers or hair [12, 23]. While a great deal is known about mammalian melanocyte morphogenesis and pigment type switching, little is know about how differences in these processes produce the myriad variation of patterns found in nature.

Recent work in domestic cats suggests pattern formation occurs through a two-step process of pre-pattern followed by pigmentation, similar to butterflies and *Drosophila* [12]. The membrane bound metalloprotease, Transmembrane aminopeptidase Q (Taqpep) is expressed in the skin during development and is responsible for variation in tabby markings [12]. Positional information established by Taqpep is later implemented by differential expression of Edn3 to

generate dark and light stripes [12]. This same connection between Taqpep and Edn3 is found in cheetahs and could serve as a more general mammalian pattern forming mechanism.

An autonomous pattern forming mechanism requires a single step process, in which pattern and pigmentation are linked. Only in fish, amphibians and reptiles, do pigment patterns reflect the precise spatial organization and interactions amongst the cells that produce them. In fish, unlike birds or mammals, pigment cells retain pigment granules intracellularly and are readily visible through the skin [24, 25]. Multiple pigment cell types, including black melanophores, yellow xanthophores, red erythrophores, iridescent iridophores and white leucophores, are organized during development to generate these stunning patterns, and differing complements and arrangements of these cells produce the diversity of teleost patterns [24, 25]. Thus far, pigment pattern development has been most extensively studied in the zebrafish, *Danio rerio*, making the genus *Danio*, which includes the zebrafish, a particularly attractive system for studying the molecular and cellular basis of pigment pattern development and evolution [26-29].

Zebrafish develop two distinct pigment patterns during their lifetime. Embryonic pigment cells, originating directly from the neural crest, produce the first of these patterns, which consists of melanophore stripes along the horizontal myoseptum and the dorsal and ventral edges of the myotomes, xanthophores scattered across the flank and iridophores associated with melanophores in the stripes [30-33]. The adult pattern begins to develop at about two weeks post fertilization. At this time, new pigment cells differentiate from post-embryonic latent precursors and over the next two weeks these cells organize to produce the juvenile pattern, which consists of two primary melanophore stripes on either side of primary interstripe consisting of xanthophores and iridophores [34-37]. Additional stripes and interstripes are added as the fish grows and in the adult, iridophores are also found within melanophores stripes [38].

Several lines of evidence suggest interactions between melanophores and xanthophores are critical for adult stripe formation [39-41]. Xanthophores express the receptor tyrosine kinase, Colony stimulating factor-1 receptor (Csf1r), which is required cell autonomously for differentiation, survival and migration [40, 42]. Zebrafish *csf1r* mutants do not develop xanthophores and have disorganized melanophore stripes, but stripes can be rescued when xanthophores are transplanted into *csf1r* mutants [39, 40]. Additional studies have provided support for both short range repulsive and long range activating interactions between melanophores and xanthophores, consistent with zebrafish stripes being generated by a self organizing "Turing mechanism" involving local activation and long range inhibition [7, 41, 43, 44]. Recently, it was shown long range positive effects of xanthophores on melanophore survival are mediated through delta-notch signaling [45]. Initially, it seems surprising that membrane-bound receptor-ligand pairs could act as a long rang signal, but Hamada *et al*, showed that pigment cells extend long projections making it possible for direct cell-cell interactions to be interpreted as long range, further supporting the hypothesis of pattern formation in zebrafish occurring through a Turing mechanism [45].

Nearly all zebrafish mutants with adult pattern defects have been mapped to genes expressed by one or more pigment cell lineages [42, 46-52], supporting the model that stripe formation occurs autonomously through interactions amongst those cells types. However, the role of iridophores in these interactions has been largely unexplored. Additionally, analysis of the *basonuclin-2* (*bnc2*) mutant, argues for an environmental component of pattern formation [53]. *basonuclin-2* mutants have severely disrupted adult patterns with fewer melanophores, xanthophores and iridophores. Genetic mosaic analysis revealed that *bnc2* acts non-autonomously to melanophore lineage during pattern development and consistent with this,

bnc2+ cells are abundant in the hypodermis, where pigment cells reside [53]. A potential role for the environment in pattern formation suggests the possibility of pre-patterns providing positional information to pigment cell during development.

The insights gained from studies of zebrafish stripe develop suggest possible mechanisms through which pattern diversity could have evolved. In fact, many zebrafish mutants develop patterns that are remarkably similar to patterns found in other species [26]. Patterns within the danios range from stripe and spot to vertical bars to nearly uniform distributions of pigment cells. The accessibility of zebrafish and other danios to genetic and cellular manipulation allow one to pose and test hypotheses for the evolution of pattern-forming mechanisms. Previous comparisons of pigment pattern development between *D. rerio* and other *Danio* species suggest that adult pattern variation results from differences in the numbers and arrangements of post-embryonic precursor derived pigment cells [27, 28, 34, 35]. *D. albolineatus* develops an evolutionarily derived pattern of intermingled melanophores and xanthophores that is dramatically different from the strict boundaries between xanthophore interstripes and melanophores stripes in *D. rerio* [26, 27, 29]. *D. albolineatus* retains latent stripe forming capabilities, as the few melanophores that appear in *D. albolineatus kit* mutants develop along the residual interstripe similar to *kit* mutant *D. rerio* [29]. It has been hypothesized that evolutionary differences in these patterns result from changes in melanophore–xanthophore interactions [27].

In my first chapter, I identify roles for both iridophores and the environment in zebrafish adult stripe formation. I found that *bnc2* mutants have reduced expression of Csf1r ligands and the ligand for the Kit receptor tyrosine kinase, Kitlga, which is required for melanophore survival, migration and differentiation [52, 54]. Although restoring Csf1 and Kitlga in *bnc2*

mutants rescued melanophore and xanthophore survival, these cells failed to organize into a normal striped pattern, indicating a requirement for additional factors or cell types. I found that in *D. rerio,* iridophores are the first pigment cell type to develop during adult stripe formation and that they do so precisely at the location of the first interstripe. By ablating iridophores in wild-type and mutants I found that iridophores play a critical role in organizing both xanthophores and melanophores into stripes. Iridophores express *csf1* and this localized Csf1 expression is sufficient to direct localized xanthophore development. Previous models of zebrafish stripe development included only melanophore and xanthophore interactions. This work adds new levels to these models by demonstrating that environmental factors are required to support pigment cells during pattern formation and that adult iridophores define a critical positional cue that the other pigment cells use to form stripes.

In my second chapter, I investigate the loss of stripes in *D. albolineatus*. I show that melanophore stripe termination in *D. rerio* requires iridophore development in secondary interstripes, that these cells are missing in *D. albolineatus* and that by ablating them in *D*. rerio, melanophores are more dispersed similar to *D. albolineatus*. I demonstrate that *D. albolineatus* develops xanthophores earlier and over a wider area than *D. rerio*, and this difference is associated with similarly early and widespread expression of Csf1, owing at least in part to an interspecific difference in the *csf1a* cis-regulatory region. Finally, I show that expressing *csf1a* similarly to *D. albolineatus* in *D. rerio*, results in melanophore and xanthophore intermingling and a loss of stripes, similar to *D. albolineatus*. Together my analyses identified evolutionary changes in the development of two pigment cell types that contribute to the loss of stripes in *D. albolineatus*. These results suggest that changes in the timing of pigment cell differentiation can

have downstream effects on pattern formation and likely contribute to evolutionary diversification in this group.

References

1. Engeszer, R.E., Ryan, M.J., and Parichy, D.M. (2004). Learned social preference in zebrafish. Current biology : CB *14*, 881-884.
2. Engeszer, R.E., Wang, G., Ryan, M.J., and Parichy, D.M. (2008). Sex-specific perceptual spaces for a vertebrate basal social aggregative behavior. Proceedings of the National Academy of Sciences of the United States of America *105*, 929-933.
3. Price, A.C., Weadick, C.J., Shim, J., and Rodd, F.H. (2008). Pigments, patterns, and fish behavior. Zebrafish *5*, 297-307.
4. Turing, A.M. (1952). The chemical basis of morphogenesis. Philosophical Transactions of the Royal Society of London. Series B, Biological Sciences *237*, 37–72.
5. Meinhardt, H., and Gierer, A. (1974). Applications of a theory of biological pattern formation based on lateral inhibition. Journal of cell science *15*, 321-346.
6. Meinhardt, H., and Gierer, A. (2000). Pattern formation by local self-activation and lateral inhibition. BioEssays : news and reviews in molecular, cellular and developmental biology *22*, 753-760.
7. Kondo, S., and Miura, T. (2010). Reaction-diffusion model as a framework for understanding biological pattern formation. Science *329*, 1616-1620.
8. Gompel, N., Prud'homme, B., Wittkopp, P.J., Kassner, V.A., and Carroll, S.B. (2005). Chance caught on the wing: cis-regulatory evolution and the origin of pigment patterns in Drosophila. Nature *433*, 481-487.
9. Prud'homme, B., Gompel, N., Rokas, A., Kassner, V.A., Williams, T.M., Yeh, S.D., True, J.R., and Carroll, S.B. (2006). Repeated morphological evolution through cis-regulatory changes in a pleiotropic gene. Nature *440*, 1050-1053.
10. Werner, T., Koshikawa, S., Williams, T.M., and Carroll, S.B. (2010). Generation of a novel wing colour pattern by the Wingless morphogen. Nature *464*, 1143-1148.
11. Reed, R.D., Papa, R., Martin, A., Hines, H.M., Counterman, B.A., Pardo-Diaz, C., Jiggins, C.D., Chamberlain, N.L., Kronforst, M.R., Chen, R., et al. (2011). optix drives the repeated convergent evolution of butterfly wing pattern mimicry. Science *333*, 1137-1141.
12. Kaelin, C.B., Xu, X., Hong, L.Z., David, V.A., McGowan, K.A., Schmidt-Kuntzel, A., Roelke, M.E., Pino, J., Pontius, J., Cooper, G.M., et al. (2012). Specifying and sustaining pigmentation patterns in domestic and wild cats. Science *337*, 1536-1541.
13. Roberts, R.B., Ser, J.R., and Kocher, T.D. (2009). Sexual conflict resolved by invasion of a novel sex determiner in Lake Malawi cichlid fishes. Science *326*, 998-1001.
14. Manceau, M., Domingues, V.S., Mallarino, R., and Hoekstra, H.E. (2011). The developmental role of Agouti in color pattern evolution. Science *331*, 1062-1065.
15. Miller, C.T., Beleza, S., Pollen, A.A., Schluter, D., Kittles, R.A., Shriver, M.D., and Kingsley, D.M. (2007). cis-Regulatory changes in Kit ligand expression and parallel evolution of pigmentation in sticklebacks and humans. Cell *131*, 1179-1189.
16. Martin, A., Papa, R., Nadeau, N.J., Hill, R.I., Counterman, B.A., Halder, G., Jiggins, C.D., Kronforst, M.R., Long, A.D., McMillan, W.O., et al. (2012). Diversification of complex butterfly wing patterns by repeated regulatory evolution of a Wnt ligand. Proceedings of the National Academy of Sciences of the United States of America *109*, 12632-12637.

17. Rogers, W.A., Salomone, J.R., Tacy, D.J., Camino, E.M., Davis, K.A., Rebeiz, M., and Williams, T.M. (2013). Recurrent modification of a conserved cis-regulatory element underlies fruit fly pigmentation diversity. PLoS genetics *9*, e1003740.
18. Wittkopp, P.J., and Beldade, P. (2009). Development and evolution of insect pigmentation: genetic mechanisms and the potential consequences of pleiotropy. Seminars in cell & developmental biology *20*, 65-71.
19. Kronforst, M.R., Barsh, G.S., Kopp, A., Mallet, J., Monteiro, A., Mullen, S.P., Protas, M., Rosenblum, E.B., Schneider, C.J., and Hoekstra, H.E. (2012). Unraveling the thread of nature's tapestry: the genetics of diversity and convergence in animal pigmentation. Pigment cell & melanoma research *25*, 411-433.
20. Brunetti, C.R., Selegue, J.E., Monteiro, A., French, V., Brakefield, P.M., and Carroll, S.B. (2001). The generation and diversification of butterfly eyespot color patterns. Current biology : CB *11*, 1578-1585.
21. Monteiro, A., Glaser, G., Stockslager, S., Glansdorp, N., and Ramos, D. (2006). Comparative insights into questions of lepidopteran wing pattern homology. BMC developmental biology *6*, 52.
22. Barsh, G.S. (2006). Regulation of Pigment Type Switching by Agouti, Melanocortin Signaling, Attractin, and Mahoganoid. In The Pigmentary System: Physiology and Pathophysiology, Second Edition, R.E.B. J. J. Nordlund, V. J. Hearing, R. A. King, W. S. Oetting and J.-P. Ortonne, ed. (Oxford, UK: Blackwell Publishing Ltd).
23. Lin, S.J., Foley, J., Jiang, T.X., Yeh, C.Y., Wu, P., Foley, A., Yen, C.M., Huang, Y.C., Cheng, H.C., Chen, C.F., et al. (2013). Topology of feather melanocyte progenitor niche allows complex pigment patterns to emerge. Science *340*, 1442-1445.
24. Bagnara, J.T.M., J. (2006). Comparative Anatomy and Physiology of Pigment Cells in Nonmammalian Tissues. In The Pigmentary System: Physiology and Pathophysiology, Second Edition, J.J.N.R.E.B.V.J.H.R.A.K.W.S.O.a.J.-P. Ortonne, ed. (Oxford, UK: Blackwell Publishing Ltd).
25. Parichy, D.M., Reedy, M. V. and Erickson, C. A. (2006). Regulation of Melanoblast Migration and Differentiation. In The Pigmentary System: Physiology and Pathophysiology, Second Edition, R.E.B. J. J. Nordlund, V. J. Hearing, R. A. King, W. S. Oetting and J.-P. Ortonne, ed. (Oxford, UK: Blackwell Publishing Ltd).
26. Parichy, D.M., and Johnson, S.L. (2001). Zebrafish hybrids suggest genetic mechanisms for pigment pattern diversification in Danio. Development genes and evolution *211*, 319-328.
27. Quigley, I.K., Manuel, J.L., Roberts, R.A., Nuckels, R.J., Herrington, E.R., MacDonald, E.L., and Parichy, D.M. (2005). Evolutionary diversification of pigment pattern in Danio fishes: differential fms dependence and stripe loss in D. albolineatus. Development *132*, 89-104.
28. Quigley, I.K., Turner, J.M., Nuckels, R.J., Manuel, J.L., Budi, E.H., MacDonald, E.L., and Parichy, D.M. (2004). Pigment pattern evolution by differential deployment of neural crest and post-embryonic melanophore lineages in Danio fishes. Development *131*, 6053-6069.
29. Mills, M.G., Nuckels, R.J., and Parichy, D.M. (2007). Deconstructing evolution of adult phenotypes: genetic analyses of kit reveal homology and evolutionary novelty during adult pigment pattern development of Danio fishes. Development *134*, 1081-1090.

30. Curran, K., Lister, J.A., Kunkel, G.R., Prendergast, A., Parichy, D.M., and Raible, D.W. (2010). Interplay between Foxd3 and Mitf regulates cell fate plasticity in the zebrafish neural crest. Developmental biology *344*, 107-118.
31. Dutton, K.A., Pauliny, A., Lopes, S.S., Elworthy, S., Carney, T.J., Rauch, J., Geisler, R., Haffter, P., and Kelsh, R.N. (2001). Zebrafish colourless encodes sox10 and specifies non-ectomesenchymal neural crest fates. Development *128*, 4113-4125.
32. Kelsh, R.N., Schmid, B., and Eisen, J.S. (2000). Genetic analysis of melanophore development in zebrafish embryos. Developmental biology *225*, 277-293.
33. Raible, D.W., and Eisen, J.S. (1994). Restriction of neural crest cell fate in the trunk of the embryonic zebrafish. Development *120*, 495-503.
34. Budi, E.H., Patterson, L.B., and Parichy, D.M. (2011). Post-embryonic nerve-associated precursors to adult pigment cells: genetic requirements and dynamics of morphogenesis and differentiation. PLoS genetics *7*, e1002044.
35. Dooley, C.M., Mongera, A., Walderich, B., and Nusslein-Volhard, C. (2013). On the embryonic origin of adult melanophores: the role of ErbB and Kit signalling in establishing melanophore stem cells in zebrafish. Development *140*, 1003-1013.
36. Parichy, D.M., and Turner, J.M. (2003). Zebrafish puma mutant decouples pigment pattern and somatic metamorphosis. Developmental biology *256*, 242-257.
37. Johnson, S.L., Africa, D., Walker, C., and Weston, J.A. (1995). Genetic control of adult pigment stripe development in zebrafish. Developmental biology *167*, 27-33.
38. Hirata, M., Nakamura, K., Kanemaru, T., Shibata, Y., and Kondo, S. (2003). Pigment cell organization in the hypodermis of zebrafish. Developmental dynamics : an official publication of the American Association of Anatomists *227*, 497-503.
39. Maderspacher, F., and Nusslein-Volhard, C. (2003). Formation of the adult pigment pattern in zebrafish requires leopard and obelix dependent cell interactions. Development *130*, 3447-3457.
40. Parichy, D.M., and Turner, J.M. (2003). Temporal and cellular requirements for Fms signaling during zebrafish adult pigment pattern development. Development *130*, 817-833.
41. Yamaguchi, M., Yoshimoto, E., and Kondo, S. (2007). Pattern regulation in the stripe of zebrafish suggests an underlying dynamic and autonomous mechanism. Proceedings of the National Academy of Sciences of the United States of America *104*, 4790-4793.
42. Parichy, D.M., Ransom, D.G., Paw, B., Zon, L.I., and Johnson, S.L. (2000). An orthologue of the kit-related gene fms is required for development of neural crest-derived xanthophores and a subpopulation of adult melanocytes in the zebrafish, Danio rerio. Development *127*, 3031-3044.
43. Nakamasu, A., Takahashi, G., Kanbe, A., and Kondo, S. (2009). Interactions between zebrafish pigment cells responsible for the generation of Turing patterns. Proceedings of the National Academy of Sciences of the United States of America *106*, 8429-8434.
44. Takahashi, G., and Kondo, S. (2008). Melanophores in the stripes of adult zebrafish do not have the nature to gather, but disperse when they have the space to move. Pigment cell & melanoma research *21*, 677-686.
45. Hamada, H., Watanabe, M., Lau, H.E., Nishida, T., Hasegawa, T., Parichy, D.M., and Kondo, S. (2013). Involvement of Delta/Notch signaling in zebrafish adult pigment stripe patterning. Development.

46. Eom, D.S., Inoue, S., Patterson, L.B., Gordon, T.N., Slingwine, R., Kondo, S., Watanabe, M., and Parichy, D.M. (2012). Melanophore migration and survival during zebrafish adult pigment stripe development require the immunoglobulin superfamily adhesion molecule Igsf11. PLoS genetics *8*, e1002899.
47. Inaba, M., Yamanaka, H., and Kondo, S. (2012). Pigment pattern formation by contact-dependent depolarization. Science *335*, 677.
48. Lopes, S.S., Yang, X., Muller, J., Carney, T.J., McAdow, A.R., Rauch, G.J., Jacoby, A.S., Hurst, L.D., Delfino-Machin, M., Haffter, P., et al. (2008). Leukocyte tyrosine kinase functions in pigment cell development. PLoS genetics *4*, e1000026.
49. Parichy, D.M., Mellgren, E.M., Rawls, J.F., Lopes, S.S., Kelsh, R.N., and Johnson, S.L. (2000). Mutational analysis of endothelin receptor b1 (rose) during neural crest and pigment pattern development in the zebrafish Danio rerio. Developmental biology *227*, 294-306.
50. Watanabe, M., Iwashita, M., Ishii, M., Kurachi, Y., Kawakami, A., Kondo, S., and Okada, N. (2006). Spot pattern of leopard Danio is caused by mutation in the zebrafish connexin41.8 gene. EMBO reports *7*, 893-897.
51. Lister, J.A., Robertson, C.P., Lepage, T., Johnson, S.L., and Raible, D.W. (1999). nacre encodes a zebrafish microphthalmia-related protein that regulates neural-crest-derived pigment cell fate. Development *126*, 3757-3767.
52. Parichy, D.M., Rawls, J.F., Pratt, S.J., Whitfield, T.T., and Johnson, S.L. (1999). Zebrafish sparse corresponds to an orthologue of c-kit and is required for the morphogenesis of a subpopulation of melanocytes, but is not essential for hematopoiesis or primordial germ cell development. Development *126*, 3425-3436.
53. Lang, M.R., Patterson, L.B., Gordon, T.N., Johnson, S.L., and Parichy, D.M. (2009). Basonuclin-2 requirements for zebrafish adult pigment pattern development and female fertility. PLoS genetics *5*, e1000744.
54. Hultman, K.A., Budi, E.H., Teasley, D.C., Gottlieb, A.Y., Parichy, D.M., and Johnson, S.L. (2009). Defects in ErbB-dependent establishment of adult melanocyte stem cells reveal independent origins for embryonic and regeneration melanocytes. PLoS genetics *5*, e1000544.

Chapter 1

INTERACTIONS WITH IRIDOPHORES AND THE TISSUE ENVIRONMENT REQUIRED FOR PATTERNING MELANOPHORES AND XANTHOPHORES DURING ZEBRAFISH ADULT PIGMENT STRIPE FORMATION

1.1 Abstract

Skin pigment patterns of vertebrates are a classic system for understanding fundamental mechanisms of morphogenesis, differentiation and pattern formation, and recent studies of zebrafish have started to elucidate the cellular interactions and molecular mechanisms underlying these processes. In this species, horizontal dark stripes of melanophores alternate with light interstripes of yellow or orange xanthophores and iridescent iridophores. We showed previously that the highly conserved zinc finger protein Basonuclin-2 (Bnc2) is required in the environment in which pigment cells reside to promote the development and maintenance of all three classes of pigment cells; *bnc2* mutants lack body stripes and interstripes. Previous studies also revealed that interactions between melanophores and xanthophores are necessary for organizing stripes and interstripes. Here we show that *bnc2* promotes melanophore and xanthophore development by regulating expression of the growth factors Kit ligand a (Kitlga) and Colony stimulating factor-1 (Csf1), respectively. Yet, we found that rescue of melanophores and xanthophores was insufficient for the recovery of stripes in the *bnc2* mutant. We therefore asked whether *bnc2*-dependent iridophores might contribute to stripe and interstripe patterning as well. We found that iridophores themselves express Csf1, and by ablating iridophores in wild-type and mutant backgrounds, we showed that iridophores contribute to organizing both melanophores and xanthophores during the development of stripes and interstripes. Our results reveal an important role for the cellular environmental in promoting adult pigment pattern formation and identify

new components of a pigment-cell autonomous pattern-generating system likely to have broad implications for our understanding of how pigment patterns develop and evolve.

1.2 Introduction

The pigment patterns of teleost fishes are extraordinarily diverse and have important functions in mate choice, shoaling and predation avoidance [1-4]. These patterns result from the spatial arrangements of several classes of pigment cells including black melanophores that contain melanin, yellow or orange xanthophores with pteridines and carotenoids, and iridescent iridophores having purine-rich reflecting platelets [5-7]. In recent years, mechanisms underlying pigment pattern development, as well as pattern diversification among species, have started to be elucidated. Much of this work has used the zebrafish *Danio rerio* or its relatives [5,8].

In zebrafish, two distinct patterns develop over the life cycle. The first of these arises in embryos and persists through early larval stages [9-14]. Pigment cells of this early larval pattern develop directly from neural crest cells and generate stripes of melanophores at the edges of the myotomes and at the horizontal myoseptum; a few iridophores occur within these stripes whereas xanthophores are scattered widely over the body. The second, adult pigment pattern begins to develop during the larval-to-adult transformation and largely replaces the early larval pigment pattern [15]. Most cells comprising the adult pigment pattern differentiate from post-embryonic latent precursors, with the best studied of these cells, the melanophores, differentiating primarily between ~2–4 weeks post-fertilization [16-19]. By the end of this period a juvenile pigment pattern has developed consisting of two dark stripes of melanophores bordering a light interstripe of xanthophores and iridophores. As the fish grows, stripes and interstripes are added dorsally and ventrally; additional, ultrastructurally distinct iridophores also

develop late within the melanophore stripes [20]. Cells comprising the body stripes and interstripes are found within the hypodermis [20,21], between the epidermis and the myotome; pigment cells are also found in the scales, fins, and epidermis.

Previous studies showed that development of adult stripes and interstripes requires interactions between different pigment cell classes. For example, *colony stimulating factor 1 receptor* (*csf1r*) encodes a receptor tyrosine kinase required for xanthophore survival and migration [22]; *csf1r* mutants are deficient in xanthophores and also have disorganized melanophores. Yet stripes and interstripes could be restored in these fish by reintroducing xanthophores, either through cell transplantation or in the context of temperature-shift experiments using a temperature-sensitive *csf1r* allele [23,24]. These experiments suggested that xanthophores are required to organize melanophores into stripes. Subsequent studies identified additional short-range and long-range interactions between these cell types [25-27], the dynamics of which are consistent with an underlying Turing process [28,29].

The environment in which pigment cells reside also influences their development and patterning. Such effects are illustrated dramatically by mutants for *basonuclin-2* (*bnc2*) [30], which encodes a highly conserved zinc finger protein that may function as a transcription factor or in RNA processing [31-35]. In contrast to the wild-type, *bnc2* mutants exhibit far fewer hypodermal melanophores, xanthophores and iridophores and, consequently, lack body stripes and interstripes, though an apparently normal pigment pattern persists in the fins and in the scales (Figure 1B). During the larval-to-adult transformation of *bnc2* mutants, differentiated pigment cells of all three classes die at high frequency. Nevertheless, precursors of melanophores and xanthophores are abundant and widespread, suggesting late defects in their survival, terminal differentiation, or both. By contrast, iridophore precursors are markedly fewer, raising the

possibility of additional defects in the earlier specification of this lineage. Genetic mosaic analyses showed that *bnc2* acts non-autonomously to the melanophore lineage and likely the other pigment cell classes as well. Consistent with this interpretation, *bnc2*+ cells are initially found along horizontal and vertical myosepta but are later widely dispersed, both in the hypodermis and epidermis, a distribution resembling that of fibromodulin-expressing fibroblasts (LP and DP, unpublished data) but distinct from that of pigment cells and their precursors.

Here, we investigated the mechanisms by which *bnc2* supports pigment cell development and the subsequent interactions between pigment cells during pigment pattern formation. We found that *bnc2* mutants have reduced expression of Csf1r ligands and the ligand of the Kit receptor tyrosine kinase, Kitlga, which is required for the migration, survival and differentiation of teleost melanophores as well as mammalian melanocytes [9,36-41]. Although restoring Csf1 and Kitlga in *bnc2* mutants was sufficient to restore xanthophores and melanophores, these cells failed to organize into a normal striped pattern, indicating a requirement for additional factors or cell types. Because iridophores are deficient in *bnc2* mutants, we asked whether these cells might normally contribute to the formation of stripes and interstripes. We found that iridophores are the first adult pigment cells to develop, that they express Csf1, and that xanthophores localize in association with them. To test if iridophores contribute to pattern development, we ablated these cells in wild-type and mutant larvae, resulting in perturbations to stripes and interstripes and confirming roles for iridophores in stripe and interstripe development. Together, our analyses suggest a model in which *bnc2* supports the development and survival of melanophores, xanthophores and iridophores, and allows for subsequent interactions involving all three cell types. These results extend our understanding of environmental influences on pattern formation as well as pigment-cell autonomous patterning mechanisms.

1.3 Results

1.3.1 *bnc2*-dependent expression of Kitlga and Csf1 promotes melanophore and xanthophore development yet is insufficient for normal stripe patterning

The death of melanophores and xanthophores in *bnc2* mutants resembles the death of melanophores in mutants for *kita*, encoding a zebrafish Kit orthologue [38], and the death of xanthophores in *csf1r* mutants [24]. As *kita* and *csf1r* act autonomously to melanophore and xanthophore lineages [24,38], respectively, whereas *bnc2* acts non-autonomously [30], we speculated that *bnc2* might contribute to the development and maintenance of melanophores and xanthophores by promoting expression of the receptor ligands, Kitlga and Csf1. Consistent with this idea, quantitative RT-PCR of isolated body skins (with attached pigment cells) revealed significantly reduced expression of *kitlga*, as well as the two Csf1-encoding loci, *csf1a* and *csf1b*, in *bnc2* mutants compared to the wild-type (Figure 1C). Quantitative RT-PCR comparisons of fins, in which melanophores and xanthophores persist in *bnc2* mutants, failed to reveal differences in *kitlga*, *csf1a* or *csf1b* expression compared to the wild-type (all $P>0.5$).

If *bnc2* acts through Kitlga and Csf1 to promote the development and survival of melanophores and xanthophores on the body, then restoring the expression of these ligands in the *bnc2* mutant should restore these cells and possibly a striped pattern. To test this idea, we generated transgenic lines using the ubiquitous, heat-shock inducible promoter of *hsp70l* to express Kitlga, Csf1a, or Csf1b individually, as well as Kitlga simultaneously with either Csf1a or Csf1b.

Restoration of Kitlga expression partially rescued melanophores in *bnc2* mutants but did not restore stripes (Figure 2A); this outcome was not unexpected given requirements for interactions between melanophores and xanthophores and the continued deficiency of the latter [23,24,26].

Restoration of Csf1a rescued xanthophores, and also increased melanophore numbers (Figure 2B). Despite the abundance of both cell types, normal stripe patterns again failed to develop, with melanophores and xanthophores ranging widely over the flank (Figure 2B). Similar outcomes were observed upon expressing Kitlga simultaneously with either Csf1a or Csf1b (Figure 2C), for Csf1b alone, and in genetic mosaics combining cells from Kitlga and Csf1a transgenic embryos (data not shown). Together, these findings support the idea that *bnc2*-dependent expression of Kitlga, Csf1a and Csf1b promotes the development and survival of hypodermal body melanophores and xanthophores, yet the presence of these cell types alone is insufficient for organizing a normal pattern of body stripes and interstripes.

1.3.2 *bnc2*-dependent iridophores differentiate before melanophores and xanthophores and mark the prospective interstripe

The failure to recover a normal pigment pattern in *bnc2* mutants suggested that *bnc2* might contribute to interstripe and stripe development through another factor or cell type. We reasoned that such a role could be fulfilled by iridophores, which are dramatically fewer in *bnc2* mutants [30]. Consistent with this idea, residual xanthophores in the weak interstripe of *bnc2* mutants were found almost exclusively within patches of residual iridophores (compare images of xanthophore and iridophores between wild-type and *bnc2* mutant controls in Figure 2B).

If iridophores contribute to patterning interstripe and stripe development, these cells should develop prior to xanthophores and melanophores. We confirmed this by repeated imaging of wild-type and *bnc2* mutant larvae, which showed that iridophores are the first adult pigment cell type to develop during the larval-to-adult transformation (Figure 3). Iridophores developed as early as 4.5 mm standardized standard length (SSL) [42] and were restricted initially to the prospective interstripe region anteriorly, then developed in progressively more posterior regions.

In contrast, the first melanophores and xanthophores differentiated later at ~6.0 SSL and ~6.5 SSL, respectively. In *bnc2* mutants, xanthophore development was significantly delayed ($F_{1,5}$=383.8, P<0.001), typically occurring at ~7.5 SSL. The time and place of iridophore development relative to xanthophores and melanophores make these cells good candidates for contributing to interstripe location and orientation, and potentially later stripe patterning and maintenance.

1.3.3 Iridophores express Csf1

Given the dependence of Csf1 expression (Figure 1) and iridophore development on *bnc2* (Figure 3) [30], and the requirement of xanthophores for signaling through Csf1r [22,24], we hypothesized that iridophores supply a localized source of Csf1 to promote xanthophore development in the interstripe. We confirmed that *csf1r* is expressed by xanthophores during the larval-to-adult transformation using a transgenic reporter line (Figure S1)[43]. To test if iridophores express *csf1a* and *csf1b*, we first used RT-PCR, which detected transcripts for both loci in iridophores isolated individually (Figure 4A). By in situ hybridization, we found *csf1a* transcripts in hypodermal cells including cells likely to be iridophores according to their positions before and after in situ hybridization, and their locations at the base of the caudal fin and along the horizontal myoseptum, where iridophores develop (Figure 4B, 4C, 4D). In cross-sections, *csf1a* transcript was detectable in the hypodermis where iridophores are found, as revealed by expression of the iridophore marker, *purine nucleoside phosphorylase 4a* (*pnp4a*) [11,30] (Figure 4E, 4F). In contrast to wild-type larvae, far fewer cells stained for *pnp4a* and *csf1a* in the prospective interstripe region of *bnc2* mutants. To further test the correspondence of *csf1a* expression and iridophores we examined the iridophore-free mutant of *leucocyte tyrosine kinase* (*ltk*), which is expressed by iridophores and required for their development [44]. *ltk*

mutants lacked *csf1a* expression where iridophores are found normally in wild-type larvae (Figure 4G, 4G'). We also observed strong, iridophore-independent expression of *csf1a* in fins of wild-type and *ltk* mutants (Figure 4H, 4H'). *csf1b* was expressed similarly to *csf1a* by in situ hybridization and was also detectable in a population of dorsal hypodermal cells in both wild-type and *bnc2* mutants. Together, these analyses indicate that iridophores express Csf1, and do so at a time and place that marks the prospective interstripe, though additional cell types express these ligands as well.

1.3.4 Iridophores influence the localization of xanthophores and melanophores during interstripe and stripe development

To test whether iridophores contribute to specifying the location of interstripe xanthophores, we sought to ablate iridophores specifically and autonomously. To this end, we isolated a 3.2 kb fragment upstream of the *pnp4a* transcriptional start site that drives iridophore-specific transgene expression (Figure 5A). We used this element to express bacterial nitroreductase (NTR) which converts metronidazole (Mtz) into toxic metabolites that kill cells without bystander effects, even amongst cells that are coupled gap-junctionally [45-49]. We injected embryos with this *pnp4a*:NTR construct at the one-cell stage and then treated these genetically mosaic larvae with Mtz at stages when adult iridophores develop in the prospective interstripe. Iridophores were lost over several days and reflecting-platelet containing fragments were identified in typical "extrusion bodies" [30,38,39] at the surface of the epidermis (Figure 5B, 5C, 5D). In contrast to transient, F0-injected transgenic larvae, it was not possible to ablate iridophores in stable *pnp4a*:NTR lines, presumably because of reduced transgene copy numbers. Thus, all subsequent analyses used genetically mosaic F0 larvae with repeated Mtz treatments.

Ablation of interstripe iridophores prior to xanthophore development resulted in fewer xanthophores in regions from which iridophores were lost (Figure 6A–C), although both iridophores and xanthophores were recovered gradually during later development (data not shown). Because interactions between xanthophores and melanophores contribute to organizing melanophore stripes, we anticipated that iridophore ablation and delayed xanthophore development could perturb melanophore patterning as well. Consistent with this prediction, we observed more melanophores in interstripe regions where iridophores (and xanthophores) had been depleted; nevertheless, melanophores occupying these regions were frequently found adjacent to residual or regenerated iridophores (Figure 6D, 6E, 6F).

1.3.5 Localized expression of Csf1 promotes regionally specific xanthophore development

If Csf1 expressed by iridophores provides a spatial cue for xanthophores, we reasoned that ectopic expression of Csf1 should result in ectopic xanthophore development. To test this possibility we transplanted cells at the blastula stage from *bnc2* mutant embryos transgenic for *hsp70l*:csf1a to *bnc2*/+ or *bnc2* hosts and then induced mosaic expression of Csf1a by heat shock. We additionally expressed Csf1a in a temporally controlled manner within the myotome adjacent to the hypodermis: we identified a 2.2 kb region upstream of *slow myosin heavy chain 1* (*smyhc1*) that drives expression in superficial slow muscle fibers and used this in a TetA-GBD [50] transgene to express Csf1a in these cells specifically during the larval-to-adult transformation. Using both paradigms to induce Csf1a outside of the developing interstripe, we observed corresponding patches of ectopic xanthophores in both *bnc2*/+ and *bnc2* mutant siblings (Figure 7). These findings, and analyses of *csf1a* and *csf1b* expression, support a model in which interstripe iridophores provide a localized source of these ligands that contributes to specifying the position of interstripe xanthophores.

1.3.6 Iridophores influence melanophore patterning independently of xanthophores

Because xanthophores contribute to melanophore stripe organization [23,24,26], the mis-patterning of melanophores following iridophore ablation could simply reflect perturbations to the distribution of xanthophores. Yet, iridophores also might influence melanophores independently of xanthophores. To test this possibility, we ablated iridophores in *csf1r* mutant larvae. These mutants exhibit a few very lightly pigmented xanthophores limited to the immediate vicinity of the horizontal myoseptum but lack xanthophores in the more ventral interstripe region and elsewhere (Figure S2A, S2B) [22,23,51]. Although stripes in *csf1r* mutants are disorganized and melanophores initially differentiate more widely over the flank than in wild-type larvae [22], quantitative analyses of final melanophore distributions in unmanipulated *csf1r* mutants revealed a residual stripe pattern in which melanophores tended to be dorsal or ventral to where the interstripe would form normally (Figure 8A, 8C, 8E). At later stages, melanophores tended to be situated close to, but not directly over, iridophores, and iridophores were more widely distributed than in the wild-type (Figure S2C). In *csf1r* mutants in which iridophores had been ablated, however, melanophores were more likely to occur in the middle of the flank where iridophores had been lost (Figure 8B, 8D, 8E). Repeated imaging of individual larvae showed that melanophores both migrated to, and differentiated in, regions where iridophores had been ablated; once in these regions, melanophores often settled adjacent to residual iridophores (Figure 8F, 8G, 8J). Together, these observations suggest that iridophores can influence melanophore patterning independently of interactions between xanthophores and melanophores. Although *kitlga* is a good candidate for contributing to an interaction between iridophores and melanophores, RT-PCR did not reveal *kitlga* expression by iridophores and kitlga transcripts were not detectable by in situ hybridization (data not shown).

1.3.7 Melanophore and xanthophore patterning are defective in additional iridophore-deficient mutant backgrounds

To further test inferences from cell ablation studies, we examined melanophore and xanthophore patterning in additional mutant backgrounds, *ltk*, described above, and *endothelin receptor b1a* (*ednrb1a*). *ltk* mutants lack iridophores and repeated imaging of individual larvae revealed increased frequencies of melanophore death, as well as delays in xanthophore differentiation by an average of 6±1 d (paired t=6, P<0.05) as compared to stage-matched wild-type siblings (Figure 9A). When xanthophores did develop they did so widely over the flank, rather than being restricted to the interstripe region (Figure 9B).

ednrb1a is expressed in precursors to all three pigment cell classes and is maintained at high levels in iridophores [52]. *ednrb1a* mutants exhibit severely reduced numbers of iridophores (Figure 9D). Although adults exhibit a dorsal melanophore stripe and ventral melanophore spots, examination of pattern development in daily image series showed that ventral spots arise further ventrally than the normal location of the ventral stripe, being localized instead to the site of the second ventral interstripe (Figure 9C). Together these observations indicate that melanophore and xanthophore patterning are disrupted in two additional iridophore-deficient mutants, consistent with roles for iridophores in promoting normal stripe and interstripe development.

1.4 Discussion

Our analyses together with previous studies suggest a model for adult body stripe and interstripe development in zebrafish (Figure 10). At the onset of adult pigment pattern formation, iridophores begin to differentiate in the prospective interstripe region and the expansion of this population depends on *bnc2*. Melanophores and xanthophores then start to differentiate,

supported by *bnc2*-dependent Kitlga and Csf1, respectively. Melanophores avoid settling in the interstripe region in part owing to short-range inhibitory interactions with iridophores, whereas xanthophores differentiate specifically in the interstripe, receiving Csf1 both from the skin and from iridophores already there. Subsequently, interactions among all three classes of pigment cells contribute to organizing the definitive pattern of stripes and interstripes.

Previous analyses of adult pigment pattern formation in zebrafish highlighted the importance of interactions between melanophores and xanthophores [23,24] and a combination of short-range and long-range interactions between these cell types is consistent with a Turing mechanism of pattern formation or maintenance [26,27]. In this study, however, the recovery of widespread melanophores and xanthophores in *bnc2* mutants was insufficient for stripe formation. Similarly, in studies using a temperature-sensitive allele of *csf1r*, the orientation of stripes in the fin was randomized when xanthophores developed only at late stages [24]. These observations suggested that additional factors specify the location and orientation of stripes and interstripes and support melanophores and xanthophores during pattern formation.

This study indicates that iridophores contribute to adult pigment pattern formation, with several lines of evidence implicating interstripe iridophores in the development of interstripe xanthophores. First, image analyses showed that iridophores are the first adult pigment cells to develop, and do so at the interstripe. Second, Csf1r signaling is necessary for xanthophore development [22,24] and we found that interstripe iridophores express *csf1a* and *csf1b* whereas xanthophores express *csf1r*. Third, misexpressing Csf1 resulted in the development of ectopic xanthophores, indicating this pathway can promote xanthophore localization. Fourth, xanthophore development was delayed in mutant backgrounds having few or no iridophores (*bnc2* and *ltk*, respectively). Fifth, the few xanthophores that do develop in *bnc2* mutants were

associated exclusively with residual iridophores. From these observations we suggest that iridophores promote the timely appearance of xanthophores within the interstripe (Figure 10C, interaction #1), thereby positioning xanthophores to interact with melanophores during the subsequent patterning of dorsal and ventral stripes.

Our finding that xanthophore development is delayed in iridophore-deficient *ltk* mutants is consistent with these inferences. That xanthophores ultimately differentiated in these mutants presumably reflects the persistence of iridophore-independent sources of Csf1 that are not present or not sufficient for xanthophore development in *bnc2* mutants. Interestingly, when xanthophores did develop in *ltk* mutants, they did so more widely over the flank than in the wild-type, in which xanthophores were restricted to the interstripe. A similar restriction of xanthophores to the vicinity of interstripe iridophores has been reported for *mitfa* mutants, which retain iridophores yet lack melanophores [23]. These observations raise the possibility that iridophores both promote xanthophore development at short-range and repress xanthophore development at long-range (Figure 10C, interaction #2), though we cannot yet exclude other explanations for this phenomenon.

Our analyses also suggest roles for iridophores in melanophore development and patterning. Our finding that melanophores localized to regions from which iridophores had been ablated could reflect a delay in the development of xanthophores and the inhibitory effects that xanthophores have on melanophore localization [26]. Although this may have contributed to the mis-patterning of melanophores, our finding that iridophore ablation perturbs melanophore patterning even in xanthophore-deficient *csf1r* mutants suggests that iridophores also influence melanophores independently of xanthophores. Melanophores frequently migrated to, or differentiated within, iridophore-free sites; melanophore centers (as indicated by melanosomes

contracted by epinephrine) rarely overlapped with iridophores, yet melanophores often settled adjacent to iridophores. These observations are consistent with a very short-range inhibitory effect of iridophores on melanophore localization (Figure 10C, interaction #3), as might occur if the two cell types compete for a common substrate, as well as a longer-range attractive or stimulatory effect of iridophores on melanophores (Figure 10C, interaction #4). Our findings of increased melanophore death in *ltk* mutants, and the increased death of *mitfa*:GFP+ cells [16] as well as mis-patterning of melanophores in *ednrb1a* mutants, are likewise consistent with a model in which iridophores influence melanophores. Finally, we note that our examination of *csf1r* mutants revealed iridophores to be more widespread in this xanthophore-deficient background than in the wild-type, raising the possibility that xanthophores interact reciprocally with iridophores as well as melanophores. A definitive test of the interactions hypothesized in Figure 10C will await the elucidation of molecular mechanisms underlying these various pattern-forming events.

In addition to interactions among pigment cells, our study provides new insights into *bnc2* roles in pigment pattern development. Expression analyses and rescue experiments suggested that *bnc2* promotes the development and survival of melanophores and xanthophores by ensuring adequate expression of *kitlga*, *csf1a*, and *csf1b* (Figure 10B). These observations are consistent with previously known roles for Kit ligand [16,37-41,53-55] and Csf1 [22-24,56], and identify a novel role for Bnc2 in regulating the expression of these genes. It will be interesting to learn if Bnc2 has similar functions in providing trophic support to other stem-cell derived lineages as this locus is also expressed in the ovary, central nervous system, and skeleton [30]. Indeed, zebrafish *bnc2* mutant females are infertile and human *BNC2* variants are associated with ovarian cancer predisposition [57]; potential defects in other systems have yet to be ascertained.

At least two aspects of *bnc2* function remain ambiguous. First, although it is clear that *bnc2*-dependent iridophores provide one source of Csf1 to developing xanthophores, *csf1a* and *csf1b* are also expressed more broadly, whereas *kitlga* is expressed in skin, and it has not yet been possible to establish whether *bnc2*+ cells express these factors themselves, or induce other cells to do so. The development of transgenic reporters for all of these loci will address this issue definitively. Second, iridophores are the most severely affected cell type in *bnc2* mutants [30] yet the mechanism by which *bnc2* promotes iridophore development remains unknown. The distribution of *bnc2*+ cells [30] does not perfectly mark the prospective interstripe so it seems likely that other factors specify where iridophores will develop, with *bnc2*+ cells promoting the expansion of the interstripe iridophore population once it has been established. It will be interesting to learn which *bnc2*-dependent and *bnc2*-independent factors are required for iridophore development and whether manipulation of these factors is sufficient to alter the location or orientation of stripes and interstripes. Finally, the continued high expression of Csf1 and Kitlga in the fins of *bnc2* mutants seems likely to explain the persistence of stripes and interstripes at this location; why fin melanophores and xanthophores can organize into stripes in the absence of *bnc2* activity, whereas body melanophores cannot awaits further investigation.

Several studies have highlighted the pigment-cell autonomous nature of pattern-generating mechanisms in zebrafish. Our study suggests two extensions to this paradigm. First, environmental factors are required to support pigment cells during pattern formation and are likely to provide cues that bias the initial development of pigment cells (e.g., the first interstripe iridophores) to specific regions, thereby influencing the subsequent locations and orientations of stripes and interstripes. Second, pigment cell interactions appear to involve all three major classes of pigment cells. Analyses presented here support a model in which iridophores exert

positive and negative effects on both xanthophores and melanophores and we can imagine that additional interactions will be identified as well. In this regard, it will be interesting to learn whether pigment pattern formation occurs through additional dimensions of Turing-like interactions. Finally, we envisage that evolutionary changes in factors both non-autonomous and autonomous to pigment cell lineages are likely to have contributed to the extraordinary diversification of pigment patterns among ectothermic vertebrates; it will be interesting to see what general themes emerge as mechanisms of pigment pattern formation are elucidated in other species.

1.5 Materials and Methods

1.5.1 Fish stocks, staging, transgenes, cell-transplantation and rearing conditions

Wild-type stock fish, WT(WA), were generated by crosses between the inbred genetic strains AB^{wp} and wik or the progeny of such crosses. Mutants were presumptive null alleles *bnc2*^{utr16e1} [30], *csf1r*^{j4e1} and *csf1r*^{j4blue} [22], and *mitfa*^{w2} [58], as well as hypomorphic alleles *ltk*^{j9s1} [44] and *ednrb1a*^{b140} [52]. Transgenic lines were *Tg(hsp70l:kitlga)*$^{wp.r.t2}$, *Tg(hsp70l:csf1a-IRES-nlsCFP)*$^{wp.r.t4}$; *Tg(hsp70l:csf1b-IRES-nlsCFP)*$^{wp.r.t5}$, *Tg(hsp70l:kitlga-V2a-csf1a-IRES-nlsCFP)*$^{wp.r.t6}$, *Tg(hsp70l:kitlga-V2a-csf1b-IRES-nlsCFP)*$^{wp.r.t7}$ and *Tg(fms:Gal4.VP16)*^{i186}; *Tg(UAS-E1b:nfsB.mCherry)*^{i149} [43]. Post-embryonic stages are reported as standardized standard length (SSL) measurements following [42]; SSL provides a more accurate representation of stages than days post-fertilization.

Transgenes were assembled by Gateway cloning of entry plasmids into pDest vectors containing *Tol2* repeats for efficient genomic integration [59,60]. For expressing NTR in iridophores, we cloned the upstream region of *pnp4a* [11,30] using primers (forward, reverse):

CCTGGGTTTTTGCCATTCTTTAGG, GAATGAGAGAGCAGCTCTTTCC. To express Csf1a in slow muscle cells of the myotome we cloned a region upstream of *smyhc1* using primers (forward, reverse): AACAAGAAGAGCAAGAGGTTGAGGT, CAGATGAACAAACTTATAAATATAATGTGCTTCTCT. Microinjection of plasmids and *Tol2* mRNA used standard methods. Cell transplantation followed [30].

Fish stocks were reared in standard conditions at 28.5 °C 14L:10D. For transgene inductions using *hsp70l* promoters, fish were heat-shocked at 38 °C twice daily for 1 h beginning when fish had reached 8.5 SSL and extending for period 2–4 weeks. For fish injected with plasmid *smyhc1*:TetGBD-TREtightBactinTRX:nlsVenus-V2a-csf1a, induction with dexamethasone and doxycycline followed [50]. For ablating iridophores in larvae mosaic for plasmid *pnp4a*:nlsVenus-V2a-NTR, larvae were incubated overnight in 10 mM Mtz. For time series of individual ablations in wild-type and *csf1r* mutants, larvae were allowed to recover one night prior to imaging. Fish were then imaged a second day and treated with Mtz again that evening. Repeated treatments were required to repress iridophore regeneration, though in many cases, iridophores eventually recovered. Treatments alternating every third night were also administered to batches of wild-type or *csf1r* mutant larvae mosaic for pnp4a:nlsVenus-V2a-NTR that were later assessed for iridophore ablations.

1.5.2 In situ hybridization

Characterization of mRNA transcript distributions in whole mount and transverse vibratome sections followed [61]. For comparing distributions of *csf1a* transcripts and iridophores, larvae were imaged prior to fixation, processed individually and then the corresponding regions re-imaged after color development.

1.5.3 RT-PCR and quantitative RT-PCR

For quantitative RT-PCR, single skins were collected from ~9.0 SSL *bnc2* or *bnc2/+* larvae and placed in either Trizol Reagent (Invitrogen) or RNAlater (Ambion). RNA was isolated using either Trizol or RNaqueous Microkit (Ambion), followed by LiCl precipitation. cDNA was synthesized with either Superscript III First-Strand Synthesis (Invitrogen) or iScript cDNA Synthesis Kit (Bio-Rad). Quantitative RT-PCRs were performed and analyzed with a StepOnePlus System (Life Technologies) using a Custom Taqman Gene Expression Assay for *kitlga* (Life Technologies) and the following Taqman Gene Expression Assays (Life Technologies): *csf1a*, Dr03432536_m1; *csf1b*, Dr03110811_m1; *gapdh*, Dr03436842_m1.

For RT-PCR of isolated iridophores, 10–14 SSL larvae were euthanized and 3 skins placed in PBS. Tissue was briefly vortexed to remove scales, then centrifuged and washed again in PBS. Skins were incubated 10 min at 37 degrees C in 0.25% trypsin-EDTA (Invitrogen). Trypsin was removed and tissue incubated 10 min at 37 °C in tyrpsin-inhibitor (Sigma T6414) with 3 mg/ml collagenase, and 2 µl RNase-free DNase I (Thermo Scientific), followed by 3 h at 28 C in a Benchmark Multi-Therm Shaker set to 800 rpm. Cells were washed in PBS and filtered through a 40 µm cell strainer (BD Falcon). Cell mixtures were placed on a glass bottom dish and examined on a Zeiss Observer inverted compound microscope. Individual iridophores were picked using a pulled capillary and Narishige 1M 9B microinjector then expelled directly into resuspension buffer from the Superscript III Cells Direct cDNA Synthesis Kit (Invitrogen). cDNA was synthesized from approximately 50 cells per sample and RT-PCR performed with the following primers designed to span introns (forward, reverse):
actb1, ACTGGGATGACATGGAGAAGAT, GTGTTGAAGGTCTCGAACATGA;
pnp4a, GAAAAGTTTGGTCCACGATTTC, TACTCATTCCAACTGCATCCAC;

csf1a, TACACCTTCACAGAGCGTCAGA, CTTCGTTGGACTGTCCTCAATC;

csf1b, AACACCCCTGTTAACTGGACCT, GAGGCAGTAGGCAGTGAGAAGA.

1.5.4 Imaging and quantitative analyses

For time-course imaging of interstripe development, fish from *bnc2*/+, *ltk*/+, or *ednrb1a*/+ backcrosses were reared individually and imaged daily on a Zeiss Observer inverted compound microscope or an Olympus SZX-12 stereomicroscope, using Zeiss Axiocam HR cameras and Axiovision software. Individuals from *bnc2*/+ backcrosses were genotyped retrospectively for the $bnc2^{utr16e1}$ lesion [30].

For transgenic rescue experiments of *bnc2* mutant melanophores and xanthophores, larvae were viewed and imaged as described above. For assessing melanophore numbers, all melanophores were counted ventral to the horizontal myoseptum in a region bounded by the anterior margin of the dorsal fin and the posterior margin of the anal fin. For assessing xanthophore numbers and localization, xanthophores were counted at three separate locations along the anterior to posterior axis, (posterior swim bladder, anus, center of anal fin) within the interstripe region (as marked by iridophores).

To quantify melanophore dorsal–ventral location in *csf1r* mutants mosaic for pnp4a:nlsVenus-V2a-NTR and uninjected controls, we measured the distance of each melanophore from the dorsal and ventral margins of the myotomes, then divided dorsal length by total distance. Positions were determined for all melanophores between the anterior of the dorsal fin and posterior of the anal fin. Regions were considered ablated when they lacked most iridophores.

For presentation, images were color-balanced and in some cases adjusted for color saturation to assist in visualizing xanthophores.

All statistical analyses were performed using JMP 8.0.2 (SAS Institute, Cary, NC). For analyses of xanthophore numbers, counts were square-root transformed prior to analysis to correct for unequal variances across groups.

1.6 Acknowledgements

Thanks to Dae Seok Eom, Tiffany N. Gordon, and Erine H. Budi for assistance with injections and in situ hybridizations, as well as Ian K. Quigley for imaging *ednrb1a* mutants. We thank Jay Parrish and David Raible for helpful suggestions as well as Christiane Nüsslein-Volhard and Hans-Georg Frohnhöfer for stimulating discussion.

1.7 References

1. Price AC, Weadick CJ, Shim J, Rodd FH (2008) Pigments, Patterns, and Fish Behavior. Zebrafish 5: 297-307.
2. Engeszer RE, Wang G, Ryan MJ, Parichy DM (2008) Sex-specific perceptual spaces for a vertebrate basal social aggregative behavior. Proc Natl Acad Sci U S A 105: 929-933.
3. Streelman JT, Peichel CL, Parichy DM (2007) Developmental genetics of adaptation in fishes: The case of novelty. Annual Review of Ecology Evolution and Systematics 38: 655-681.
4. Houde AE (1997) Sex, Color, and Mate Choice in Guppies. Princeton, NJ: Princeton University Press.
5. Kelsh RN (2004) Genetics and evolution of pigment patterns in fish. Pigment Cell Res 17: 326-336.
6. Parichy DM, Reedy MV, Erickson CA (2006) Chapter 5. Regulation of melanoblast migration and differentiation. In: Nordland JJ, Boissy RE, Hearing VJ, King RA, Oetting WS et al., editors. The Pigmentary System: Physiology and Pathophysiology 2nd Edition. New York, New York: Oxford University Press.
7. Bagnara JT, Matsumoto J (2006) Chapter 2. Comparative anatomy and physiology of pigment cells in nonmammalian tissues. In: Nordland JJ, Boissy RE, Hearing VJ, King RA, Oetting WS et al., editors. The Pigmentary System: Physiology and Pathophysiology. New York, New York: Oxford University Press.
8. Parichy DM (2006) Evolution of danio pigment pattern development. Heredity 97: 200-210.
9. Kelsh RN, Harris ML, Colanesi S, Erickson CA (2009) Stripes and belly-spots-A review of pigment cell morphogenesis in vertebrates. Semin Cell Dev Biol 20: 90–104.
10. Kelsh RN, Schmid B, Eisen JS (2000) Genetic analysis of melanophore development in zebrafish embryos. Dev Biol 225: 277-293.
11. Curran K, Lister JA, Kunkel GR, Prendergast A, Parichy DM, et al. (2010) Interplay between Foxd3 and Mitf regulates cell fate plasticity in the zebrafish neural crest. Dev Biol 344: 107–118.
12. Raible DW, Eisen JS (1994) Restriction of neural crest cell fate in the trunk of the embryonic zebrafish. Development 120: 495-503.
13. Dutton KA, Pauliny A, Lopes SS, Elworthy S, Carney TJ, et al. (2001) Zebrafish colourless encodes sox10 and specifies non-ectomesenchymal neural crest fates. Development 128: 4113-4125.
14. Hultman KA, Budi EH, Teasley DC, Gottlieb AY, Parichy DM, et al. (2009) Defects in ErbB-dependent establishment of adult melanocyte stem cells reveal independent origins for embryonic and regeneration melanocytes. PLoS Genetics 5: e1000544.
15. Kirschbaum F (1975) Untersuchungen über das Farbmuster der Zebrabarbe *Brachydanio rerio* (Cyprinidae, Teleostei). Wilhelm Roux's Arch 177: 129–152.
16. Budi EH, Patterson LB, Parichy DM (2011) Post-embryonic nerve-associated precursors to adult pigment cells: genetic requirements and dynamics of morphogenesis and differentiation. PLoS Genet In press.
17. Parichy DM, Turner JM (2003) Zebrafish puma mutant decouples pigment pattern and somatic metamorphosis. Developmental Biology 256: 242-257.
18. Johnson SL, Africa D, Walker C, Weston JA (1995) Genetic control of adult pigment stripe development in zebrafish. Dev Biol 167: 27–33.

19. Budi EH, Patterson LB, Parichy DM (2008) Embryonic requirements for ErbB signaling in neural crest development and adult pigment pattern formation. Development 135: 2603-2614.
20. Hirata M, Nakamura K, Kanemaru T, Shibata Y, Kondo S (2003) Pigment cell organization in the hypodermis of zebrafish. Dev Dyn 227: 497-503.
21. Hawkes JW (1974) The structure of fish skin. I. General organization. Cell Tiss Res 149: 159–172.
22. Parichy DM, Ransom DG, Paw B, Zon LI, Johnson SL (2000) An orthologue of the *kit*-related gene *fms* is required for development of neural crest-derived xanthophores and a subpopulation of adult melanocytes in the zebrafish, *Danio rerio*. Development 127: 3031-3044.
23. Maderspacher F, Nusslein-Volhard C (2003) Formation of the adult pigment pattern in zebrafish requires leopard and obelix dependent cell interactions. Development 130: 3447-3457.
24. Parichy DM, Turner JM (2003) Temporal and cellular requirements for Fms signaling during zebrafish adult pigment pattern development. Development 130: 817-833.
25. Inaba M, Yamanaka H, Kondo S (2012) Pigment pattern formation by contact-dependent depolarization. Science 335: 677.
26. Nakamasu A, Takahashi G, Kanbe A, Kondo S (2009) Interactions between zebrafish pigment cells responsible for the generation of Turing patterns. Proc Natl Acad Sci U S A 106: 8429-8434.
27. Yamaguchi M, Yoshimoto E, Kondo S (2007) Pattern regulation in the stripe of zebrafish suggests an underlying dynamic and autonomous mechanism. Proc Natl Acad Sci U S A 104: 4790-4793.
28. Kondo S, Miura T (2010) Reaction-diffusion model as a framework for understanding biological pattern formation. Science 329: 1616-1620.
29. Meinhardt H, Gierer A (2000) Pattern formation by local self-activation and lateral inhibition. Bioessays 22: 753-760.
30. Lang MR, Patterson LB, Gordon TN, Johnson SL, Parichy DM (2009) Basonuclin-2 requirements for zebrafish adult pigment pattern development and female fertility. PLoS Genet 5: e1000744.
31. Vanhoutteghem A, Bouche C, Maciejewski-Duval A, Herve F, Djian P (2010) Basonuclins and disco: Orthologous zinc finger proteins essential for development in vertebrates and arthropods. Biochimie.
32. Vanhoutteghem A, Maciejewski-Duval A, Bouche C, Delhomme B, Herve F, et al. (2009) Basonuclin 2 has a function in the multiplication of embryonic craniofacial mesenchymal cells and is orthologous to disco proteins. Proc Natl Acad Sci U S A 106: 14432-14437.
33. Vanhoutteghem A, Djian P (2007) The human basonuclin 2 gene has the potential to generate nearly 90,000 mRNA isoforms encoding over 2000 different proteins. Genomics 89: 44-58.
34. Vanhoutteghem A (2006) Basonuclins 1 and 2, whose genes share a common origin, are proteins with widely different properties and functions. Proceedings of the National Academy of Sciences 103: 12423-12428.
35. Vanhoutteghem A (2004) Basonuclin 2: An extremely conserved homolog of the zinc finger protein basonuclin. Proceedings of the National Academy of Sciences 101: 3468-3473.

36. Besmer P, Manova K, Duttlinger R, Huang EJ, Packer A, et al. (1993) The kit-ligand (steel factor) and its receptor c-kit/W: pleiotropic roles in gametogenesis and melanogenesis. Dev Suppl: 125-137.
37. Wehrle-Haller B (2003) The role of Kit-ligand in melanocyte development and epidermal homeostasis. Pigment Cell Res 16: 287-296.
38. Parichy DM, Rawls JF, Pratt SJ, Whitfield TT, Johnson SL (1999) Zebrafish sparse corresponds to an orthologue of c-kit and is required for the morphogenesis of a subpopulation of melanocytes, but is not essential for hematopoiesis or primordial germ cell development. Development 126: 3425-3436.
39. Hultman KA, Bahary N, Zon LI, Johnson SL (2007) Gene Duplication of the zebrafish kit ligand and partitioning of melanocyte development functions to kit ligand a. PLoS Genet 3: e17.
40. Mellgren EM, Johnson SL (2004) A requirement for kit in embryonic zebrafish melanocyte differentiation is revealed by melanoblast delay. Dev Genes Evol 214: 493-502.
41. Dooley CM, Mongera A, Walderich B, Nusslein-Volhard C (2013) On the embryonic origin of adult melanophores: the role of ErbB and Kit signalling in establishing melanophore stem cells in zebrafish. Development.
42. Parichy DM, Elizondo MR, Mills MG, Gordon TN, Engeszer RE (2009) Normal table of postembryonic zebrafish development: staging by externally visible anatomy of the living fish. Developmental Dynamics 238: 2975-3015.
43. Gray C, Loynes CA, Whyte MK, Crossman DC, Renshaw SA, et al. (2011) Simultaneous intravital imaging of macrophage and neutrophil behaviour during inflammation using a novel transgenic zebrafish. Thromb Haemost 105.
44. Lopes SS, Yang X, Muller J, Carney TJ, McAdow AR, et al. (2008) Leukocyte tyrosine kinase functions in pigment cell development. PLoS Genet 4: e1000026.
45. Chen CF, Chu CY, Chen TH, Lee SJ, Shen CN, et al. (2011) Establishment of a transgenic zebrafish line for superficial skin ablation and functional validation of apoptosis modulators in vivo. PLoS ONE 6: e20654.
46. Curado S, Stainier DY, Anderson RM (2008) Nitroreductase-mediated cell/tissue ablation in zebrafish: a spatially and temporally controlled ablation method with applications in developmental and regeneration studies. Nat Protoc 3: 948-954.
47. Pisharath H, Rhee JM, Swanson MA, Leach SD, Parsons MJ (2007) Targeted ablation of beta cells in the embryonic zebrafish pancreas using E. coli nitroreductase. Mech Dev 124: 218-229.
48. Bridgewater JA, Knox RJ, Pitts JD, Collins MK, Springer CJ (1997) The bystander effect of the nitroreductase/CB1954 enzyme/prodrug system is due to a cell-permeable metabolite. Hum Gene Ther 8: 709-717.
49. Sisson G, Jeong JY, Goodwin A, Bryden L, Rossler N, et al. (2000) Metronidazole activation is mutagenic and causes DNA fragmentation in Helicobacter pylori and in Escherichia coli containing a cloned H. pylori RdxA(+) (Nitroreductase) gene. J Bacteriol 182: 5091-5096.
50. Knopf F, Schnabel K, Haase C, Pfeifer K, Anastassiadis K, et al. (2010) Dually inducible TetON systems for tissue-specific conditional gene expression in zebrafish. Proc Natl Acad Sci U S A 107: 19933-19938.
51. Parichy DM, Turner JM. Cellular interactions during adult pigment stripe development in zebrafish; 2003. Academic Press Inc Elsevier Science. pp. 486.

52. Parichy DM, Mellgren EM, Rawls JF, Lopes SS, Kelsh RN, et al. (2000) Mutational analysis of endothelin receptor b1 (rose) during neural crest and pigment pattern development in the zebrafish Danio rerio. Dev Biol 227: 294-306.
53. Reid K, Nishikawa S, Bartlett PF, Murphy M (1995) Steel factor directs melanocyte development in vitro through selective regulation of the number of c-kit+ progenitors. Dev Biol 169: 568-579.
54. Wehrle-Haller B, Weston JA (1995) Soluble and cell-bound forms of steel factor activity play distinct roles in melanocyte precursor dispersal and survival on the lateral neural crest migration pathway. Development 121: 731–742.
55. Jordan SA, Jackson IJ (2000) MGF (KIT ligand) is a chemokinetic factor for melanoblast migration into hair follicles. Dev Biol 225: 424-436.
56. Stanley ER, Berg KL, Einstein DB, Lee PS, Pixley FJ, et al. (1997) Biology and action of colony stimulating factor-1. Mol Reprod Dev 46: 4-10.
57. Song H, Ramus SJ, Tyrer J, Bolton KL, Gentry-Maharaj A, et al. (2009) A genome-wide association study identifies a new ovarian cancer susceptibility locus on 9p22.2. Nat Genet 41: 996-1000.
58. Lister JA, Robertson CP, Lepage T, Johnson SL, Raible DW (1999) nacre encodes a zebrafish microphthalmia-related protein that regulates neural-crest-derived pigment cell fate. Development 126: 3757-3767.
59. Kwan KM, Fujimoto E, Grabher C, Mangum BD, Hardy ME, et al. (2007) The Tol2kit: a multisite gateway-based construction kit for Tol2 transposon transgenesis constructs. Dev Dyn 236: 3088-3099.
60. Suster ML, Kikuta H, Urasaki A, Asakawa K, Kawakami K (2009) Transgenesis in zebrafish with the tol2 transposon system. Methods Mol Biol 561: 41-63.
61. Larson TA, Gordon TN, Lau HE, Parichy DM (2010) Defective adult oligodendrocyte and Schwann cell development, pigment pattern, and craniofacial morphology in puma mutant zebrafish having an alpha tubulin mutation. Dev Biol 346: 296-309.
62. Goll MG, Anderson R, Stainier DY, Spradling AC, Halpern ME (2009) Transcriptional silencing and reactivation in transgenic zebrafish. Genetics 182: 747-755.

1.8 Figure Legends

Figure 1. *bnc2* mutants exhibited reduced expression of melanogenic and xanthogenic factors. (A) Wild-type. (B) Homozygous *bnc2* mutant. (C) Quantitative RT-PCR for *csf1a*, *csf1b*, and *kitlga* revealed significantly reduced transcript abundances in skins isolated from 8.5 SSL *bnc2* mutants as compared to stage-matched, wild-type *bnc2*/+ siblings. Shown are means±SE. Values are derived from 3 replicate experiments each consisting of 3 biological replicates for each genotype (*n*=9 larvae total per genotype). Scale bar: in (B) 3 mm for (A,B).

Figure 2. Re-expression of Kitlga, Csf1a, and Csf1b in *bnc2* mutants promoted melanophore and xanthophore development but were insufficient for stripe patterning. (A) Melanophore recovery following heat-shock induction of *Tg(hsp70l:kitlga)*. Although Kitlga expression increased melanophore numbers in *bnc2* mutant larvae, the restored melanophores failed to develop into stripes. Plots show means±SE with different letters above bars denoting means that differed significantly from one another in Tukey Kramer *post hoc* comparisons. All wild-type larvae are *bnc2*/+ siblings to *bnc2* mutants. Sample sizes: *bnc2*/+, *n*=10; *bnc2*, *n*=10, *bnc2*/+ *hsp70l:kitlga*, *n*=14; *bnc2*, *hsp70l:kitlga*, *n*=14. (B) Xanthophore and melanophore recovery following heat-shock induction of *Tg(hsp70l:csf1a)*. Upper plot, xanthophores were classed as either associated with iridophores (larger, lower segment of each bar), or not associated with iridophores (smaller, upper segment of each bar): total xanthophore numbers, including xanthophores not associated with iridophores were increased in *bnc2* mutants by Csf1a expression. Lower plot indicates that melanophore numbers were increased as well. Images show xanthophores (yellow–orange cells) over iridophores (patches of grey cells in this illumination, denoted by arrowheads in the *bnc2* mutant). Red dashed circle in *bnc2* mutant +Csf1 panel

shows a xanthophore that has developed at a distance from iridophores. Lower magnification images (bottom) show typical patterns and the absence of organized stripes in the *bnc2* mutant after Csf1 expression, despite increased numbers of melanophores and xanthophores (compare to controls in A). Sample sizes: *bnc2*/+, *n*=15; *bnc2*, *n*=19, *bnc2*/+ *hsp70l:csf1a*, *n*=19; *bnc2*, *hsp70l:csf1a*, *n*=22. Results for *Tg(hsp70l:csf1b)* were equivalent (not shown; total sample size, *N*=17). (C) Xanthophore and melanophore numbers were restored by heat shock induction of *Tg(hsp70l:kitlga-csf1a)* and *Tg(hsp70l:kitlga-csf1b)* yet stripes failed to form (total sample sizes, *N*=7, 12, respectively). Scale bars: in (A) 500 μm for (A); in (B, upper) 80 μm for (B upper for images); in (B, lower) 500 μm for (B bottom 2 images); in (C) 500 μm for (C).

Figure 3. Interstripe xanthophores developed after iridophores in wild-type larvae and were further delayed in *bnc2* mutants. Shown are a representative wild-type (*bnc2*/+) larva (A) and a sibling *bnc2* mutant (B) imaged repeatedly over 27 d beginning at 6.0 SSL, just prior to the appearance of iridophores at the anteroposterior region imaged, dorsal to the anus . In both the wild-type and the *bnc2* mutant iridophores started to appear by day 2 of imaging (blue arrowheads). Xanthophores started to differentiate by day 9 of imaging in wild-type; newly arising xanthophores are indicated by red dashed circles. In contrast, xanthophores did not appear until day 25 of imaging in the *bnc2* mutant. As iridophores (and xanthophores) in the interstripe became more abundant, some early larval melanophores along the horizontal myoseptum disappeared from view (e.g., green arrows in A, d12 and d15). For easier visualization of melanophores and other cell type, fish were treated briefly with epinephrine immediately prior to imaging, which contracts melanosomes towards the cell body; the distribution of melanin thus indicates the centers of melanophores whereas processes extending out from the cell body are not visible. Bottom panels schematize the distribution of iridophores

(light blue) and xanthophores (red) on the final day shown. Samples sizes for which complete image series were obtained were: *bnc2*, *n*=4; *bnc2/+*, *n*=6. Scale bar: in (B, d27) 80 μm for (A,B).

Figure 4. *csf1a* and *csf1b* were expressed by interstripe iridophores as well as hypodermal and fin cells. (A) RT-PCR of isolated iridophores (irid) and skin containing pigment cells for the iridophore marker *pnp4a* as well as *csf1a* and *csf1b*. –, no template control. (B) A larva (~6 SSL) imaged to show iridophores prior to fixation (upper) and after whole-mount staining for *csf1a* transcript. Not all iridophore reflecting platelets are visible and platelets that are apparent may not precisely delineate cell bodies and processes. (C,D) Whole-mount larvae (~8.5 SSL) stained for *csf1a* transcript. (C) csf1a was expressed in the posterior trunk at the base of the caudal fin (arrow) where a patch of posterior iridophores develops [42] and also within the fin (f). (D) *csf1a* staining near the horizontal myoseptum (arrow). (E–J) In situ hybridizations on vibratome cross-sections through the midtrunk (~7 SSL). (E,E') *pnp4a* staining indicated iridophore locations (arrowheads) within the hypodermis of wild-type (*bnc2*/+) larvae (E) and revealed fewer of these cells in *bnc2* mutants (E'). Arrow, melanophore. (F,F') *csf1a* staining (arrowheads) was reduced in *bnc2* mutants. (G–H) Staining for *csf1a* in wild-type (*ltk*/+) and *ltk* mutants, which lack iridophores. (G,G') *csf1a* staining was absent in *ltk* mutants at the location where iridophores are found in the wild-type (arrowhead). (H,H') In the fins, however, iridophore-independent *csf1a* expression was present in both wild-type and *ltk* mutant larvae. (I–J) *csf1b* expression was at the limit of detection by in situ hybridization. (I,I') Along the lateral trunk, *csf1b* transcript (arrowheads) was evident in wild-type larvae, representing either hypodermal cells, iridophores or both, but transcript was not apparent in *bnc2* mutant sections stained for equivalent times. (J,J') Along the dorsal trunk, *csf1b* transcript (arrowheads) was

evident in both wild-type and *bnc2* mutants. Scale bars: in (B) 60 μm for (B); in (C) 100 μm for (C); in (D) 100 μm for (D); in (E) 80 μm for (E,E',F,F',G,G',I,I'), in (H) 80 μm for (H,H'); in (J) 20 μm for (J,J').

Figure 5. Ablation of iridophores by Mtz treatment of fish injected with *pnp4a*:NTR. (A) Iridophores in a wild-type larva (6.5 SSL) were marked by Venus fluorescence following injection of *pnp4a*:nlsVenus-V2a-NTR plasmid as the 1-cell stage, as shown in bright-field (A), fluorescence (A') and merged (A'') views. (B–D) The same larva following Mtz treatment exhibited fewer, rounded iridophores that were progressively lost over several days. Inset in B shows reflecting-platelet containing extrusion bodies at the surface of the epidermis. Scale bar: in (A'') 60 μm for (A–D).

Figure 6. Iridophore ablation perturbed xanthophore and melanophore patterning. (A, B) Wild-type siblings that were either not injected (A) or injected (B) with *pnp4a*:NTR plasmid and then treated with Mtz beginning at 5 SSL, prior to the the onset of xanthophore differentiation. Controls (A) exhibited normal interstripe iridophores and xanthophores whereas iridophore-ablated individuals developed xanthophores primarily in association with residual iridophores (e.g., dashed red circle in B). (C) Numbers of xanthophores (means±SE) in stage-matched siblings treated with Mtz that were either uninjected or injected with *pnp4a*:NTR plasmid. Xanthophore numbers did not differ between groups at the onset of the experiment but iridophore-ablated individuals showed an increasingly severe xanthophore deficiency compared to uninjected larvae as the experiment proceeded (genotype x day interaction, $F_{1,10}$=2.7, P<0.005; initial sample sizes: uninjected, n=13; *pnp4*:NTR, n=13). During later development, new xanthophores ultimately developed more broadly over the flank and in association with regenerating iridophores; iridophore ablations after xanthophores had differentiated typically did

not affect these cells (not shown). (D–F) Examples of larvae (9.5 SSL) exhibiting melanophore patterning defects following earlier iridophore ablations (started at 6.0 SSL). Melanophores have colonized regions from which iridophores were ablated, though a few regenerative or persisting iridophore remained. In the lighting used here, iridophores are blue or gold iridescent. (D) Melanophores occupy a region from which iridophores were ablated (residual or regenerated iridophores outlined by dashed yellow lines). Green arrowhead, one of several melanophores localized adjacent to remaining iridophores. Fish shown in A, C and D were treated with epinephrine prior to imaging. (E) Melanophore stripes are broken at site of iridophore ablation and melanophores appear to "wrap around" residual interstripe iridophores on either side of the ablation. (F) In another individual, melanophores stripes are constricted where iridophores have been ablated (arrow). Close-up in F'. Fish in E and F were not treated with epinephrine, so that melanin reveals peripheral processes of melanophores. (Total sample size, *N*=40.) Scale bars: in (B) 60 μm for (A,B); in (D) 200 μm for (D); in (E) 500 μm for (E); in (F) 100 μm for (F); in (F') 60 μm for (F').

Figure 7. Localized Csf1 expression directed xanthophore development. (A) Ectopic xanthophores (red dashed line) developed over the dorsal myotome in association with Csf1a-expressing cells transplanted from a wild-type, *Tg(hsp70l:csf1a-IRES-nlsCFP)* donor to a *bnc2* mutant host. Larva shown at 7.9 SSL. (A') Nuclear CFP expression in the myotome. (A'') Merge. (B) Ectopic xanthophores in a wild-type larva developed over the dorsal myotome in association with a slow muscle fiber of the myotome expressing Csf1a from plasmid smyhc1:TetGBD-TREtightBactinTRX:nlsVenus-V2a-csf1a. Larva shown at 7.5 SSL. (B') Nuclear Venus expression. (B'') Merge. (Sample sizes: *hsp70l*, *n*=8*; smyhc1, n=10.*) Scale bars: in (A'') 100 μm for (A); in (B) 100 μm for (B).

Figure 8. Iridophores influenced melanophore pattern in xanthophore-deficient *csf1r* mutants. (A,B) In stage-matched siblings treated with Mtz, a region on the tail from which iridophores have been ablated (dashed yellow lines in B) exhibits more melanophores than the corresponding region of the control larva (shown here at ~8.5 SSL). Both larvae were treated with epinephrine immediately before imaging. (C,D) Iridophore ablation at the mid-trunk region (dashed yellow lines in D) likewise resulted in increased numbers of melanophores compared to stage-matched control (C)(shown here at ~10.2 SSL). Note that some iridophores have regenerated within previously ablated regions and that melanophores are present at the left edge of the ablated region, adjacent to remaining interstripe iridophores. Larvae in these images were not treated with epinephrine. (E) Quantification of melanophore distributions within dorsal–ventral regions of the flank for larvae that were uninjected but treated with Mtz (left) and for regions of injected, Mtz-treated larvae from which iridophores were unablated (middle) or ablated (right). Plots show means±SE within each region. Asterisk denotes the residual interstripe in *csf1r* mutants, where melanophore numbers differed significantly between unablated and ablated regions (paired t=5.6, d.f.=2, P<0.05). (F,G) Details showing melanophore behaviors in an uninjected control larva (F) and an injected larva (G) in the region of iridophore ablation. Day 0 panels show initial distribution of iridophores and melanophores, prior to Mtz treatment (7.0 SSL). Following iridophore ablation (G), some melanophores moved short distances ventrally (red arrows at d0 and d2 show starting and stopping positions of two melanophores). Melanophores also differentiated within the ablated region (dashed red circles in G, d2); dashed orange circle in G, d7 shows a lightly melanized cell just beneath the surface of the myotome that emerges within the skin by d8. In unablated individuals (F), melanophores typically differentiated further ventrally at sites lacking iridophores (an exception is the left-most

melanophore that appeared at d7). Also see Figure S3C. (H) Detail from another individual showing a lightly melanized cell initially near an iridophore that was ablated (blue arrowhead); the melanophore subsequently translocated to settle adjacent to another iridophore. All larvae in F–H were treated with epinephrine. (Total sample size, *N*=55.) Scale bars: in (A) 200 μm for (A,C); in (B) 400 μm for (D); in (F, d0) 80 μm for (F,G); in (H, d0) 20 μm for (H).

Figure 9. Melanophore and xanthophore development is disrupted in additional iridophore-deficient mutants. (A) Comparison of xanthophore and melanophore development in wild-type and *ltk* mutants. Shown are details at the horizontal myoseptum from larger images of representative wild-type (*ltk*/+) and *ltk* mutant, stage-matched siblings imaged daily (beginning at 6 SSL). In the wild-type, nearly all melanophores persisted through the image series. A xanthophore had already developed at the onset of imaging (day 0, red dashed circle), and additional xanthophores differentiated shortly thereafter. In the *ltk* mutant, however, melanophores were frequently lost between days (green arrowheads) and melanin-containing debris and extrusion bodies were often apparent (green arrows). Unlike the wild-type, no xanthophores differentiated until day 5 of imaging. (B) During later development (9.6 SSL), xanthophores were confined principally to the interstripe region of the wild-type whereas xanthophore developed widely over the flank in the *ltk* mutant. The horizontal myoseptum lies at the lower edge of both images. Lower panels show positions of xanthophores in red. (C) Comparison of wild-type and *ednrb1a* mutant. Shown are ventral flanks of representative stage-matched, sibling wild-type (*ednrb1a*/+) and *ednrb1a* mutant larvae imaged daily (8.8–10 SSL). At the onset of imaging, wild-type melanophores are largely absent from a region where the second interstripe will form by day 7 of imaging (blue bars). In *ednrb1a* mutants, however, melanophores are relatively uniformly distributed in this region at the onset of imaging, and, by

day 7 of imaging, formed clusters where the second interstripe would normally form (green bars). Images shown were rescaled to control for growth. (D) Closeups showing reduced iridophores in *ednrb1a* mutant compared to wild-type (9.0 SSL) as well as wider distribution of xanthophores. Fish in A, B and D were treated briefly with epinephrine prior to imaging. Sample sizes for which complete image series were obtained were: *ltk*, *n*=6; *ltk/+*, *n*=5; *ednrb1a*, *n*=4; *ednrb1a/+*, *n*=5. Scale bars: in (A, d0) 60 μm for (A); in (B) 100 μm for (B); in (C, d0) 200 μm for (C, d0); in (D) 100 μm for (D).

Figure 10. Summary of results and model for stripe and interstripe patterning in zebrafish. (A) Development of pigment pattern phenotypes in wild-type, *bnc2* mutants, iridophore-ablated larvae (pnp4a:NTR), and *ltk* mutants. Blue circles, iridophores; orange circles, xanthophores; grey and black circles, melanophores. In *bnc2* mutants, there are fewer iridophores and increased rate of cell death (open circles) amongst all three pigment cell classes. Xanthophores are restricted to the vicinity of iridophores. In iridophore-ablated larvae, melanophores localize where iridophores have been lost but also organize adjacent to residual iridophore patches. In ltk mutants, iridophores are missing, melanophores tend to die, and xanthophores develop both later and over a wider area than in wild-type larvae. (B) An unknown, *bnc2*-dependent factor expands an initial population of iridophores, whereas *bnc2*-dependent Kitlga and Csf1 support the expansion of melanophore and xanthophore populations. (C) Hypothesized interactions amongst pigment cell classes. Black lines, suggested by this study; grey lines, suggested previously **[23,24,26]**. Solid lines, short-range interactions; dotted lines; longer-range interactions. See main text for details.

Supplementary Figure S1. Expression of *csf1r* reporter by xanthophores during the larval-to-adult transformation. Interstripe xanthophores autofluoresce in the same channel as GFP

and coexpress an mCherry *csf1r* reporter (arrowhead). Variegation of reporter is likely due to epigenetic silencing of Gal4VP16-UAS **[62]**.

Supplementary Figure S2. Pigment cell distributions in *csf1r* mutants. (A) Despite the absence of well-differentiated xanthophores over the flank, csf1r mutants often exhibited a few lightly pigmented xanthophores at the level of the horizontal myoseptum and lateral line nerve (dashed blue line). (A') Higher magnification view of boxed region in A. (B) In an individual in which iridophores have been ablated, residual xanthophores remained confined to the horizontal myoseptum and did not enter the region from which iridophores had been lost (likely owing to csf1r requirements for xanthophore migration **[22,51]**). Shown here is the same region of the larva shown in main text Figure 7G (d8), with higher magnification view of boxed region and residual xanthophores in B'. (C) Image showing distributions of iridophores and melanophores along the ventral trunk of an unmanipulated *csf1r* mutant (10.4 SSL). Most melanophores are centered in regions lacking iridophores. (C') Schematic showing distribution of iridophores (blue) and melanophores (black). Larvae in A and B were treated with epinephrine immediately before imaging (not all melanosomes have contracted in A). Scale bars: in (A) 40 μm for (A); in (B) 60 μm for (B); in (C) 400 μm for (C,C').

1.9 Figures

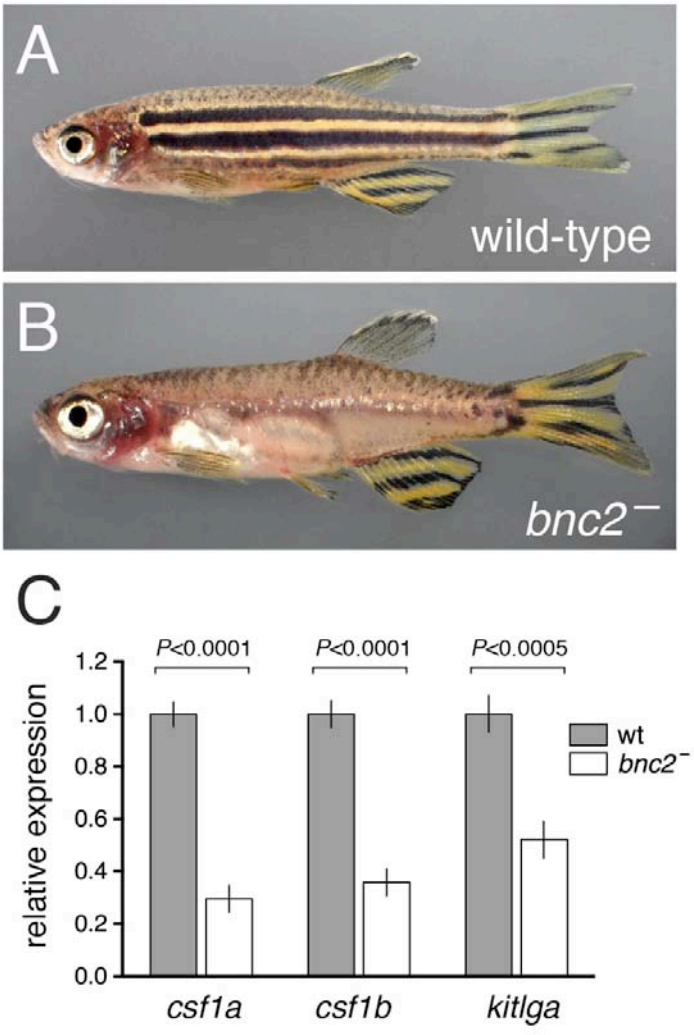

Figure 1.1

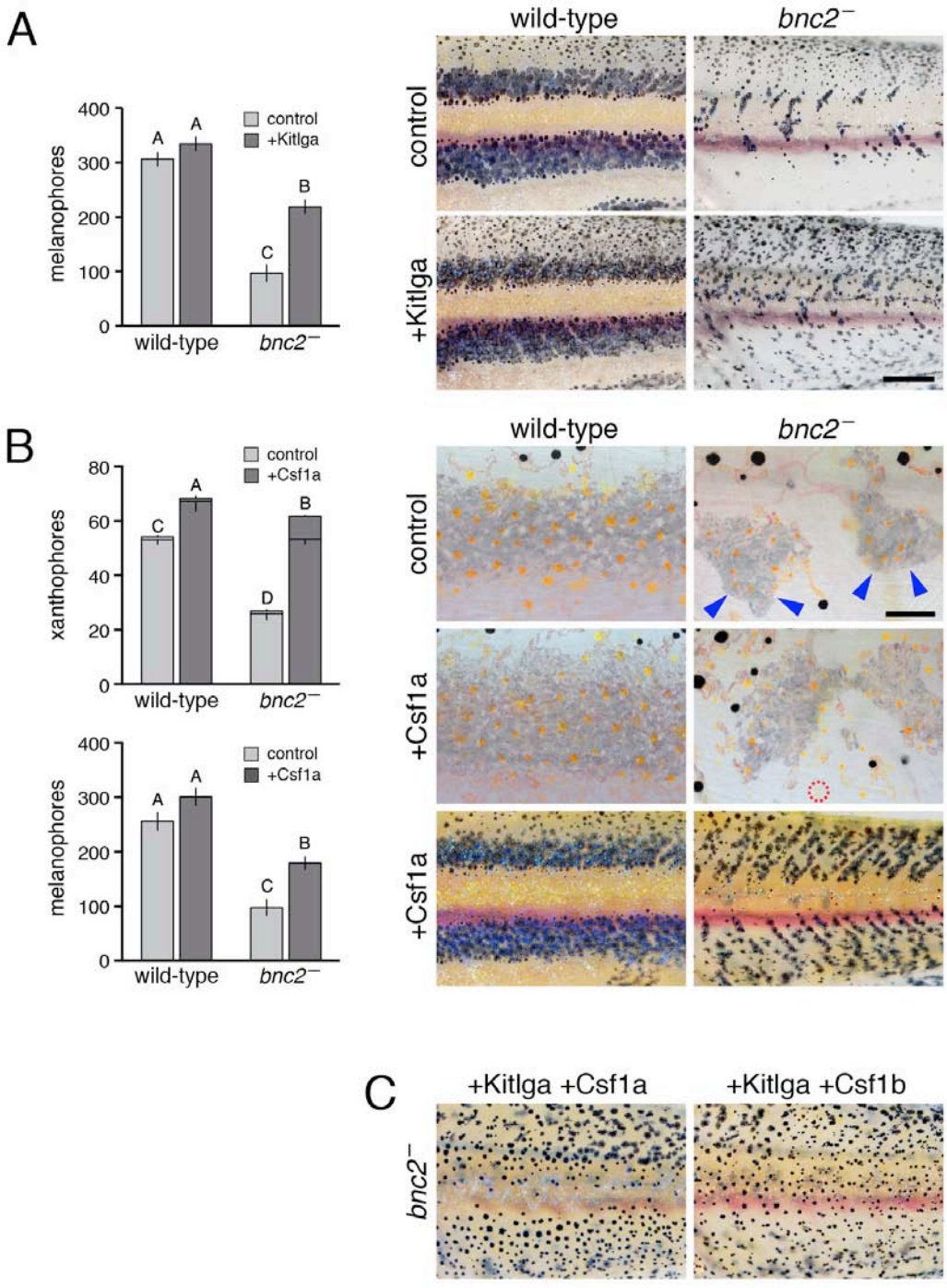
A
melanophores
400
300
200
100
0
control
+Kitlga
A
A
C
B
wild-type
bnc2−
wild-type
bnc2−
control
+Kitlga
B
xanthophores
80
60
40
20
0
control
+Csf1a
C
A
D
B
wild-type
bnc2−
melanophores
400
300
200
100
0
control
+Csf1a
A
A
C
B
wild-type
bnc2−
wild-type
bnc2−
control
+Csf1a
+Csf1a
C
+Kitlga +Csf1a
+Kitlga +Csf1b
bnc2−

Figure 1.2

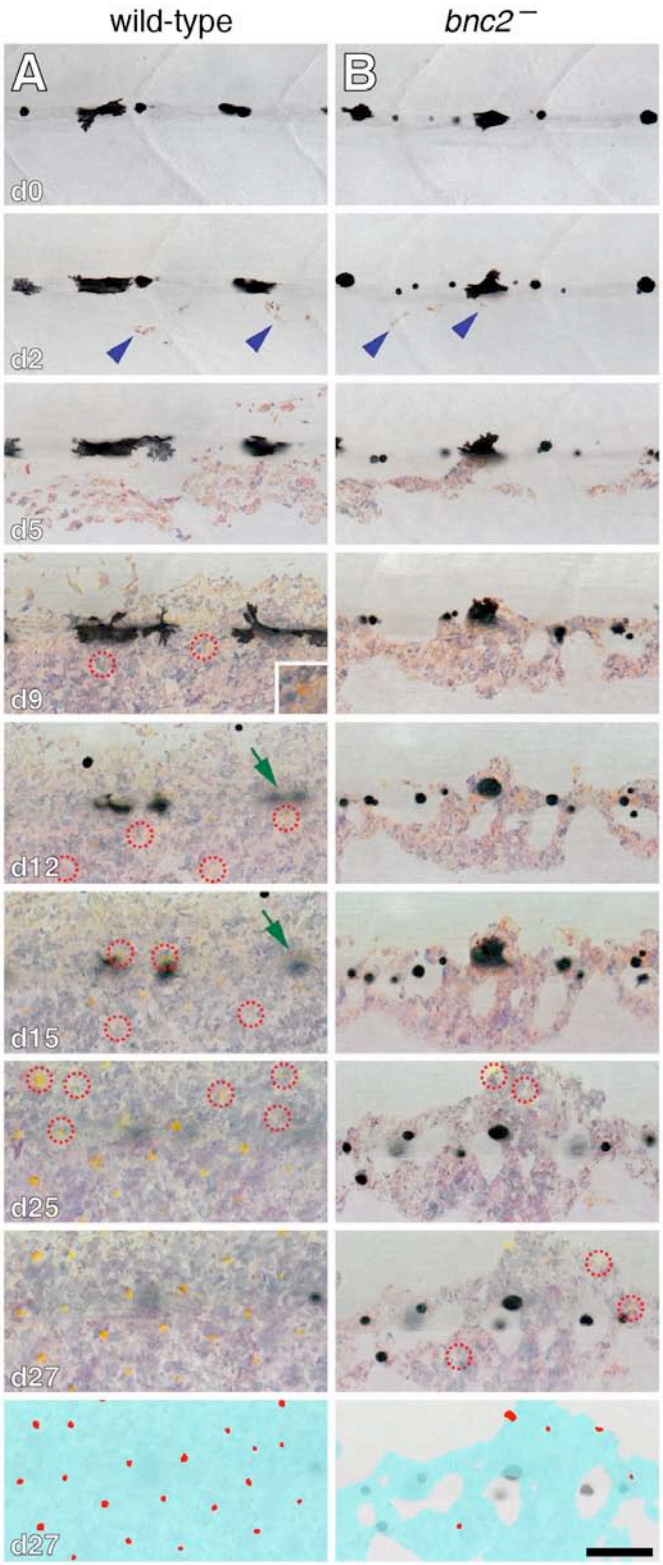

Figure 1.3

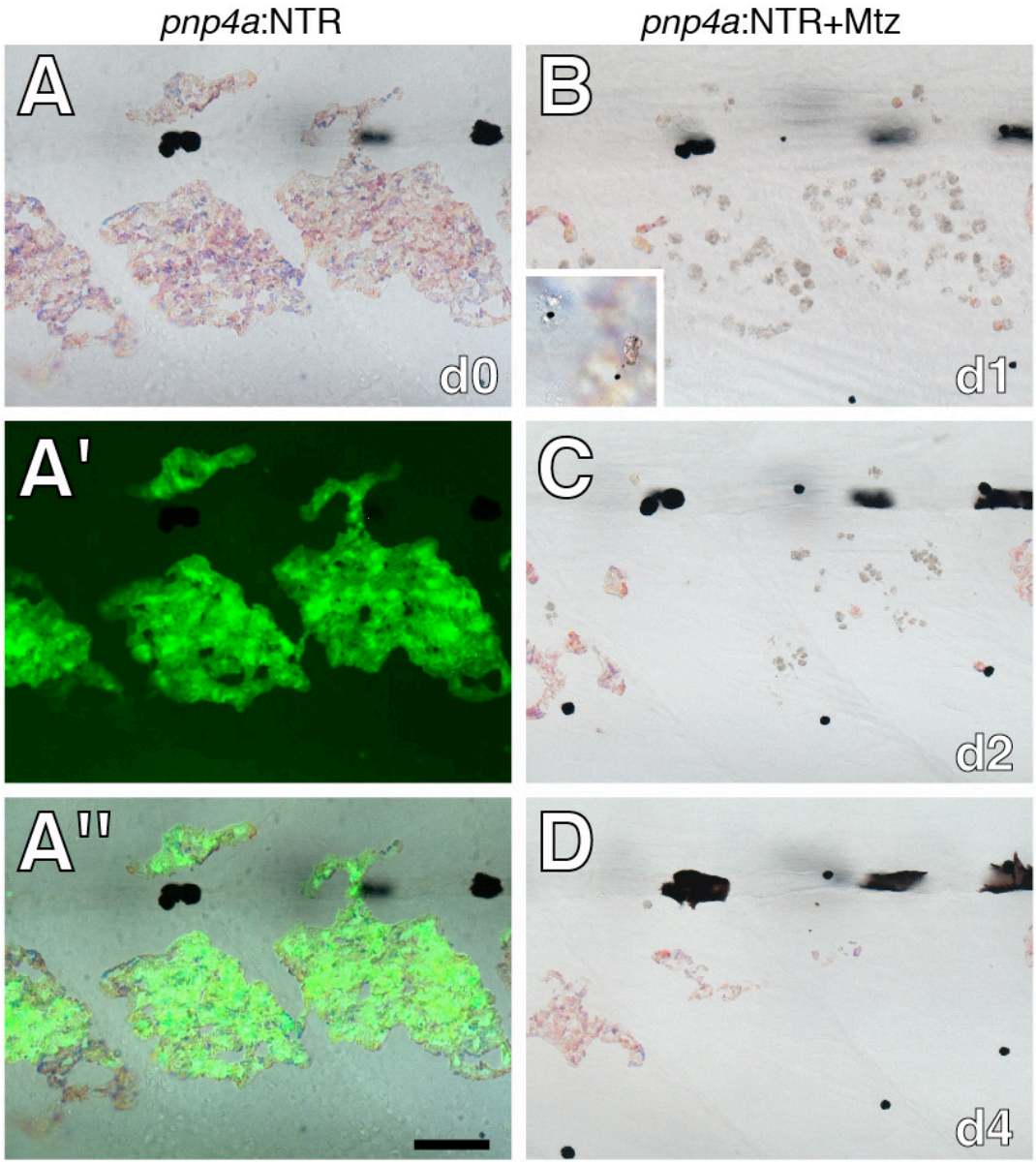

Figure 1.4

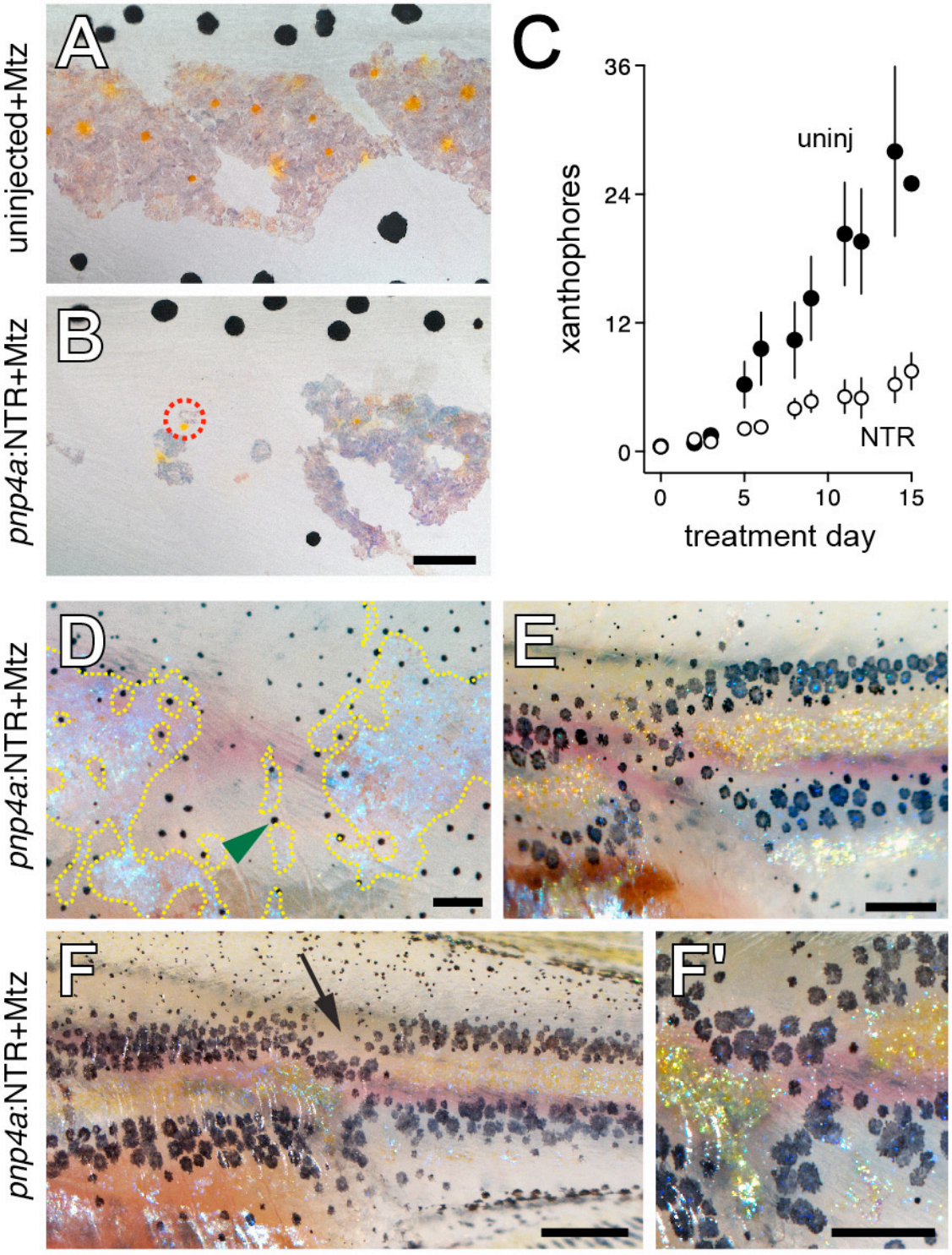
A
uninjected+Mtz
B
pnp4a:NTR+Mtz
C
xanthophores
36
24
12
0
uninj
NTR
0
5
10
15
treatment day
D
pnp4a:NTR+Mtz
E
F
pnp4a:NTR+Mtz
F'

Figure 1.5

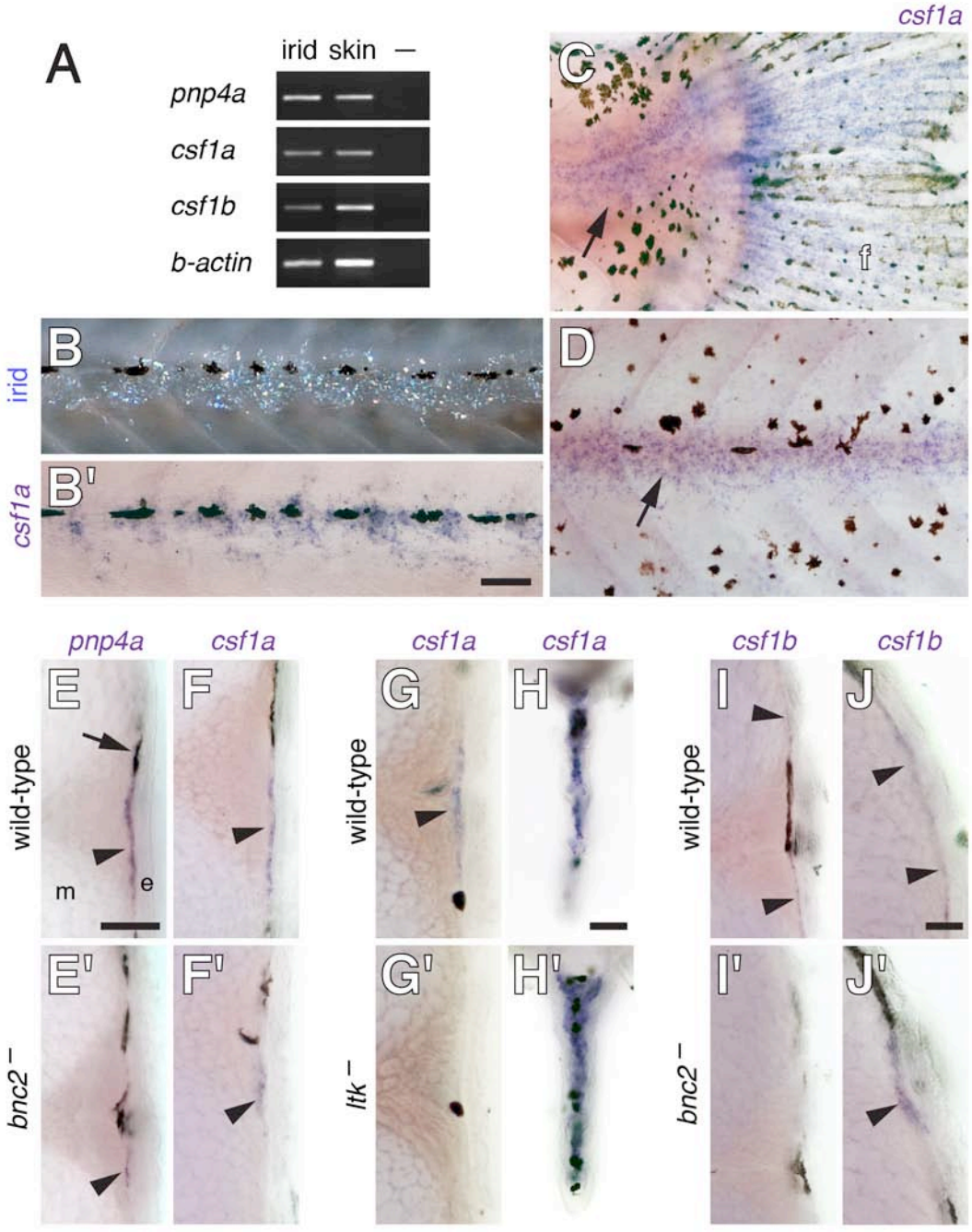
A
irid skin
pnp4a
csf1a
csf1b
b-actin
csf1a
C
f
B
irid
B'
csf1a
D
pnp4a
csf1a
csf1a
csf1a
csf1b
csf1b
E
F
G
H
I
J
wild-type
m
e
E'
F'
G'
H'
I'
J'
bnc2−
ltk−
bnc2−

Figure 1.6

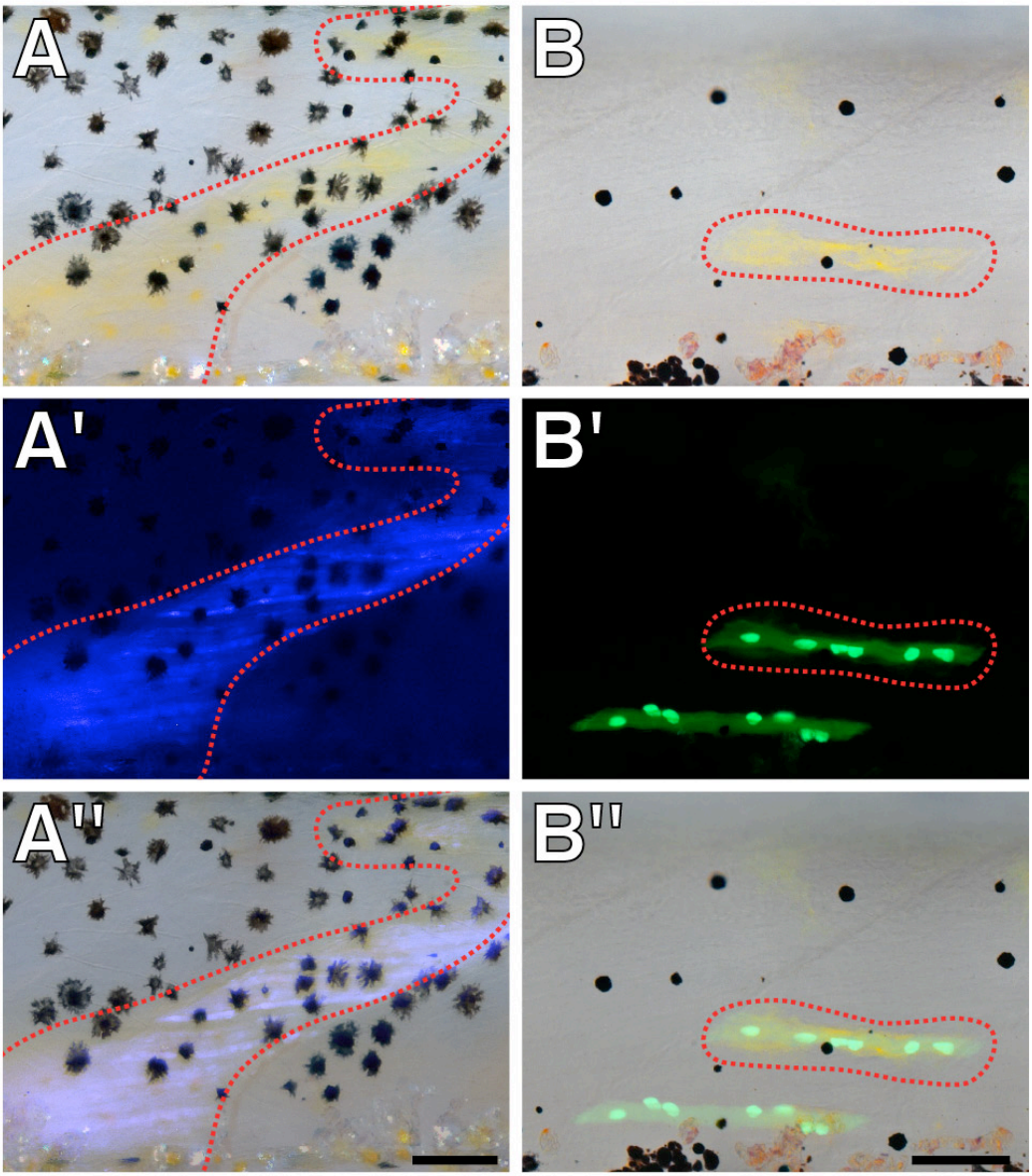

Figure 1.7

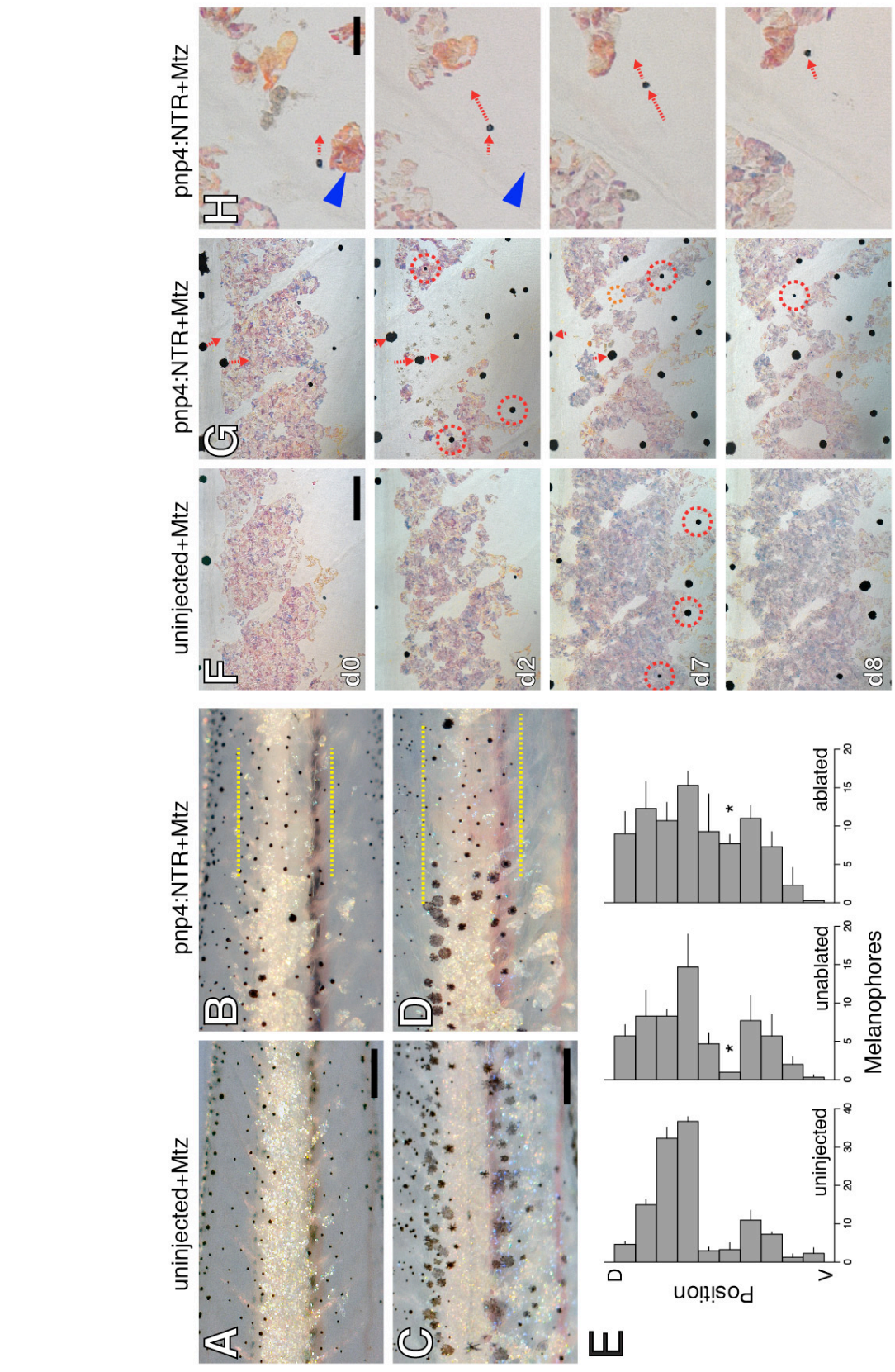
uninjected+Mtz
pnp4:NTR+Mtz
uninjected+Mtz
pnp4:NTR+Mtz
pnp4:NTR+Mtz
A
B
C
D
E
F
G
H
d0
d2
d7
d8
Position
D
V
uninjected
unablated
ablated
Melanophores
0
10
20
30
40
5
15
*

Figure 1.8

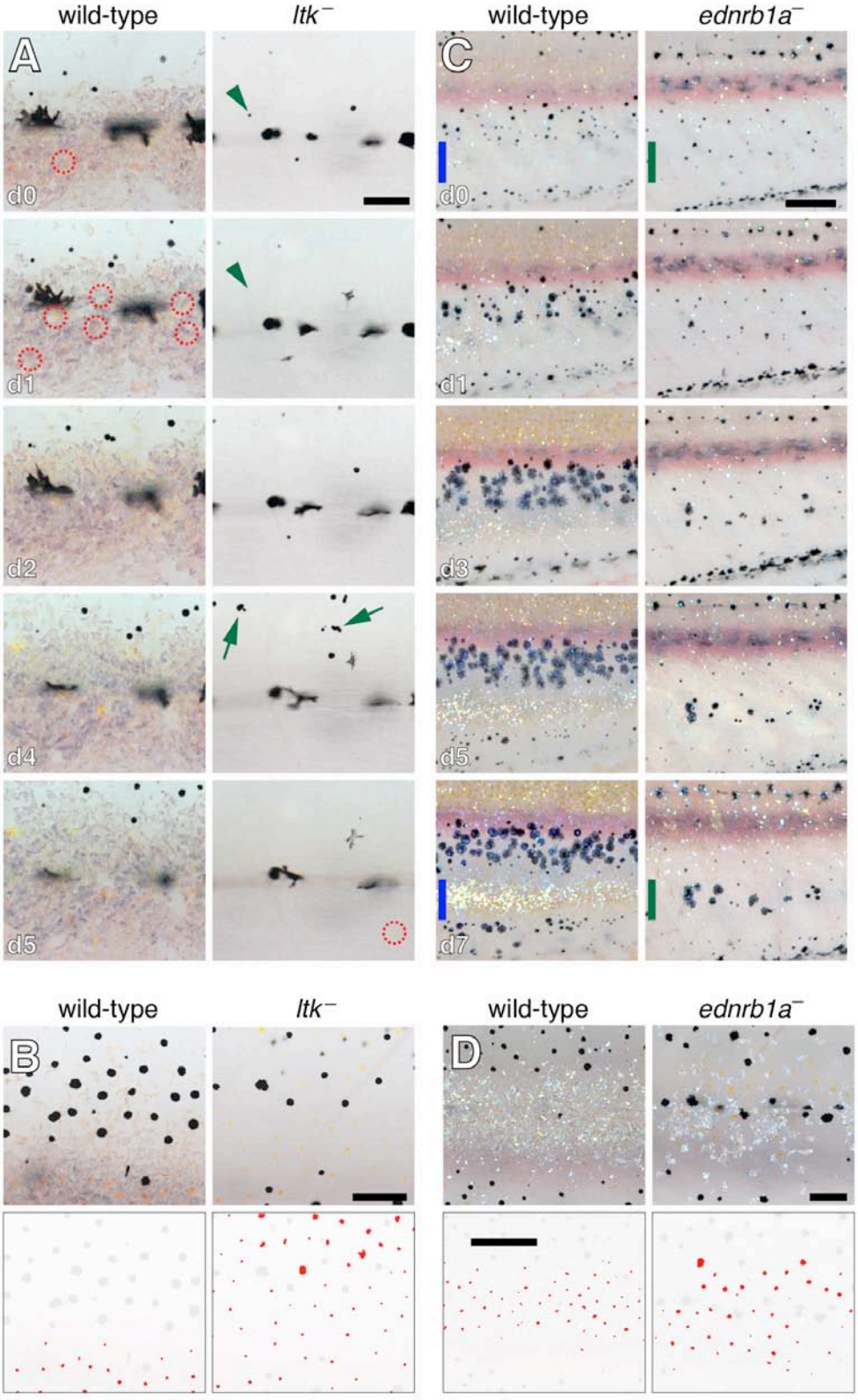
wild-type
ltk⁻
wild-type
ednrb1a⁻
A
C
d0
d0
d1
d1
d2
d3
d4
d5
d5
d7
wild-type
ltk⁻
wild-type
ednrb1a⁻
B
D

Figure 1.9

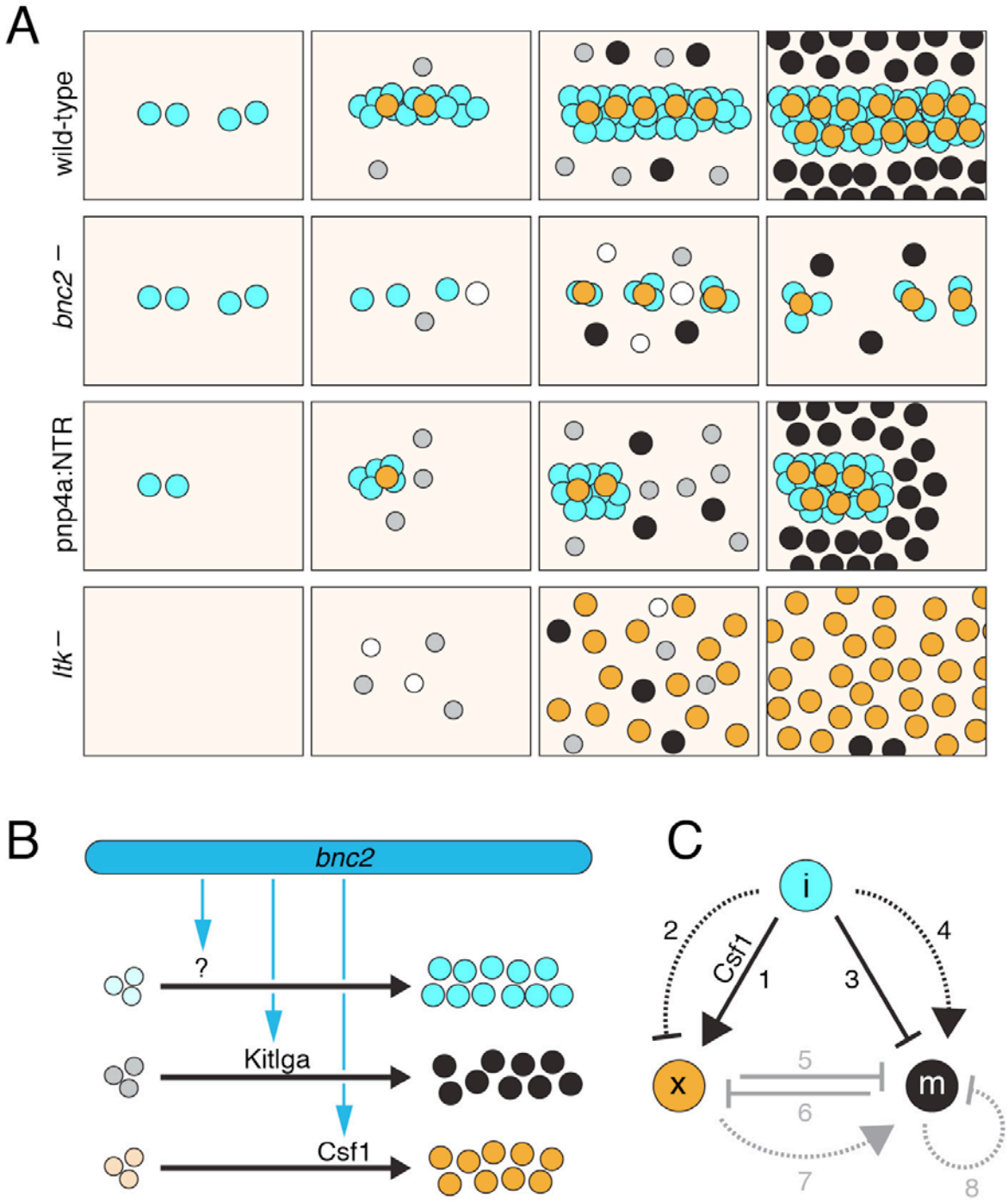
A
wild-type
bnc2 −
pnp4a:NTR
ltk −
B
bnc2
?
Kitlga
Csf1
C
i
x
m
Csf1
1
2
3
4
5
6
7
8

Figure 1.10

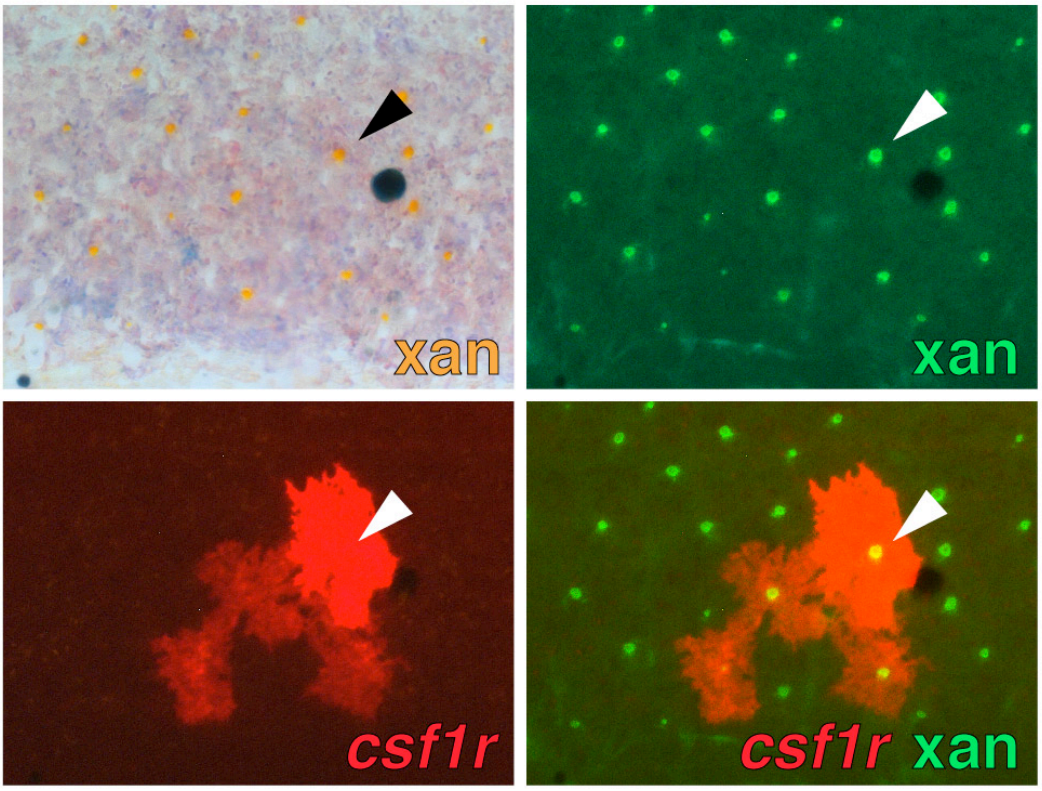

Figure S1.1

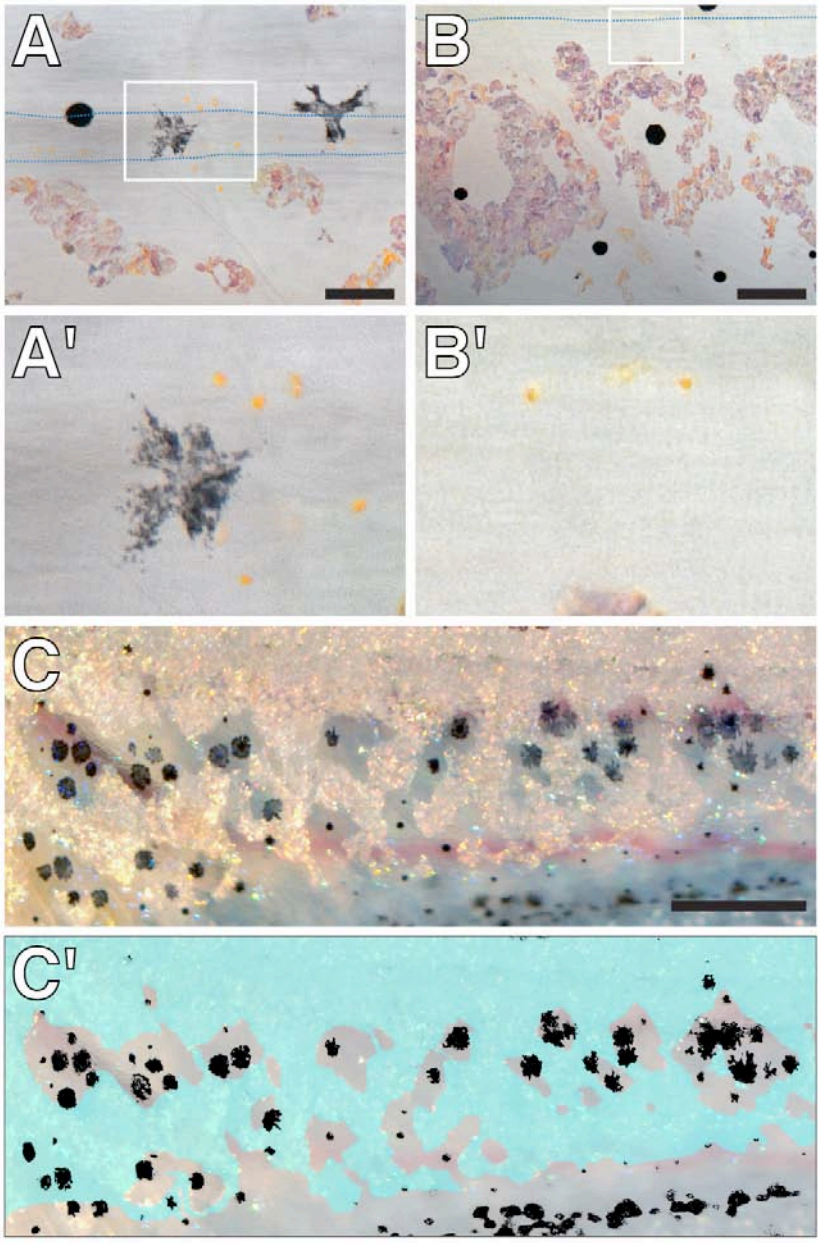

Figure S1.2

Chapter 2

PIGMENT CELL HETEROCHRONIES UNDERLYING STRIPE EVOLUTION IN DANIO FISHES

2.1 Abstract

Teleost fishes have striking and diverse pigment patterns, yet we know little about how evolutionary changes in pigment cell development generate this variation. Adult zebrafish, *Danio rerio*, exhibit light interstripes of yellow xanthophores with abundant, iridescent iridophores that alternate with dark stripes of black melanophores having a few scattered iridophores [1, 2] In contrast, *D. albolineatus* has an evolutionarily derived, uniform pattern in which melanophores, xanthophores and iridophores are intermingled [3, 4]. Here we show that iridophores not only initiate and orient stripes [5, 6], but also form boundaries that terminate developing stripes in *D. rerio*. By contrast, these boundaries do not form in *D. albolineatus*, and ablation of boundary-forming iridophores in *D. rerio* partially recapitulated the *D. albolineatus* pattern of uniform melanophores. Our analyses further show that in *D. albolineatus* xanthophores developed precociously and over a broader area than in *D. rerio*, a change associated with *cis*-regulatory evolution at the xanthogenic Colony stimulating factor-1a (Csf1a) locus. To test if a loss of not only iridophore-derived but also xanthophore-derived positional information might have contributed to stripe loss in *D. albolineatus*, we misexpressed Csf1a in *D. rerio* at stages comparable to those of *D. albolineatus*. Under these conditions, of excess xanthophore differentiation, development of interstripe iridophores was repressed and boundaries that normally terminate melanophore stripes did not form, generating a uniform pattern in which melanophores, xanthophores and iridophores were intermingled, as in *D. albolineatus*. Together we identified evolutionary changes in the development of two pigment cell types that contribute

to the loss of stripes in *D. albolineatus*. These results suggest that heterochronic changes in pigment cell differentiation can have cascading effects on pattern formation and have likely contributed to evolutionary diversification in this group.

2.2 Introduction

The beauty, diversity and ecological importance of animal pigment patterns have attracted the attention of geneticists as well as mathematicians seeking to understand processes of pattern formation. Remarkably, mathematical models, most notably reaction-diffusion models, can predict pattern variation and suggest possible mechanisms for pattern evolution [7, 8]. Thus far, the genes responsible for pattern variation have been identified in only a few cases [9-16]. The pigment patterns of teleost fish are an attractive system for elucidating the genetic underpinnings of species differences and how such differences are translated through changes in cell behavior into differences in adult form. In fish, unlike birds or mammals, pigment cells retain pigment granules intracellularly and are readily visible through the skin [17, 18]. The genus *Danio*, which includes zebrafish *D. rerio*, is a particularly tractable group for studying the molecular and cellular bases of pigment pattern development and evolution [3, 4, 19-21]. Patterns in *Danio* range from stripes and spots to vertical bars and uniform arrangements of pigment cells, and the accessibility of zebrafish and other danios to genetic and cellular manipulation allow one to pose, and test with manipulative experiments, hypotheses for the evolution of pattern-forming mechanisms. Studies of zebrafish adult stripe development have shown that interactions between melanophores and xanthophores are critical for stripe formation and maintenance and involve both short-range inhibitory and long-range activating interactions that fit the requirements for a reaction-diffusion model of pattern formation [22-28]. These interactions, as well as additional

interactions between these cells types and iridophores, constitute a pigment-cell autonomous pattern-generating system that can respond to still unidentified cues to produce stripes in *D. rerio* [5, 6]. How such interactions might have shaped pattern evolution remains unknown. To investigate this question, we chose to compare *D. rerio* to a close relative having a dramatically different adult pigment pattern, *D. albolineatus* [4, 21, 29].

2.3 Results

2.3.1 Iridophores are required for melanophore stripe termination

In zebrafish, two "primary" adult melanophore stripes develop dorsally and ventrally to a primary interstripe; as fish grow, additional interstripes and stripes arise further dorsally and ventrally (Figure 1A, 1C). Iridophores of the primary interstripe are the first adult pigment cells to differentiate and are critical to initiate the patterning of melanophores and xanthophores [5, 6]. We hypothesized that interstripe iridophores are also required to "terminate" developing stripes, thereby initiating the next cycle of interstripe and stripe development. We tested this hypothesis using comparative and experimental and approaches. If iridophores terminate stripes, we predicted that these cells should be fewer, or organized differently, in species lacking stripes. We therefore compared iridophore development during the stages of secondary interstripe formation in *D. rerio* with the equivalent stages of *D. albolineatus* (Figure 1B, 1D) [3, 4]. At three weeks post-fertilization, adult melanophores were evenly distributed along the dorsal–ventral axis in both species (Figure 1E, 1F). Over the next week in *D. rerio*, iridophores differentiated and formed patches of the secondary interstripe, and, as they did so, melanophores within this region either died or evacuated this region by migrating away (Figure 1E; Movie S1). In *D.*

albolineatus, however, no new iridophores appeared, the existing iridophores did not form distinct patches and melanophores remained dispersed (Figure 1F; Movie S2).

The correspondence between iridophore patches and melanophore loss in *D. rerio*, and the absence of iridophore patches and persistence of melanophores in *D. albolineatus*, were both consistent with a role for iridophores in terminating melanophore stripes. Thus, we predicted that a failure of secondary interstripe iridophores to develop should result in an expansion of the primary melanophore stripe. We tested this idea experimentally in *D. rerio* by ablating iridophores before and during secondary interstripe development by administering metrodnidazole to larvae expressing bacterial nitroreductase under control of the iridophore-lineage specific promoter of *purine nucleoside phosphorylase 4a* (*pnp4a*) [6, 30-33]. In genetically mosaic larvae, patches of *pnp4a*+ cells in the primary interstripe were associated with scattered *pnp4a*+ cells extending ventrally through the primary melanophore stripe and into the prospective secondary interstripe (Figure S1A). When these iridophores were ablated, melanophores persisted in this region, causing the primary melanophore stripe to extend further ventrally (Figure 1G, 1H; Figure S1B, S1C) and resulting in a pattern similar to that of *D. albolineatus* (Figure 1D). This suggests that iridophores are required to terminate melanophore stripes (and in so doing, to initiate the next round of interstripe–stripe development) and that evolutionary changes in iridophore development could lead to changes in stripe width or number, as in *D. albolineatus*. Nevertheless, quantitative analyses of melanophore distributions suggested that differences in iridophore development cannot alone account for the pattern difference between species, as melanophores were less evenly distributed even in iridophore-ablated *D. rerio* than in *D. albolineatus* (Figure S1B), possibly owing to limits of long-range trophic

support provided by xanthophores to melanophores [34]. We therefore sought additional explanations for the species difference.

2.3.2 Xanthophores develop precociously in *D. albolineatus*

Previous analyses revealed that *D. albolineatus* have many more xanthophores than *D. rerio*: xanthophores extend well beyond a residual primary interstripe (Figure 1B) and are intermingled with melanophores across the flank [4]. Because interactions between xanthophores and melanophores contribute to stripe formation [22-24], we reasoned that evolutionary changes in when or where xanthophores differentiate could alter the availability of positional information used by melanophores during stripe formation. We therefore compared the timing and anatomical locations of pigment cell differentiation between species (Figure 2A, 2B; Figure S2A). In *D. rerio*, iridophores of the prospective primary interstripe were the first adult pigment cells to differentiate, followed by scattered melanophores and, finally, xanthophores localized to the interstripe [6]. In *D. albolineatus*, however, xanthophores were the first adult pigment cells to develop; these cells differentiated widely across the flank and even were found internally, adjacent to the spinal cord and vertebral column, and within the myotomes, all locations where xanthophores were rarely found in *D. rerio.* Only after xanthophores developed did we observe newly differentiated adult iridophores and, still later, adult melanophores. Thus, *D. rerio* and *D. albolineatus* exhibit heterochronic, and heterotopic, changes in pigment cell differentiation, potentially altering the landscape of positional information available (through pigment cell interactions) for stripe development.

2.3.3 Expression of the xanthogenic factor *csf1* is increased in *D. albolineatus*

Given the extraordinary change in the time and pattern of xanthophore differentiation between species, we sought to uncover its underlying genetic basis. Extensive work in *D. rerio*

has shown that xanthophores and their precursors express the receptor tyrosine kinase, Colony stimulating factor receptor (Csf1r), which is required cell-autonomously for migration, survival and differentiation of this lineage [6, 22, 23, 35]. Genes encoding the ligands for Csf1r, Csf1a and Csf1b, are expressed in the skin of zebrafish larvae and also by adult iridophores, with the latter expression domain accounting for the differentiation of xanthophores in the developing interstripe. Moreover, Csf1 misexpression is sufficient to induce xanthophore differentiation in ectopic locations [6]. Given the critical role for this pathway in xanthophore development, and genetic analyses suggesting an interspecific difference in this pathway between *D. rerio* and *D. albolineatus* [3, 4], we hypothesized that differences in xanthophore differentiation result from corresponding changes in Csf1 expression. We therefore compared by quantitative RT-PCR the abundance of *csf1a* and *csf1b* transcripts between *D. rerio* and *D. albolineatus*, analyzing whole trunks at early larval stages and analyzing separately "internal" tissues (trunks denuded of skin) and the skin itself at later larval stages. We found that *csf1a* and *csf1b* expression were elevated significantly in *D. albolineatus* from early larval stages, and *csf1a* remained elevated, particularly internally and including the surface of the myotomes, even during later larval stages (Figure 2C, Figure S2B). Thus, *D. albolineatus* exhibit a profound upregulation of xanthogenic Csf1 expression, corresponding to the evolutionary heterochrony and heterotopy in xanthophore development in this species as compared to *D. rerio*.

2.3.4 Differences in *csf1a* expression evolved through *cis*-regulatory changes

To better understand the mechanism underlying evolutionary changes in Csf1 expression and xanthophore abundance, we focused on *csf1a*, for which the differences between species lasts into later stages. We sought to determine whether alterations in *csf1a* expression reflect changes in *cis*-regulatory elements of the *csf1a* locus itself, or alterations in *trans*-acting factors that

modulate *csf1a* expression. To test explicitly for *cis*-regulatory differences between *D. rerio* and *D. albolineatus csf1a* orthologues, we crossed these species and compared expression of the two species alleles in the common *trans*-regulatory background of the interspecific hybrid. If differences are *cis*-regulatory in nature, then we should see higher expression of the *D. albolineatus* allele even in the hybrid. If differences are in *trans*, then both alleles should be expressed similarly in the averaged hybrid background. We found by quantitative RT-PCR that the *D. albolineatus csf1a* allele was expressed more highly than the *D. rerio* allele in the hybrid strongly suggesting an interspecific change in *cis*-regulation (Figure 2D).

To further test for *cis*-regulatory differences in *csf1a* expression, we used unpublished (DMP) whole-genome sequence of *D. albolineatus* (aligned to the Ensembl Zv9 whole-genome assembly for *D. rerio* [36]) to identify corresponding ~9 kb regions extending from a conserved distal element to the translational start site of each locus. We then used each of these regions to drive mCherry and generated multiple stable transgenic lines in each species for both *csf1a*^{rerio}*:mCherry and csf1a*^{albolineatus}*:mCherry* (*csf1a*^{alb}*:mCherry*). In more than five independent lines for *csf1a*^{rerio}*:mCherry* (generated in both *D. rerio* and *D. albolineatus*), we were unable to visualize mCherry expression by native fluorescence (Figure 2E); although immunohistochemistry also failed to reveal mCherry, low levels of transgene expression were detectable by RT-PCR (Figure S2D and data not shown). In contrast, we observed robust, and indistinguishable, mCherry expression in all *csf1a*^{alb}*:mcherry* reporter lines in both *D. rerio* and *D. albolineatus* backgrounds. These findings indicate that a change within the proximal 9 kb of the regulatory region confers increased expression to *D. albolineatus csf1a* as compared to *D. rerio csf1a* (Figure 2E).

Similar to expression of *D. rerio* native *csf1a* transcript, as detected by *in situ* hybridization [6], *csf1a*^{alb}*:mCherry* was expressed in the hypodermis, where pigment cells reside, between the epidermis and underlying myotome. We also observed *csf1a*^{alb}*:mCherry* expression in the vicinity of the spinal cord and vertebral column, corresponding to locations where many internal xanthophores develop in *D. albolineatus* (Figure 2F). We have never observed *csf1a* or (*csf1b*) expression in these regions in *D. rerio*, although we cannot rule out the possibility of expression below the limits of detection by *in situ* hybridization. These analyses strongly suggest that, although interstripe iridophores supply Csf1 to promote the development of interstripe xanthophores in *D. rerio* [6], *cis*-regulatory changes in *csf1a* expression have allowed for sites of strong, iridophore-independent Csf1 expression in *D. albolineatus*. To test further if Csf1 expression is entirely decoupled from iridophores in *D. albolineatus*, we assayed *csf1a* and *csf1b* expression in isolated iridophores by RT-PCR: the presence of both transcripts in iridophores of both *D. rerio* and *D. albolineatus* indicates that enhanced expression elsewhere has not been accompanied by the loss of iridophore-specific expression (Figure S2C). Together, these results indicate that *cis*-regulatory changes, at least some of which reside within 9 kb of the *csf1a* start site, have resulted in increased expression of this xanthogenic factor, associated with an earlier and broader domain of xanthophore differentiation in *D. albolineatus* as compared to *D. rerio*.

2.3.5 Timing and Location of Pigment Cell Differentiation Establishes Positional Information Required for Pattern Development

In *D. rerio*, primary interstripe iridophores, as the first pigment cell type to differentiate, provide positional information necessary for xanthophore and melanophore organization into interstripes and stripes, respectively [6]. The evolutionary differences in the timing and pattern of xanthophore and iridophore differentiation in *D. albolineatus*, suggest melanophores of this

species develop in a very different cellular context, in which positional information used for pattern formation is likely to be altered. In turn, we hypothesized that evolutionary changes in differentiation time and location of a single cell type—the xanthophore—could have had cascading effects on pattern formation, mediated by interactions amongst all pigment cell classes, thereby preventing the formation of ancestral stripes [4, 21] in favor of a uniform pattern. We tested this hypothesis by experimentally manipulating xanthophore development in *D. rerio*. We predicted that if *D. rerio* developed earlier, more widespread xanthophores, as in *D. albolineatus*, this might alter the subsequent patterning of melanophores, iridophores, or both, potentially recapitulating the *D. albolineatus* pigment pattern.

To increase xanthophore numbers in *D. rerio* we used a stable transgenic line, *Tg(hsp70l:csf1a-IRES-nCFP*), to overexpress Csf1. To best understand the dynamics of this system, we first supplied excess Csf1 beginning at a relatively late stage (PR+; [37]), after *D. rerio* secondary stripe iridophores had started to develop and also after the species differences in Csf1 expression were apparent. In this context, excess xanthophores were produced and melanophores and xanthophores were partially intermingled, as in *D. albolineatus* (Figure 3A, 3A', 3B, 3B', 3H). Nevertheless, patches of secondary interstripe iridophores still developed as did a normally positioned ventral margin to the primary melanophore stripe, resulting in no significant change in the overall distribution or number of melanophores relative to controls (Figure 3I; Figure S3A). These observations indicate that once an interstripe is established, the resulting boundary is robust to perturbations in xanthophore number.

To more closely approximate the dynamics of pattern formation in *D. albolineatus*, we then supplied excess Csf1a to *D. rerio* at an early stage (AR+), before secondary interstripe iridophores arise in *D. rerio* and corresponding to when increased Csf1 expression and extra

xanthophores are evident in *D. albolineatus*. Under these conditions, we observed supernumerary xanthophores in *D. rerio*, both in the hypodermis and at internal sites corresponding to where xanthophores develop internally in *D. albolineatus* (Figure 3C'C', Figure S3B). Xanthophores were extensively intermingled with melanophores, as in *D. albolineatus* (Figure 3C', 3D', 3H), and, remarkably, primary stripe melanophores extended to the ventral edge of the flank, a distribution significantly different from that of controls but indistinguishable from that of *D. albolineatus* (Figure 3I). Inspection of iridophores revealed that these cells were scattered amongst melanophores across the flank, as in *D. albolineatus* or within melanophore stripes of *D. rerio*, but were not found in patches in the prospective interstripe region, as would normally be true in wild-type *D. rerio*. The absence of interstripe iridophores, and possibly trophic support from xanthophores [34] may have contributed to a significantly increased number of melanophores overall (Figure S3A). Thus, precocious and widespread development of xanthophores is sufficient to "override" the development of secondary interstripe iridophores, and to prevent the normal termination of the primary melanophore stripe.

Our finding that an excess of xanthophores arising only late in development does not alter melanophore distributions (Figure 3B, 3I) is consistent with a role for pre-existing interstripe iridophores in terminating melanophore stripes (e.g., Figure 1G, 1H). A formal alternative possibility would be that other positional cues arising at late stages, independent of iridophores, prevented a xanthophore-mediated expansion of the primary melanophore stripe. To distinguish between these scenarios and further test the role of iridophores in terminating melanophore stripes, we repeated these analyses using the *basonuclin-2* mutant, which has fewer melanophores and xanthophores and also fails to develop secondary interstripe iridophores [31]. We reasoned that if previously developed interstripe iridophores terminate melanophore stripes

at late stages, then iridophore-deficient *basonuclin-2* mutants should exhibit broader stripes whenever excess Csf1a and xanthophores are supplied. Consistent with this expectation, when we supplied excess Csf1a in *basonuclin-2* mutants, beginning at either early or late stages, additional xanthophores and melanophores developed and melanophores distributions were indistinguishable from the melanophore distribution resulting from early Csf1a overexpression in wild-type *D. rerio* as well as the naturally occurring melanophore distribution of *D. albolineatus* (Figure 3E–G, 3I, Figure S3A).

Together, these results suggest that differences in the timing of xanthophore differentiation can have cascading effects on the development of iridophores and melanophores, dramatically altering the pigment pattern.

2.4 Discussion

Our results, together with previous analyses suggest a model through which evolutionary changes in the timing and location of pigment cell differentiation can produce dramatically different pigment patterns. In *D. rerio*, adult stripe development begins with an unknown signal that promotes iridophore differentiation in the primary interstripe [6]. Melanophores differentiate broadly, but avoid settling in the primary interstripe due to short-range inhibitory interactions with iridophores. Xanthophores, in response to Csf1 expressed by iridophores, differentiate within the interstripe region. Additional interactions between all three pigment cells refine the boundary between the primary interstripe and primary stripes by simultaneously repelling melanophores from the interstripe and promoting their settlement nearby. This process is reinitiated when iridophores develop in the secondary interstripe, again in response to an unidentified signal. Secondary interstripe iridophores interact with existing melanophores to

remove them from this region, terminating development of the primary stripe and also promote xanthophore differentiation in the interstripe, presumably through Csf1 signaling. Thus, primary interstripe iridophores provide early positional information that is utilized in all subsequent steps of pattern development. Adult pattern development in *D. albolineatus* begins with an abundant source of iridophore-independent Csf1, which promotes widespread xanthophore differentiation. Unlike primary interstripe iridophores, this uniform distribution of xanthophores lacks positional information. When melanophores and iridophores differentiate they engage in the same types of interactions as they do in *D. rerio*, but without positional information to guide them, the combination of positive and negative interactions experienced by melanophores results in decreased melanophore motility [4]. Melanophores and xanthophores remain dispersed and a uniform pattern results.

The above model does not require changes in the interactions between pigment cells, merely changes in the cellular environment in which those interactions take place. Changes in cell behavior in response to uniform verses localized signals have been observed in other contexts as well [38]. For example spinal ganglion neurons, which express ephrin-B2 and -B3, are repulsed at EphA4 stripe boundaries, by turning, stopping or growth cone termination, but when EphA4 is uniformly distributed, turning is random and no growth cone termination is observed [38]. Even though these cell behaviors are mediated through the same interaction, an asymmetric source of the signal elicits a different response than a global one. In our case, a melanophore that differentiates in the presence of an interstripe filled with iridophores and xanthophores will behave differently than one that differentiates amidst a field of xanthophores, even though it is participating in the same cellular interactions. We propose that changes in the timing of differentiation establish priority effects between pigment cells. In this model, the consequences

of pigment cell interactions depend on the cellular context in which pigment cells develop. The first pigment cell type to differentiate determines whether that cellular context contains positional information or not. If the first cell type to differentiate establishes asymmetries in cell distributions, then all subsequent interactions are initiated from this start point. However, if the first cell type to differentiate does so broadly, directional cues are absent and the other cells likewise interact without direction.

While our results suggest that changes in timing of pigment cell differentiation contribute to pattern differences between *D. rerio* and *D. albolineatus,* they don't rule out additional evolutionary changes. Indeed, several lines of evidence suggest additional evolutionary changes have occurred in either the melanophore or xanthophore lineages. Xanthophores provide trophic support to melanophores in *D. rerio* and when xanthophores are lost, melanophores are also reduced [22, 23, 34]. The opposite is seen, in *D. albolineatus*, which has increased melanophore death despite the presence of numerous xanthophores [4]. Additionally, studies of *kit* mutant *D. albolineatus*, revealed not only that *D. albolineatus* retains latent stripe forming capabilities (at the residual primary interstripe suggesting melanophore-iridophore interactions are conserved in *D. albolineatus*), but also that the numbers of *kit*-independent late metamorphic melanophores are drastically reduced in *D. albolineatus* [21]. Whether these differences reflect evolutionary changes xanthophores, melanophores or both, remains to be explored.

2.5 Materials and Methods

2.5.1 Fish stocks, staging and rearing conditions

D. rerio wild-type stock fish, WT(WA), were produced by crosses between the inbred genetic strains AB^{wp} and wik or the progeny of these crosses. Iridophore-deficient *bonaparte*

mutants are presumptive null alleles *bnc2*^{utr16e1}[31]. *D. albolineatus* stocks were originally obtained from M. McClure and independently from tropical fish suppliers and have been inbred and maintained in the lab for more than 8 generations. Transgenic lines were *Tg(hsp70l:csf1a-IRES-nlsCFP)*$^{wp.r.t4}$, *Tg(csf1a*^{rerio}*:mCherry)*, *Tg(csf1a*^{alb}*:mCherry)* in *D. rerio* and *Tg(csf1a*^{rerio}*:mCherry*), *Tg(csf1a*^{alb}*:mCherry)* in *D. albolineatus*. Post-embryonic staging followed [37]. *D. albolineatus* reached each developmental stage at a larger size than *D. rerio* so criteria such as fin ray development were used as an indicator of stage rather than standardized standard length (SSL). All fish stocks were reared in standard conditions of 14L:10D at 28.5°C. For transgene inductions of *Tg(hsp70l:csf1a-IRES-nlsCFP)*$^{wp.r.t4}$, fish were heat-shocked at 38°C twice daily for 1 h beginning at 6.0SSL and continuing until they reached 11SSL (+Csf1 early) or beginning at 9.5SSL until 11SSL (+Csf1 late).

2.5.2 Transgene construction and microinjection

To generate *csf1a* reporter lines, we cloned ~9 kb proximal to the *csf1a* start site from both species into a 5' Gateway vector using isothermal single reaction assembly cloning, allowing us to insert this region in precisely the same location in the backbone [39, 40]. Transgenes were then assembled by Gateway cloning of entry plasmids into pDestTol2CG2 vector containing Tol2 repeats for efficient genomic integration and *cmlc2:EGFP* as a transgenesis marker [41, 42]. Microinjection of plasmids and *Tol2* mRNA followed standard methods. Progeny of F0 injected fish were screened for *cmlc2:EGFP* expression and used to establish stable transgenic lines(*Tg(csf1a*^{rerio}*:mCherry)*, *n=5; Tg(csf1a*^{alb}*:mCherry, n=3)* in *D. rerio* and *Tg(csf1a*^{rerio}*:mCherry*), *n*=1; *Tg(csf1a*^{alb}*:mCherry), n*=3 in *D. albolineatus*). For ablating secondary interstripe iridophores in larvae mosaic for plasmid *pnp4a*:nlsVenus-V2a-NTR we followed [6], starting MTZ treatment at 8.5-9.0SSL.

2.5.3 RT-PCR and Quantitative RT-PCR

For quantitative RT-PCR in *D. rerio* and *D. albolineatus*, skins and underlying tissue were collected from AR+, DR+, PB+ and J stage larvae. To generate interspecific hybrids for quantitative RT-PCR, a *D. rerio* female was crossed to a *D. albolineatus* male by *in vitro* fertilization and resulting larvae were collected at AR+. All tissues were placed directly into either Trizol Reagent (Invitrogen) or RNalater (Ambion). RNA was isolated using either RNaqueous Microkit (Ambion) or Trizol, followed by LiCl precipitation. cDNA was synthesized with iScript cDNA Synthesis Kit (Bio-Rad). Quantitative RT-PCRs were performed and analyzed on a StepOnePlus System (Life Technologies) using Custom Taqman Gene Expression Assays designed to bind either conserved sites (*csf1a, csf1b, rpl13a*) or species specific sites (*csf1a* hybrid analysis) and Taqman Gene Expression Master Mix (Life Technologies).

To detect *mCherry* transcripts in *D. rerio Tg*($csf1a^{rerio}$*:mcherry*) and *Tg*($csf1a^{alb}$*:mcherry*), individual larvae were collected at stage PR. Heads and tails were removed and trunks were placed in RNalater (Ambion). RNA was isolated using Direct-zol RNA Kit (Zymo Research, R2050) and cDNA synthesized using iScript cDNA Synthesis Kit (Bio-Rad). For RT-PCR of isolated iridophores, late metamorphic/early juvenile larvae were euthanized and skins were collected in PBS. Skins were vortexed briefly to remove scales, then spun down and washed again in PBS. Tissue was incubated 10 min at 37ºC in 0.25% Tyrpsin-EDTA (Invitrogen). Trypsin was removed and tissue incubated 10 min at 37°C in tyrpsin-inhibitor (Sigma T6414) with 3 mg/ml collagenase, and 2µl Dnase I, RNase-Free (Thermo Scientific), followed by gentle pipetting until skins were completely dissociated. Cells were then washed in PBS and filtered through a 40um cell strainer. Cell were placed on a glass bottom dish and examined on a Zeiss Observer inverted compound microscope. A minimum of 50 iridophores were picked up using a

Narishige 1M 9B microinjector, expelled into PBS, then repicked and expelled directly into Resuspension Buffer. cDNA was synthesized using Superscript III Cells Direct cDNA Synthesis Kit (Invitrogen). RT-PCR was performed with the following primer sets (forward, reverse): *actb1,* ACTGGGATGACATGGAGAAGAT, GTGTTGAAGGTCTCGAACATGA*;* *csf1a,* CAACAACTGAGCCAACACATAAATA, GGGATCTGTGGTCTTTGCTGAT*;* *csf1b,* AACACCCCTGTTAACTGGACCT, GAGGCAGTAGGCAGTGAGAAGA*;* *mdkb,* AGTGAATGGCAGTATGGGAAAT*,* TGGACACTTTAATGGTGGTCTG; *mCherry,* CCAGCTTGATGTTGACGTTG, AGGACGGCGAGTTCATCTAC*;* *pnp4a,* GAAAAGTTTGGTCCACGATTTC, TACTCATTCCAACTGCATCCAC.

2.5.4 Immunohistochemistry

For immunohistochemistry, fish were fixed in 4% paraformaldehyde for 30 minutes at room temperature, washed with PBS, transferred to 15% sucrose, followed by 30% sucrose, and then embedded and frozen in OCT media. Cyrosections of 20μm thickness were collected on microfrost slides and allowed to dry. Slides were washed in PBS and then fixed in 4% paraformaldehyde for 10 minutes at room temperature followed by additional PBS washes. Sections were blocked in PBS containing 5% heat inactivated goat serum and 0.1% Triton-X, then incubated overnight at 4°C with primary antibody. Antibodies used were monoclonal rat anti-mCherry (1:250; Life Technologies, M11217), and polyclonal rabbit anti-Human bnc2 antibody (1:350; P. Djian [43]). After washes, slides were incubated with secondary antibodies (Alexa Fluor 488, 568), washed in PBS and imaged on Zeiss Observer Spinning Disc.

2.5.5 Imaging and Quantitative Analysis

Fish were imaged on an Olympus SZX-12 stereomicroscope, Zeiss Axioplan 2 compound

microscope or Zeiss Observer inverted compound microscope using Zeiss Axiocam HR, MRC and spinning disc cameras and Axiovision software.

To quantify melanophore dorsal-ventral position, we measured the distance of each melanophore to the dorsal and ventral margins of the myotome and divided dorsal length by the total distance. For *pnp4a*:nlsVenus-V2a-NTR mosaic ablations and controls, positions were determined for all melanophores ventral to the horizontal myoseptum, in the area bordered by the anterior and posterior ends of the anal fin. For *D. albolineatus*, *D. rerio*, *D. rerio bonaparte* mutants, and induced *Tg(hsp70l:csf1a-IRES-nlsCFP)*$^{wp.r.t4}$, positions were determined for all melanophores ventral to the horizontal mysoseptum, in the anterior third of the area between the anterior and posterior ends of the anal fin.

To determine whether melanophore and xanthophore were intermingled k-nearest-neighbour (kNN) classification was conducted using a MATLAB routine written in-house (MATLAB R2011a, Mathworks, Natick, MA, USA). For each fish, an average of the five nearest neighbour distances were calculated for each cell from images taken at the border of the ventral melanophore stripe and the secondary ventral iridophore stripe or this presumptive region from images that did show iridophores in this region.

2.6 Acknowledgements

Michael Nishizaki for pigment cell k-nearest-neighbor (kNN) analysis in MATLAB, Jessica Spiewak for performing AC stage quantitative RT-PCR, Anna McCann for staging and embedding fish for cyrosectioning, Amandine Vanhoutteghem and Philippe Djian for Bnc2 antibody.

2.7 References

1. Johnson, S.L., Africa, D., Walker, C., and Weston, J.A. (1995). Genetic control of adult pigment stripe development in zebrafish. Developmental biology *167*, 27-33.
2. Parichy, D.M., and Turner, J.M. (2003). Zebrafish puma mutant decouples pigment pattern and somatic metamorphosis. Developmental biology *256*, 242-257.
3. Parichy, D.M., and Johnson, S.L. (2001). Zebrafish hybrids suggest genetic mechanisms for pigment pattern diversification in Danio. Development genes and evolution *211*, 319-328.
4. Quigley, I.K., Manuel, J.L., Roberts, R.A., Nuckels, R.J., Herrington, E.R., MacDonald, E.L., and Parichy, D.M. (2005). Evolutionary diversification of pigment pattern in Danio fishes: differential fms dependence and stripe loss in D. albolineatus. Development *132*, 89-104.
5. Frohnhofer, H.G., Krauss, J., Maischein, H.M., and Nusslein-Volhard, C. (2013). Iridophores and their interactions with other chromatophores are required for stripe formation in zebrafish. Development *140*, 2997-3007.
6. Patterson, L.B., and Parichy, D.M. (2013). Interactions with iridophores and the tissue environment required for patterning melanophores and xanthophores during zebrafish adult pigment stripe formation. PLoS genetics *9*, e1003561.
7. Meinhardt, H., and Gierer, A. (1974). Applications of a theory of biological pattern formation based on lateral inhibition. Journal of cell science *15*, 321-346.
8. Meinhardt, H., and Gierer, A. (2000). Pattern formation by local self-activation and lateral inhibition. BioEssays : news and reviews in molecular, cellular and developmental biology *22*, 753-760.
9. Gompel, N., Prud'homme, B., Wittkopp, P.J., Kassner, V.A., and Carroll, S.B. (2005). Chance caught on the wing: cis-regulatory evolution and the origin of pigment patterns in Drosophila. Nature *433*, 481-487.
10. Prud'homme, B., Gompel, N., Rokas, A., Kassner, V.A., Williams, T.M., Yeh, S.D., True, J.R., and Carroll, S.B. (2006). Repeated morphological evolution through cis-regulatory changes in a pleiotropic gene. Nature *440*, 1050-1053.
11. Werner, T., Koshikawa, S., Williams, T.M., and Carroll, S.B. (2010). Generation of a novel wing colour pattern by the Wingless morphogen. Nature *464*, 1143-1148.
12. Reed, R.D., Papa, R., Martin, A., Hines, H.M., Counterman, B.A., Pardo-Diaz, C., Jiggins, C.D., Chamberlain, N.L., Kronforst, M.R., Chen, R., et al. (2011). optix drives the repeated convergent evolution of butterfly wing pattern mimicry. Science *333*, 1137-1141.
13. Kaelin, C.B., Xu, X., Hong, L.Z., David, V.A., McGowan, K.A., Schmidt-Kuntzel, A., Roelke, M.E., Pino, J., Pontius, J., Cooper, G.M., et al. (2012). Specifying and sustaining pigmentation patterns in domestic and wild cats. Science *337*, 1536-1541.
14. Roberts, R.B., Ser, J.R., and Kocher, T.D. (2009). Sexual conflict resolved by invasion of a novel sex determiner in Lake Malawi cichlid fishes. Science *326*, 998-1001.
15. Miller, C.T., Beleza, S., Pollen, A.A., Schluter, D., Kittles, R.A., Shriver, M.D., and Kingsley, D.M. (2007). cis-Regulatory changes in Kit ligand expression and parallel evolution of pigmentation in sticklebacks and humans. Cell *131*, 1179-1189.
16. Manceau, M., Domingues, V.S., Mallarino, R., and Hoekstra, H.E. (2011). The developmental role of Agouti in color pattern evolution. Science *331*, 1062-1065.

17. Bagnara, J.T.M., J. (2006). Comparative Anatomy and Physiology of Pigment Cells in Nonmammalian Tissues. In The Pigmentary System: Physiology and Pathophysiology, Second Edition, J.J.N.R.E.B.V.J.H.R.A.K.W.S.O.a.J.-P. Ortonne, ed. (Oxford, UK: Blackwell Publishing Ltd).
18. Parichy, D.M., Reedy, M. V. and Erickson, C. A. (2006). Regulation of Melanoblast Migration and Differentiation. In The Pigmentary System: Physiology and Pathophysiology, Second Edition, R.E.B. J. J. Nordlund, V. J. Hearing, R. A. King, W. S. Oetting and J.-P. Ortonne, ed. (Oxford, UK: Blackwell Publishing Ltd).
19. Quigley, I.K., Turner, J.M., Nuckels, R.J., Manuel, J.L., Budi, E.H., MacDonald, E.L., and Parichy, D.M. (2004). Pigment pattern evolution by differential deployment of neural crest and post-embryonic melanophore lineages in Danio fishes. Development *131*, 6053-6069.
20. Parichy, D.M. (2006). Evolution of danio pigment pattern development. Heredity *97*, 200-210.
21. Mills, M.G., Nuckels, R.J., and Parichy, D.M. (2007). Deconstructing evolution of adult phenotypes: genetic analyses of kit reveal homology and evolutionary novelty during adult pigment pattern development of Danio fishes. Development *134*, 1081-1090.
22. Parichy, D.M., and Turner, J.M. (2003). Temporal and cellular requirements for Fms signaling during zebrafish adult pigment pattern development. Development *130*, 817-833.
23. Maderspacher, F., and Nusslein-Volhard, C. (2003). Formation of the adult pigment pattern in zebrafish requires leopard and obelix dependent cell interactions. Development *130*, 3447-3457.
24. Inaba, M., Yamanaka, H., and Kondo, S. (2012). Pigment pattern formation by contact-dependent depolarization. Science *335*, 677.
25. Nakamasu, A., Takahashi, G., Kanbe, A., and Kondo, S. (2009). Interactions between zebrafish pigment cells responsible for the generation of Turing patterns. Proceedings of the National Academy of Sciences of the United States of America *106*, 8429-8434.
26. Takahashi, G., and Kondo, S. (2008). Melanophores in the stripes of adult zebrafish do not have the nature to gather, but disperse when they have the space to move. Pigment cell & melanoma research *21*, 677-686.
27. Yamaguchi, M., Yoshimoto, E., and Kondo, S. (2007). Pattern regulation in the stripe of zebrafish suggests an underlying dynamic and autonomous mechanism. Proceedings of the National Academy of Sciences of the United States of America *104*, 4790-4793.
28. Kondo, S., Iwashita, M., and Yamaguchi, M. (2009). How animals get their skin patterns: fish pigment pattern as a live Turing wave. The International journal of developmental biology *53*, 851-856.
29. He, S., Mayden, R.L., Wang, X., Wang, W., Tang, K.L., Chen, W.J., and Chen, Y. (2008). Molecular phylogenetics of the family Cyprinidae (Actinopterygii: Cypriniformes) as evidenced by sequence variation in the first intron of S7 ribosomal protein-coding gene: further evidence from a nuclear gene of the systematic chaos in the family. Molecular phylogenetics and evolution *46*, 818-829.
30. Curran, K., Lister, J.A., Kunkel, G.R., Prendergast, A., Parichy, D.M., and Raible, D.W. (2010). Interplay between Foxd3 and Mitf regulates cell fate plasticity in the zebrafish neural crest. Developmental biology *344*, 107-118.

31. Lang, M.R., Patterson, L.B., Gordon, T.N., Johnson, S.L., and Parichy, D.M. (2009). Basonuclin-2 requirements for zebrafish adult pigment pattern development and female fertility. PLoS genetics *5*, e1000744.
32. Curado, S., Stainier, D.Y., and Anderson, R.M. (2008). Nitroreductase-mediated cell/tissue ablation in zebrafish: a spatially and temporally controlled ablation method with applications in developmental and regeneration studies. Nature protocols *3*, 948-954.
33. Pisharath, H., Rhee, J.M., Swanson, M.A., Leach, S.D., and Parsons, M.J. (2007). Targeted ablation of beta cells in the embryonic zebrafish pancreas using E. coli nitroreductase. Mechanisms of development *124*, 218-229.
34. Hamada, H., Watanabe, M., Lau, H.E., Nishida, T., Hasegawa, T., Parichy, D.M., and Kondo, S. (2013). Involvement of Delta/Notch signaling in zebrafish adult pigment stripe patterning. Development.
35. Parichy, D.M., Ransom, D.G., Paw, B., Zon, L.I., and Johnson, S.L. (2000). An orthologue of the kit-related gene fms is required for development of neural crest-derived xanthophores and a subpopulation of adult melanocytes in the zebrafish, Danio rerio. Development *127*, 3031-3044.
36. Howe, K., Clark, M.D., Torroja, C.F., Torrance, J., Berthelot, C., Muffato, M., Collins, J.E., Humphray, S., McLaren, K., Matthews, L., et al. (2013). The zebrafish reference genome sequence and its relationship to the human genome. Nature *496*, 498-503.
37. Parichy, D.M., Elizondo, M.R., Mills, M.G., Gordon, T.N., and Engeszer, R.E. (2009). Normal table of postembryonic zebrafish development: staging by externally visible anatomy of the living fish. Developmental dynamics : an official publication of the American Association of Anatomists *238*, 2975-3015.
38. Brors, D., Bodmer, D., Pak, K., Aletsee, C., Schafers, M., Dazert, S., and Ryan, A.F. (2003). EphA4 provides repulsive signals to developing cochlear ganglion neurites mediated through ephrin-B2 and -B3. The Journal of comparative neurology *462*, 90-100.
39. Gibson, D.G., Young, L., Chuang, R.Y., Venter, J.C., Hutchison, C.A., 3rd, and Smith, H.O. (2009). Enzymatic assembly of DNA molecules up to several hundred kilobases. Nature methods *6*, 343-345.
40. Gibson, D.G., Smith, H.O., Hutchison, C.A., 3rd, Venter, J.C., and Merryman, C. (2010). Chemical synthesis of the mouse mitochondrial genome. Nature methods *7*, 901-903.
41. Urasaki, A., Morvan, G., and Kawakami, K. (2006). Functional dissection of the Tol2 transposable element identified the minimal cis-sequence and a highly repetitive sequence in the subterminal region essential for transposition. Genetics *174*, 639-649.
42. Kwan, K.M., Fujimoto, E., Grabher, C., Mangum, B.D., Hardy, M.E., Campbell, D.S., Parant, J.M., Yost, H.J., Kanki, J.P., and Chien, C.B. (2007). The Tol2kit: a multisite gateway-based construction kit for Tol2 transposon transgenesis constructs. Developmental dynamics : an official publication of the American Association of Anatomists *236*, 3088-3099.
43. Vanhoutteghem, A., and Djian, P. (2006). Basonuclins 1 and 2, whose genes share a common origin, are proteins with widely different properties and functions. Proceedings of the National Academy of Sciences of the United States of America *103*, 12423-12428.

2.8 Figure Legends

Figure 1: Iridophores terminate ventral melanophore stripe in *D. rerio*

(A) *D. rerio* young adult, boxed region shown in C. (B) *D. albolineatus* young adult, boxed region shown in D. Double blue arrowheads denote iridophores in residual primary interstripe. (C) In *D. rerio*, iridophores and xanthophores are found in the primary and secondary interstripes (1I, 2Iv). Iridophores also associate with melanophores in the primary ventral stripe (1V, blue arrow). (D) In *D. albolineatus* iridophore aggregations outside of a residual primary interstripe are drastically fewer, although scattered iridophores are present (blue arrow). (E,F) Pigment cell distributions in representative *D. rerio* (D) and *D. albolineatus* (E) imaged daily during the stages of secondary interstripe development in *D. rerio* (beginning at three weeks post-fertilization; PB+[37]). (E) In *D. reri*o scattered iridophores were intermingled with melanophores (blue arrow), iridophores then organize to form the secondary interstripe (blue arrowhead) and melanophores in this region either die (yellow circles) or migrate short distances dorsally or ventrally (red dashed arrow). Xanthophores later develop in interstripe (green circle). Blue bar in rightmost panel, approximate dorsoventral extent of interstripe iridophores. Also see: Supplementary Movie S1. (F) *D. albolineatus* (stage-matched to *D. rerio* in E) had widely distributed melanophores and xanthophores (green arrowheads) and few iridophores extending ventrally from the primary interstripe region (blue arrow). During this time, no new iridophores appeared, those present at the start did not expand ventrally and melanophores remained broadly distributed. (G, H) Ablating iridophores during adult stripe formation in fish mosaic for *pnp4a*:nlsVenus-V2a-NTR, results in broadly dispersed melanophores (MTZ), compared to control individuals, which develop iridophores and form stripes (DMSO).

Blue bar in G, approximate dorsoventral extent of interstripe iridophores; See also

Supplementary Figure S1.

Figure 2: Precocious xanthophore development in *D. albolineatus* is associated with evolutionary differences in Csf1 expression

(A) Differences in adult pattern development are apparent between *D. rerio* and *D. albolineatus* by two weeks post-fertilization (AR+). At this stage, *D. rerio* had developed iridophores in the primary interstripe (blue arrowheads), just ventral to the horizontal myoseptum (hm); melanophores present have persisted from the embryonic/early larval pattern. At the same stage, *D. albolineatus* exhibited xanthophores already dispersed widely over the flank (e.g., green arrowheads) between the skin and myotomes. Additional xanthophores were evident internally in the vicinity of the spinal cord, and vertebral column (v), and within the myotomes. (B) The relative timing of pigment cell differentiation differs between species. Shown are the first appearances (mean±SE) of pigment cell classes for each species in larvae reared individually (*D. rerio*, n=5; *D. albolineatus*, n=3; species x cell-type interaction: $F_{2,18}$=158, P<0.0001). For details see Supplementary Figure S2A. (C) Increased *csf1a* expression in *D. albolineatus*. Shown are the relative abundances (means±SE) of *csf1a* transcript in *D. rerio* and *D. albolineatus* as assayed across stages by quantitative RT-PCR, using internal trunk tissues (i.e., denuded of skin). Levels in *D. rerio* are set to 1 for each stage and comparisons made within stages (see Methods). ***, P<0.0001; *, P<0.05. See Supplemental Figure S2B for relative transcript abundances for *csf1a* and *csf1b* in both internal tissues and in isolated skin. (D) Increased *csf1a* expression in *D. albolineatus* compared to *D. rerio* reflects differences in cis-regulation revealed by quantitative RT-PCR for species-specific expression of *csf1a* alleles in hybrids. Level of the *D. rerio* allele was set to 1 in each hybrid; means±SE are shown. Paired t=12.8, d.f.=4, P<0.0005. (E) mCherry expression in AR+ stage *Tg*(*csf1a*^{rerio}*:mcherry*) and *Tg*(*csf1a*^{alb}*:mcherry*)

in *D. rerio* and *D. albolineatus*. No fluorescence was detectable in either species transgenic for *csf1a*^{rerio}*:mCherry*, but robust mCherry expression was visible in the hypodermis in both species transgenic for *csf1a*^{alb}*:mCherry*. Images shown for *csf1a*^{rerio}*:mCherry* were exposed twice as long as for *csf1a*^{alb}*:mCherry*. (F) Immunohistochemistry in transverse sections of AR+ stage *D. rerio Tg*(*csf1a*^{alb}*:mCherry*), show mCherry (magenta) in hypodermal cells, but not *bnc2*+ cells (green) (left), as well as internally, surrounding the vertebral column and spinal cord (middle). Internal staining for mCherry in *Tg*(*csf1a*^{alb}*:mcherry*), correlates with sites of internal xanthophores in AR+ stage *D. albolineatus* (right).

Figure 3: Timing of interactions between xanthophores and iridophores are critical for stripe pattern formation

(A-D) Brightfield images showing melanophore patterns above the anal fin in Tg(*hsp70l:csf1a*) *D. rerio* and *D. albolineatus*. When Tg(*hsp70l:csf1a*) is induced after the secondary interstripe has begun to develop (+Csf1 late), melanophores formed stripes, as they do in control *D. rerio* (stripe width indicated by red bar at left edge of images). However, when Tg(*hsp70l:csf1a*) inductions began in *D. rerio* at AR+ (+Csf1 early), melanophores extended all the way to the ventral edge of the myotomes, as they do in *D. albolineatus* (as show by red line on left side of image). (See also Supplementary Figure S3). (A'-D') High magnification images of xanthophore, melanophore and iridophores distributions. In *D. rerio* control and +Csf1 late, iridophores developed into secondary interstripes and melanophores were organized into stripes, although xanthophores were found in the stripe region when Csf1 was increased. Images taken at the corresponding region in *D. rerio*, following early induction of Tg(*hsp70l:csf1a*) (+Csf1 Early), revealed only scattered iridophores and intermingled melanophores and xanthophores throughout this region, similar to *D. albolineatus*. Blue arrowheads, densely organized

iridophores of the secondary interstripe; blue arrows, scattered iridophores. (E-G) Regardless of the timing of Tg(*hsp70l:csf1a*) inductions, iridophore-deficient *bonaparte* mutants developed increased xanthophores and melanophores and never formed stripes. (H) Ratio nearest-neighbor melanophore-xanthophore distances over melanophore-melanophores distances reveals melanophore-xanthophore structure in wild-type *D. rerio*, and decreased distances indicating intermingling in *D. rerio* whenever excess xanthophores develop as a result of increased Csf1, similarly to *D. albolineatus*. Shown are means±SE; letters indicate means that were not significantly different from one another ($P>0.05$) in Tukey Kramer post hoc comparisons (overall $F_{3,27}=7.3$, $P=0.001$). (I) Quantification of melanophore distributions ventral to the horizontal myoseptum, where 0.5 on the y-axis corresponds to the horizontal myoseptum and 1 corresponds to the ventral edge of the myotomes. Differently colored bars indicate means that are not significantly different from one another in Tukey-Kramer post hoc comparisons (for clarity only a subset of means comparisons are shown). Letters in the lower right of each plot indicate distributions in which the frequencies of melanophores in the ventral region of the flank, corresponding to the normal location of the secondary ventral interstripe (at D–V positions 0.8–0.9), did not differ significantly from one another by contingency table analysis: e.g., melanophore distributions in control *D. rerio* did not differ significantly from +Csr1 late *D. rerio* ($\chi^2=0.3$, d.f.=2, $P<0.0001$; $N=235$ melanophores) but did differ from +Csf1 early *D. rerio* ($\chi^2=25.1$, d.f.=2, $P<0.0001$; $N=412$) and other phenotypes shown (all $P<0.0001$); by contrast, the distribution of melanophores in *D. rerio* +Csf1 early did not differ significantly from that of *D. albolineatus* ($\chi^2=3.4$, d.f.=2, $P=0.2$; $N=654$). Fish sample sizes: *D. rerio* $n=13$; *D. rerio* +Csf1 late, $n=14$; *D. rerio* +Csf1 early, $n=8$; *bon*, $n=10$; *bon* +Csf1 late, $n=10$; *bon* +Csf1 early, $n=9$; *D. albolineatus*, $n=7$)

Supplemental Figure S1: Secondary interstripe iridophores terminate melanophore stripes in *D. rerio*

(A) Patch of iridophores expressing nlsVenus in the primary interstripe with scattered nlsVenus positive cells extending ventrally in wild-type *D. rerio* injected at the one cell stage with *pnp4a*:nlsVenus-2a-NTR. (B) Quantification of melanophore distributions ventral to the horizontal myoseptum in control, unablated *D. rerio* (left, n=5 fish), and iridophore-ablated *D. rerio* (middle, n=4 fish), and wild-type *D. albolineatus* (right, n=7 fish). Although significantly more melanophores were found in the ventral region of the flank (D–V positions 0.9–1.0) in iridophore-ablated *D. rerio* as compared to control *D. rerio* (χ^2=15.0, d.f.=2, P<0.001; N=103 melanophores), even ablated individuals exhibited melanophore distributions less uniform than that observed in *D. albolineatus*. (C) Detail of A showing iridophore and melanophore behaviors during secondary interstripe development in *pnp4a*:nlsVenus-V2a-NTR injected larvae treated with MTZ (below) and control siblings (above).

Supplemental Figure S2: Heterochronic shift in xanthophore development correlates with increased *csf1* expression in *D. albolineatus*

(A) First appearances of the three pigment cell classes in representative *D. rerio* (left) and *D. albolineatus* (right) individuals imaged daily through the stages of adult pigment pattern formation. Days post-fertilization shown in upper left of each frame. Prior to the onset of adult pigment pattern development, embryonic melanophores were found along the horizontal myoseptum; no adult pigment cell were present and the two species were practically indistinguishable. By 15 dpf, the first iridophore differentiated in *D. rerio* (blue circle, inset) and the first xanthophore has appeared in *D. albolineatus* (green circle, inset). In *D. rerio*, melanophores were the next cell type to appear (yellow circle, d17) and xanthophores (green

circle and inset, day 24) appeared about a week later, after iridophores had filled the primary interstripe. In *D. albolineatus*, xanthophores were the first pigment cell type to develop (green circle and inset, d15), doing so independently of iridophores. Iridophore differentiated subsequently (blue circle and inset, d24) but did not fill the interstripe region as in *D. rerio.* Melanophores developed only much later (yellow circle, d41). (B) Results of quantitative RT-PCR (means±SE) comparing *csf1a* and *csf1b* expression in trunks denuded of skin (internal) and skins of *D. rerio* and *D. albolineatus* at four distinct developmental stages [37]. Within each stage, expression of the zebrafish locus is set to 1. ***$P<0.0001$, *$P<0.05$. (C) *D. albolineatus* iridophores express *csf1a* and *csf1b*, similar to *D. rerio* iridophores[6]. Shown are RT-PCR amplifications for isolated iridophores (irid) and skins with pigment cells for *actinb1,* the iridophore marker, *pnp4a*, *csf1a* and *csf1b* in *D. rerio* and *D. albolineatus*. nt, no template control. (D) The *D. rerio Tg*(*csf1a*^{rerio}*:mcherry*) is expressed at low levels. Shown are RT-PCR amplifications for *mCherry* and *mdkb* transcripts isolated from larval (AR+) *Tg*(*csf1a*^{rerio}*:mCherry*) *D. rerio* and *Tg*(*csf1a*^{alb}*:mCherry*) *D. rerio*. *mdkb* serves as an input control and amplifies an 259 bp fragment from cDNA and a 334 bp fragment from genomic DNA (gDNA), demonstrating the absence of genomic DNA contamination in RT-PCR samples.

Supplemental Figure S3: Melanophore numbers are increased in wild-type and *bonaparte* mutant larvae by early over-expression of *csf1a*

(A) Inducing Tg(*hsp70l:csf1a*), beginning at AR+, resulted in significantly increased melanophores numbers in wild-type *D. rerio* (+Csf1 early), but inducing expression after the start of secondary interstripe development did not significantly alter melanophore numbers (+Csf1 late). In *basonuclin-2* mutants, melanophore numbers were significantly increased

regardless of when Csf1 expression began. Plot shows means±SE; letters over bars denote means that are not significantly different from one another in Tukey Kramer post hoc comparisons.

Figures 2.9

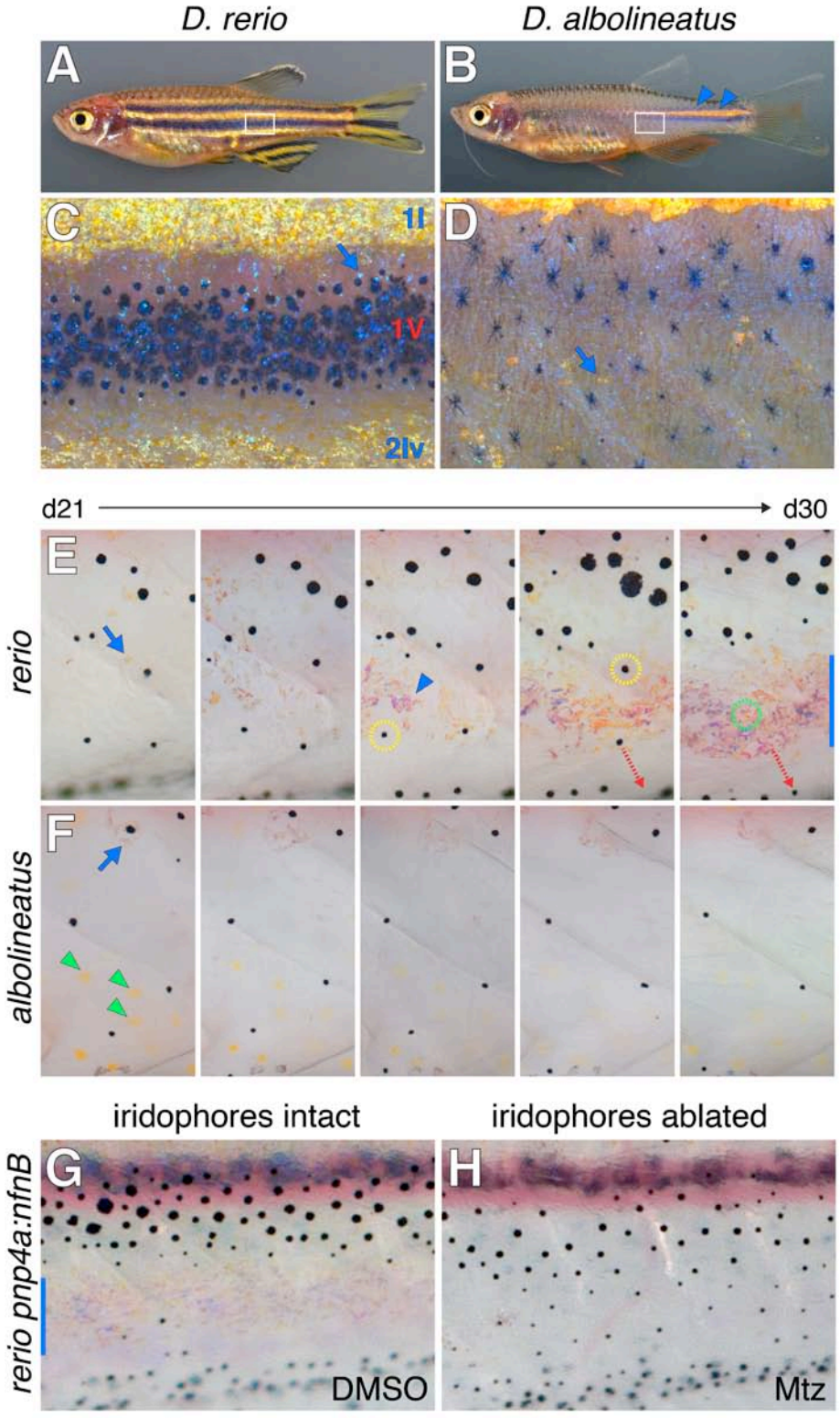

Figure 2.1

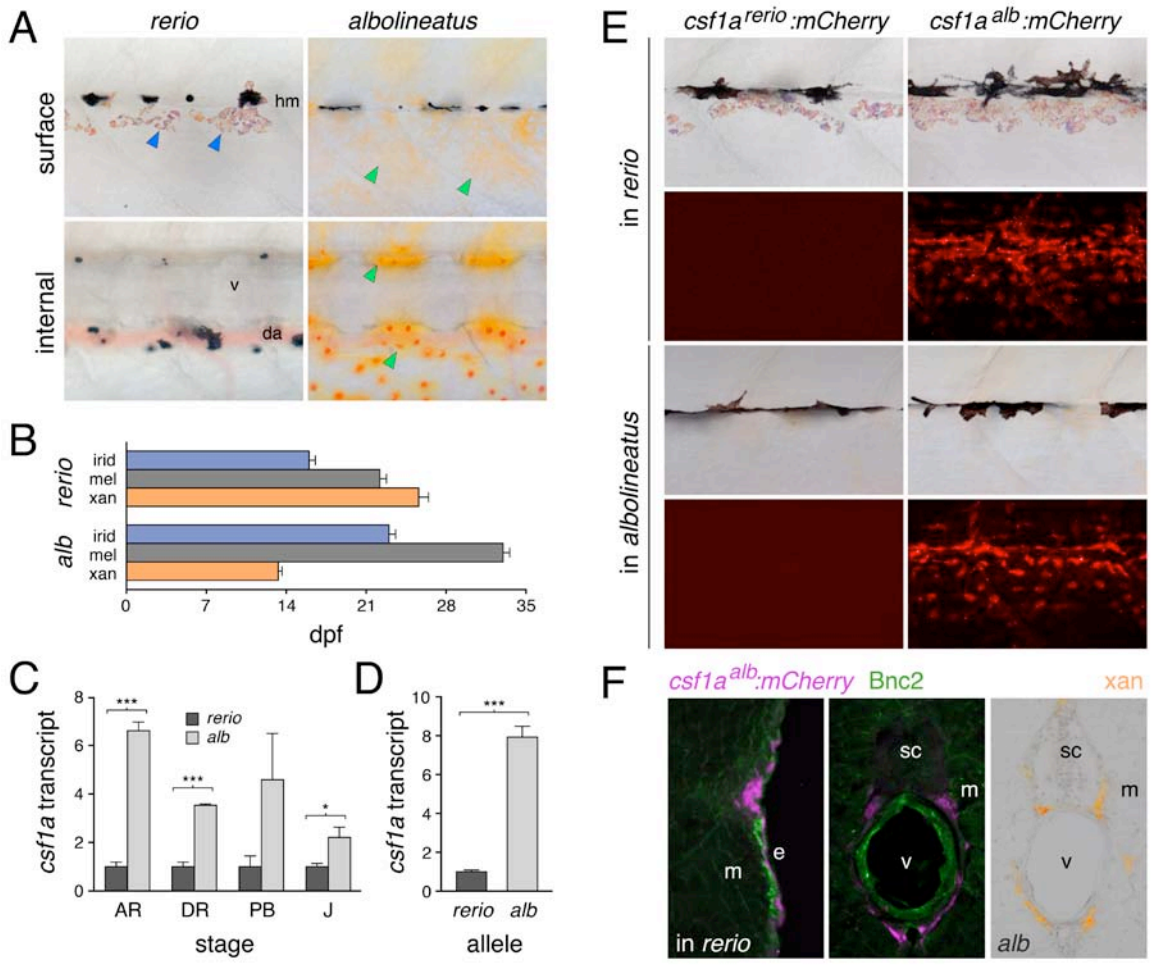
A
rerio
albolineatus
surface
internal
hm
v
da
B
rerio
alb
irid
mel
xan
0
7
14
21
28
35
dpf
C
csf1a transcript
rerio
alb
AR
DR
PB
J
stage
D
csf1a transcript
rerio
alb
allele
E
csf1a rerio :mCherry
csf1a alb :mCherry
in rerio
in albolineatus
F
csf1a alb :mCherry
Bnc2
xan
sc
m
e
v
in rerio
alb

Figure 2.2

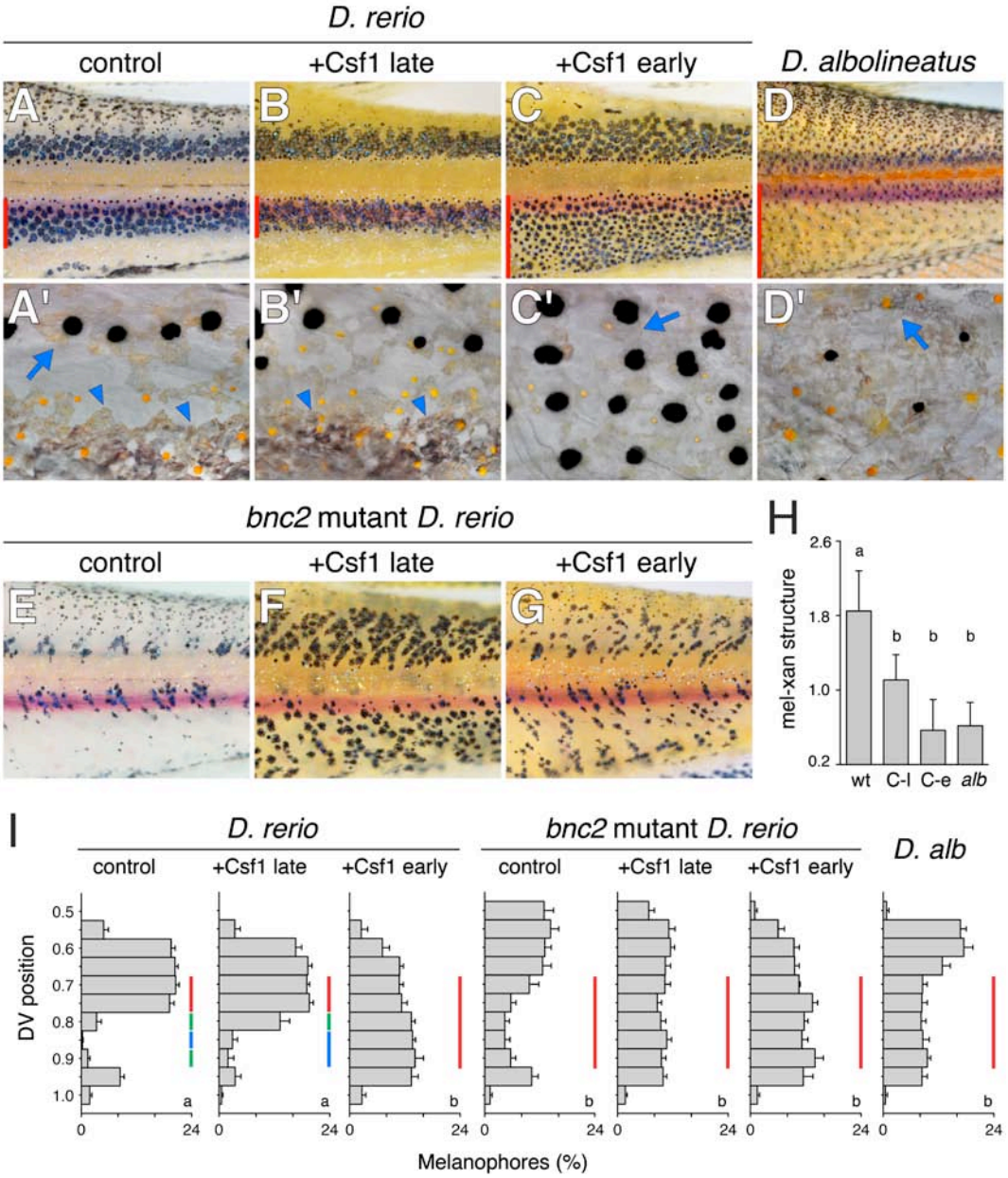
D. rerio
control
+Csf1 late
+Csf1 early
D. albolineatus
A
B
C
D
A'
B'
C'
D'
bnc2 mutant D. rerio
control
+Csf1 late
+Csf1 early
E
F
G
H
mel-xan structure
2.6
1.8
1.0
0.2
a
b
b
b
wt
C-l
C-e
alb
I
D. rerio
bnc2 mutant D. rerio
D. alb
control
+Csf1 late
+Csf1 early
control
+Csf1 late
+Csf1 early
DV position
0.5
0.6
0.7
0.8
0.9
1.0
a
a
b
b
b
b
b
0
24
Melanophores (%)

Figure 2.3

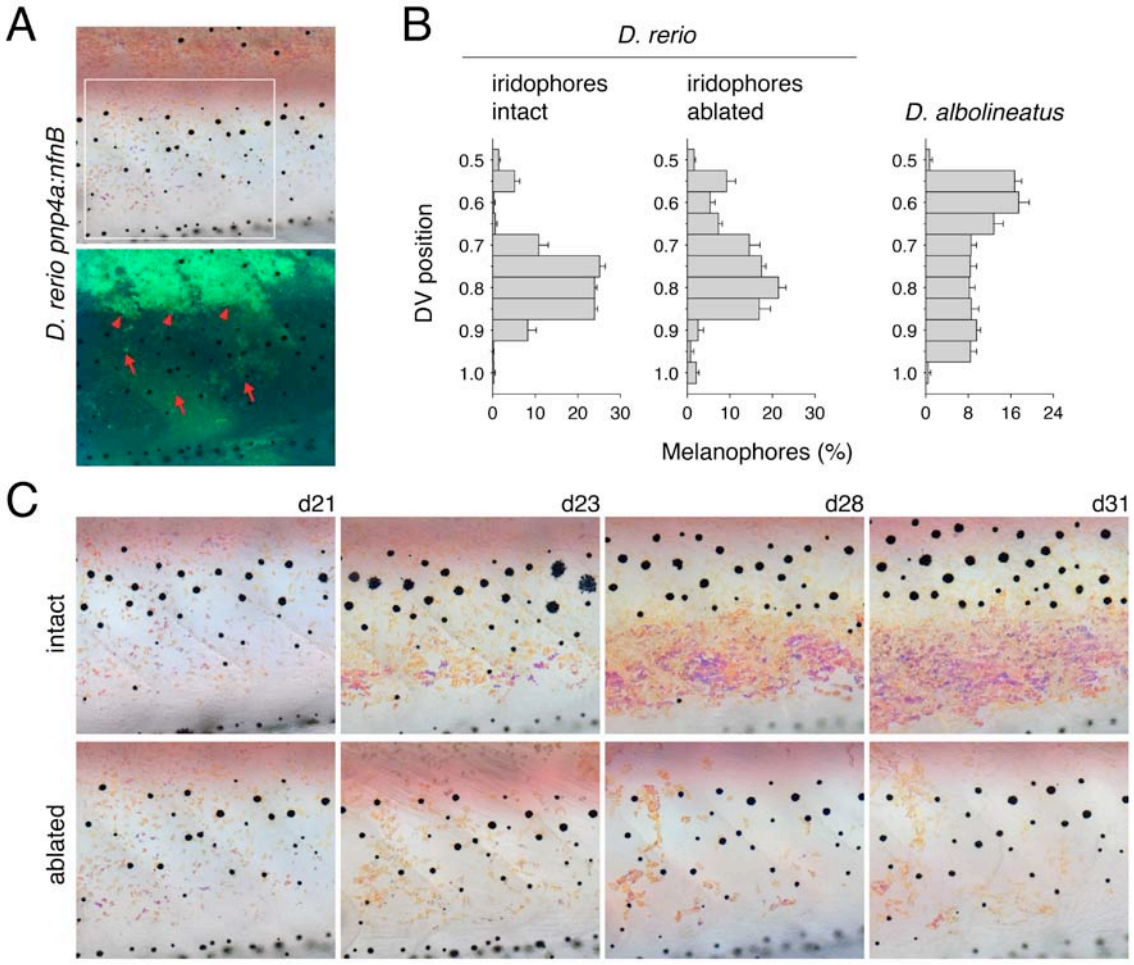
A
D. rerio pnp4a:nfnB
B
D. rerio
iridophores intact
iridophores ablated
D. albolineatus
DV position
0.5
0.6
0.7
0.8
0.9
1.0
0
10
20
30
8
16
24
Melanophores (%)
C
d21
d23
d28
d31
intact
ablated

Figure S2.1

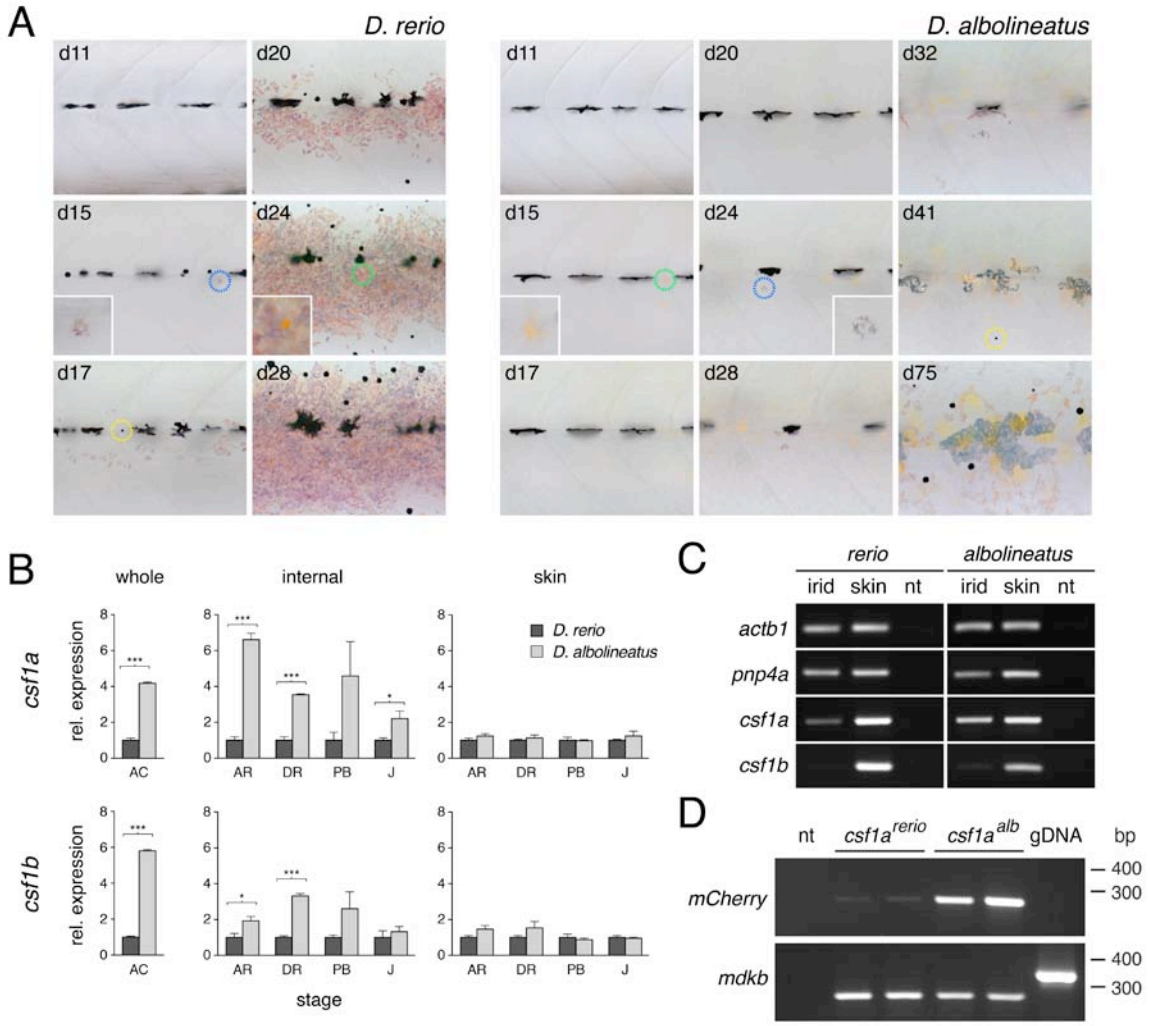
A
D. rerio
D. albolineatus
d11
d20
d32
d15
d24
d41
d17
d28
d75
B
whole
internal
skin
csf1a
csf1b
rel. expression
D. rerio
D. albolineatus
AC
AR
DR
PB
J
stage
C
rerio
albolineatus
irid
skin
nt
actb1
pnp4a
csf1a
csf1b
D
nt
csf1a rerio
csf1a alb
gDNA
bp
mCherry
mdkb
400
300

Figure S2.2

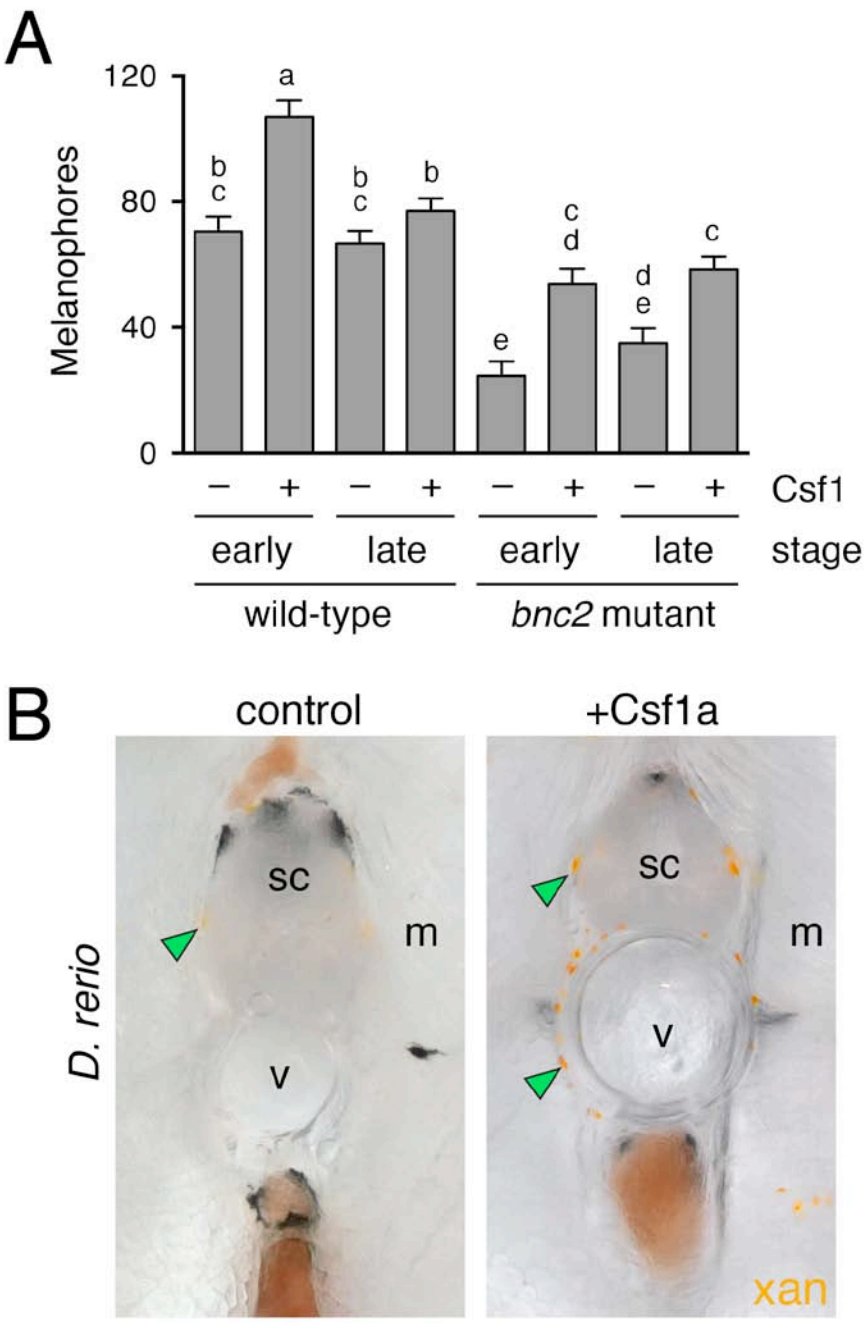
A
Melanophores
120
80
40
0
a
b
c
b
c
b
e
c
d
d
e
c
– + – + – + – +
Csf1
early late early late
stage
wild-type
bnc2 mutant
B
control
+Csf1a
D. rerio
sc
m
v
sc
m
v
xan

Figure S2.3